M 2014

U.PORTO
INSTITUTO DE CIÊNCIAS BIOMÉDICAS ABEL SALAZAR
UNIVERSIDADE DO PORTO

7α-ALLYLANDROSTANES AS NEW AROMATASE INHIBITORS:

BIOLOGICAL EFFECTS IN HORMONE-DEPENDENT AND HORMONE-RESISTANT BREAST CANCER CELLS

JOÃO CARLOS PAIS MAURÍCIO

DISSERTAÇÃO DE MESTRADO APRESENTADA

AO INSTITUTO DE CIÊNCIAS BIOMÉDICAS ABEL SALAZAR

DA UNIVERSIDADE DO PORTO EM

ONCOLOGIA – ONCOLOGIA MOLECULAR

JOÃO CARLOS PAIS MAURÍCIO

7α-ALLYLANDROSTANES AS NEW AROMATASE INHIBITORS: BIOLOGICAL EFFECTS IN HORMONE-DEPENDENT AND HORMONE-RESISTANT BREAST CANCER CELLS

Dissertação de Candidatura ao grau de Mestre em Oncologia – Oncologia Molecular, submetida ao Instituto de Ciências Biomédicas de Abel Salazar da Universidade do Porto.

Orientador – Doutora Natércia Teixeira

Categoria – Professora Catedrática

Afiliação – Faculdade de Farmácia da Universidade do Porto.

Co-orientador – Doutora Georgina Correia-da-Silva

Categoria – Professora Auxiliar

Afiliação – Faculdade de Farmácia da Universidade do Porto.

ORAL/POSTER COMMUNICATIONS

J. Maurício, C. Amaral, C. Varela, E. Tavares da Silva, F. Roleira, S. Costa, G. Correia-da-Silva and N. Teixeira, *New 7α-allylandrostanes as Aromatase Inhibitors: Biological Effects in Hormone-dependent and Hormone-resistant Breast Cancer Cells*. Presented at IJUP'14 – 7º Encontro de Jovens Investigadores da Universidade do Porto, Feb. 2014, Porto, Portugal – Oral Communication.

J. Maurício, C. Amaral, C. Varela, E. Tavares da Silva, F. Roleira, S. Costa, G. Correia-da-Silva and N. Teixeira, *7α-allylandrostanes as Aromatase Inhibitors: Biological Effects in ER+ Breast Cancer Cells*. Presented at XV Jornadas de Senologia, Sociedade Portuguesa de Senologia, Oct 2014, Luso, Portugal – Abstract selected by the juri for Oral Communication.

J. Maurício, C. Amaral, C. Varela, E. Tavares da Silva, F. Roleira, S. Costa, G. Correia-da-Silva and N. Teixeira, *7α-allylandrostanes as New Aromatase Inhibitors: Biological Effects in MCF-7aro and LTEDaro Cells*. Presented at 1st ASPIC International Congress, Associação Portuguesa de Investigação em Cancro (ASPIC), Nov 2014, Lisboa, Portugal – Poster Communication.

AKNOWLEGMENTS

Due to personal reasons, I will keep this section written in Portuguese and not in English.

Mais uma etapa que termina…Um percurso de altos e baixos, de desafios e constantes batalhas. É certo que estes momentos das nossas vidas só têm verdadeiro significado por os podermos partilhar com quem nos é importante, estejam onde estiverem. São as pessoas que fazem parte do nosso mundo que nos encorajam e nos apoiam a cada passo que damos. Por isso, deixo aqui vários obrigados…

Às Professoras Natércia Teixeira e Georgina Correia-da-Silva, por me terem acolhido no laboratório de Bioquímica, por terem acreditado em mim ao longo do caminho, quando, muitas vezes, era eu a duvidar, pelo constante apoio e preocupação e, acima de tudo, pelo inestimável conhecimento que tão bem souberam transmitir. Obrigado pela experiência enriquecedora que me proporcionaram.

À (Doutora) Cristina Amaral, pelo acompanhamento diário no laboratório, pela paciência e empenho, pelo saber transmitido e fascínio pela ciência contagiante, por ter contribuído, de forma inegável, para que eu pudesse crescer neste meu início tímido na carreira científica. Aos meus restantes colega do laboratório, que sempre foram presenças sorridentes e bem-dispostas e que tornaram a minha estadia nesta "casa" muito mais agradável. Obrigado por me socorrerem quando precisei e por também estarem disponíveis para aplacar as minhas dúvidas. Um obrigado muito especial, então, à Marta, Maria, David, João, Bruno, Susana, Sandra e Mariana. E, claro, um obrigado enorme à D. Casimira e à Ana Paula, pela simpatia e por não me baterem de cada vez que ia pedir algo do armazém!

Aos meus pais, um obrigado do fundo do coração! Pelos sacrifícios feitos, pelas preocupações, pelo apoio incondicional. Jamais teria chegado onde cheguei se não fosse tudo isso e não seria quem sou hoje se não fosse por vocês. Obrigado por me ouvirem, por saberem aconselhar, por procurar fazer sempre mais, quando, muitas vezes, isso é difícil. Estarei eternamente grato por tudo! Amo-vos!

À minha restante família, muito obrigado pelo vosso apoio e por sempre ter podido contar convosco. Aos meus tios Francisca e João, aos meus tios/primos Lurdes e José Luís e ao meu quase-irmão Jorge. Sabem o quanto vos adoro!

Às minhas avós, Bia e Catarina, que, por diferentes razões, não podem testemunhar este meu objectivo alcançado, deixo o meu amor eterno! Sei que se iriam orgulhar de mim…

À Ana Lúcia, pelos já 21 anos de amizade! O que nos une vai muito além do que alguém possa imaginar. Mesmo longe, sabemos que os nossos corações estão sempre ligados. Obrigado por tudo, por me aceitares tal e qual eu sou e por fazeres o meu mundo um lugar mais luminoso. Tenho saudades…Adoro-te coração!

À Lúcia Apolo pela amizade inestimável e as confidências que nos pertencem. Obrigado por teres estado sempre lá. Love you!
Um obrigado caloroso e repleto de amor à Rute Morais, Filipe Torres, Inês Oliveira, Andreia Ferreira, Marta Barbosa, Sara Salazar, Mariana Pinhão, Ana Nascimento, Samuel Silva e Pedro Gonçalves. É quase impossível expressar o quanto vocês significam para mim. Não consigo imaginar a minha vida sem vocês! Obrigado por tudo, por serem o meu abrigo e a infinita fonte de sorrisos e gargalhas, lágrimas desfeitas e saudades imensas. Amo-vos!
Aos meus afilhados académicos, pelo carinho e orgulho de ser vosso padrinho!
Ao Marco Ferreira e ao João Sá, pela amizade especial e que nós tão bem sabemos estimar!
À Joana Galante, Teresa Bento, Mário Sousa e Jorge Comendinha, pelas aventuras em Londres e a amizade que daí surgiu. Saudades de todos!
À Bela Teixeira e todo o pessoal da Associação Juvenil de Ciência (AJC)! A minha passagem pela associação foi uma experiência única e orgulho-me do meu contributo para o seu crescimento. Adoro-vos a todos e espero um dia voltar à azáfama das nossas actividades.
Aos amigos especiais que me conquistaram nestes últimos dois anos a viver no Porto. À Liliana Raimundo, Pedro Jorge, Hélio Costa, Bruno Pereira e Ismael Carneiro. Ao mais recente grupo, João Ferreira, Aníbal Évora, Filipe Geraldes, Tiago Sequeira, Luís Guardado e Paulo Laranjeira. Obrigado pelo companheirismo, pela amizade genuína e inestimável, pelos momentos partilhados. Adoro-vos!

"Our lives are not our own. We are bound to others, past and present and by each crime and every kindness we birth our future"

By David Mitchell *in "*Cloud Atlas"

RESUMO

O subtipo mais comum de cancro da mama é o hormono-dependente (ER+). Terapias endócrinas para este subtipo incluem moduladores e inactivadores selectivos do receptor de estrogénio e inibidores da aromatase (IAs). Estes últimos inibem a aromatase, impedindo a conversão de androgénios em estrogénios. Contudo, existem aspectos negativos quanto ao seu uso, nomeadamente desenvolvimento de resistência e ocorrência de perda de massa óssea. O foco deste trabalho é, portanto, identificar novos inibidores da aromatase mais potentes e que consigam contornar a resistência endócrina e, ao mesmo tempo, clarificar os seus mecanismos de acção a nível das células tumorais da mama.

Recentemente, os compostos esteróides 7α-allylandrostanes foram descritos como inibidores potentes em microssomas de placenta: 7α-allylandrost-4-ene-3,17-dione (**6**), 7α-allylandrost-4-en-17-one (**9**), 7α-allyl-3-oxoandrosta-1,4-dien-17β-ol (**10**) e 7α-allylandrosta-1,4-diene-3,17-dione (**12**). Os novos esteróides são potentes IAs em células MCF-7aro e induzem um decréscimo da viabilidade celular independente da inibição da aromatase e, no caso do IA **10**, dependente do receptor de estrogénio. Estes compostos não induzem citotoxicidade em células não-tumorais. Após tratamento, as células MCF-7aro apresentaram características morfológicas típicas de apoptose, tais como condensação e fragmentação de cromatina, para além da presença de vacúolos citoplasmáticos em algumas células. Os IAs induziram um bloqueio do ciclo celular nas fases G0/G1 ou G2/M e activaram a caspase-9. O esteróide **10** demonstrou ser o mais potente. As células LTEDaro, resistentes aos IAs usados na clínica, são sensíveis ao composto **10**. A inibição da autofagia com 3-MA sensibiliza as células resistentes, o que sugere que, para períodos curtos, a autofagia é um mecanismo de sobrevivência. Contudo, para períodos mais longos, a inibição da autofagia já não promove uma maior diminuição da viabilidade celular. As células hormono-resistentes e -sensíveis mostram ter o mesmo comportamento para tempos de exposição prolongados, independentemente da presença de 3-MA. Em suma, os dados mostram que o composto **10** é o mais promissor e futuros estudos devem ser realizados para melhor compreender os seus mecanismos celulares específicos. Estes estudos são importantes para obter informação sobre os efeitos biológicos dos IAs esteróides e permitir determinar quais as características químicas que contribuem para a obtenção de IAs mais potentes, com menos efeitos secundários e capazes de superar a resistência endócrina.

Palavras-chave: cancro da mama, inibidores da aromatase, apoptose, autofagia, ciclo celular

ABSTRACT

The most common subtype of breast cancer is the hormone-dependent one (ER+). Targeted therapies include selective estrogen receptor modulators, down-regulators and aromatase inhibitors (AIs). AIs inhibit the aromatase enzyme, preventing the conversion of androgens to estrogens. However, there are drawbacks concerning their use, namely the development of acquired resistance and the occurrence of bone loss. The focus of this work was to identify new potent steroidal AIs that can overcome endocrine resistance and, at the same time, clarify their biological mechanisms in breast cancer cells.

Recently, the steroidal compounds 7α-allylandrostanes were described as potent AIs in placental microsomes: 7α-allylandrost-4-ene-3,17-dione (**6**), 7α-allylandrost-4-en-17-one (**9**), 7α-allyl-3-oxoandrosta-1,4-dien-17β-ol (**10**) and 7α-allylandrosta-1,4-diene-3,17-dione (**12**). The new steroids were shown to be potent AIs when studied their anti-aromatase activity in MCF-7aro cells. All the compounds induced a decrease in MCF-7aro cells' viability independent of aromatase inhibition and, for compound **10**, dependent on ER. The new AIs did not present cytotoxicity in non-tumor cells. After treatment, MCF-7aro cells presented typical features of apoptosis such as chromatin condensation and fragmentation, besides presence of cytoplasmic vacuoles in some cells. They were able to induce a cell cycle arrest in G0/G1 or G2/M phases and activate initiator capase-9. AI **10** was demonstrated to be the most potent one. LTEDaro cells, which are resistant to the AIs used in the clinic, are sensitive to steroid **10**. Inhibition of autophagy by 3-MA sensitizes resistant cells, which suggests that, for short periods of time, autophagy is a mechanism of cell survival. However, for longer exposure times, autophagy inhibition no longer enhances the decrease in cell viability. Both hormone-resistant and –dependent cells show the same behaviour for prolonged times of treatment, regardless of the presence of 3-MA.

In summary, our data showed that compound **10** is the most promising AI and future studies should be designed, in order to understand the specific cellular mechanisms for this steroid. These studies are important to provide new insights on the cellular effects of steroidal AIs, allowing to determine which features of the chemical structure contribute to the design of more potent AIs with fewer side effects than the ones currently used in clinic and with the ability to overcome endocrine resistance.

Key-words: breast cancer, aromatase inhibitors, apoptosis, autophagy, cell cycle

INDEX

FIGURES

TABLES

ABBREVIATIONS

3β-HSD	3β-hydroxysteroid dehydrogenase
3-MA	3-methyladenine
17β-HSD	17β-hydroxysteroid dehydrogenase
A	Androstenedione
ABC	Advanced breast cancer
AF-1/2	Activation function 1/2
AI	Aromatase inhibitor
AIB1	Amplified in breast 1 (NCOA3/SRC-3)
AKT	Protein kinase B
AO	Acridine Orange
AP-1	Activator protein 1
Atg	Autophagy-related gene
AVO	Acid vesicular organelle
BAFs	Breast adipose fibroblasts
Bcl-2	B-Cell Lymphoma 2
cAMP	Cyclic adenosine monophosphate
CCCP	Carbonyl cyanide *m*-chlorophenylhydrazone
cDNA	Complementary DNA
CFBS	Charcoal-treated fetal bovine serum
CK	Cytokeratin
CMF	Cyclophosphamide, methotrexate and 5-fluorouracil
COX	Cyclooxygenase
CPR	Cytochrome P450 reductase
CR	Complete response
CREs	cAMP response elements
CREB1	cAMP-responsive element binding protein 1
CYPs	Cytochromes P450
CYP11A1	Cholesterol side-chain cleavage enzyme
CYP17A1	17α-hydroxylase/17,20-lyase
DBD	DNA binding domains
$DCFH_2$-DA	2',7'-dichlorodihydrofluorescein diacetate
DEX	Dexamethasone
DFI	Disease-free interval
DFS	Disease-free survival

DHT	Dihydrotestosterone
DHEA	Dehydroepiandrosterone
DHEAS	Dehydroepiandrosterone sulfate
$DiOC_6(3)$	3,3-dihexyloxacarbocyanine iodide
DMEM	Dulbecco's Modified Eagle Medium
DMSO	Dimethylsulfoxide
E1	Estrone
E1-S	Estrone-sulfate
E2	Estradiol/17β-estradiol
E3	Estriol
EBC	Early breast cancer
EDTA	Ethylenediaminetetraacetic acid
EGFR	Epidermal growth factor receptor 1 (HER1)
EMT	Epithelial-Mesenchymal Transition
ER	Estrogen receptor
ERE	Estrogen-response element
ERK	Extracellular signal-regulated kinase
EST	Estrogen sulfotransferase
FAC	5-fluorouracil, doxorubicin and cyclophosphamide
FBS	Fetal bovine serum
HB-EGF	Heparin-binding epidermal growth factor
HER2	Human epidermal growth factor receptor 2
HR	Hormone receptors
HSDs	Hydroxysteroid dehydrogenases
IDC	Infiltrating/Invasive ductal carcinomas
IGFR1	Insulin-like growth factor receptor 1
IHC	Immunohistochemical/Immunohistochemistry
IL	Interleukin
ILC	Infiltrating/Invasive lobular carcinomas
Jak	Janus kinase
JNK	c-Jun-NH2-terminal kinase
LCIS	Lobular carcinoma in situ
LBD	Ligand binding domain
LDH	Lactate dehydrogenase
MAPK	Mitogen-activated protein kinase
MBC	Metastatic breast cancer

MEM	Minimum essential medium
mTOR	Mammalian target of rapamycin
MTT	3-(4,5-dimethylthiazol-2-yl)-2,5-difenyltetrazolium
NACT	Neoadjuvant chemotherapy
NAD+	Nicotinamide adenine dinucleotide
NADPH	Nicotinamide adenine dinucleotide phosphate
NAET	Neoadjuvant endocrine therapy
NCOA1/2/3	Nuclear receptor co-activator 1/2/3 (SRC-1/2/3)
NSAI	Non-steroidal aromatase inhibitor
OFS	Ovarian function suppression
ORR	Objective response rate
OS	Overall survival
OSM	Oncostatin M
OTR	Oxytocin receptor
p53	Tumor protein p53
PARP1	poly(adenosine diphosphate [ADP]-ribose) polymerase 1
pCR	Pathological complete response
PDGFR	Platelet-derived growth factor receptor
PFS	Progression-free survival
PGE2	Prostaglandin E2
PI	Propidium iodide
PI3K	Phosphatidylinositol-4,5-bisphosphate 3-kinase
PKA/PKC	Protein kinase A/C
PMA	Phorbol 12-myristate 13-acetate
PgR	Progesterone receptor
PR	Partial response
RFS	Recurrence-free survival
RNA	Ribonucleic acid
RS	Recurrence score
RTK	Receptor tyrosine kinase
RT-PCR	Real-time polymerase chain reaction
SAI	Steroidal aromatase inhibitor
SERM	Selective estrogen receptor modulator
SERD	Selective estrogen receptor down-regulator
siRNA	Short interfering RNA
SP-1	Specificity protein 1

STA	Staurosporine
STAT	Signal transducer and activator of transcription
STS	Steroid sulfatase
T	Testosterone
TGF	Transforming growth factor
TIC	Tumor initiating cells
TN	Triple-Negative
TNF	Tumor necrosis factor
TTP	Time-to-progression
VEGF	Vascular endothelial growth factor
VEGFR	Vascular endothelial growth factor receptor

Chapter I

Introduction

1.1. BREAST CANCER

Breast cancer is the second most common cancer in the world and, by far, the most frequent cancer among women, with an estimated 1.67 million new cancer cases diagnosed in 2012 (25% of all cancers). Incidence rates vary across the world regions, with rates ranging from 27 per 100,000 in Middle Africa and Eastern Asia to 96 in Western Europe. Breast cancer is the most frequent cause of cancer death in women in less developed regions and it is now the second cause of cancer death in more developed regions, after lung cancer. The range in mortality rates between world regions is lower than that for incidence, because of the more favorable survival rates of breast cancer in (high-incidence) developed regions (Ferlay et al. 2013).

Breast cancer is a complex disease including clinical, histological and molecular distinct entities. This heterogeneity cannot be explained exclusively by clinical parameters such as tumor size, lymph node (LN) involvement, histological grade and age or by pathological biomarkers like estrogen receptor (ER), progesterone receptor (PgR) and epidermal growth factor receptor 2 (HER2), which are routinely used in the diagnosis and treatment decision. During the last decade, research has focused in depth on the molecular biology of the disease. The interconnection of several signaling pathways and both the tumor microenvironment and the inherent characteristics of the patient influence disease pathophysiology, outcome and treatment response (Eroles et al. 2012; Prat and Perou 2011). About 20-40% of patients develop metastatic disease, with a median survival between 2 and 4 years depending on the subtype (Eroles et al. 2012; Guarneri and Conte 2009).

The data stipulated by the quantitative evaluation of numerous genes is more precise for biological characterization than that offered by the tumor histopathological studies used for diagnosis (Eroles et al. 2012). Perou et al. (2000) published the first paper classifying breast cancer into intrinsic subtypes based on gene expression profile. Variation in growth rates, activated signaling pathways and cellular composition of the tumors were all mirrored in the corresponding variation in the expression of specific subsets of genes. Also, the finding that a metastasis and primary tumor were similar in their overall pattern of gene expression suggested that the molecular program of a primary tumor may generally be retained in its metastases (Perou et al. 2000).

The hierarchical cluster analysis revealed four molecular subtypes (Figure 1A): luminal, HER2-positive (HER2+), basal-like and normal breast-like. This last category is now believed to be a misconception, since it clusters together with normal breast samples and this happens due to the samples being composed, predominantly, of normal breast tissue

and not tumor tissue (Prat and Perou 2011; Eroles et al. 2012). The subsequent expansion of this work allowed the identification of two groups within the luminal subtype (luminal A and B) and showed that different molecular subtypes were linked to distinct incidence, prognosis (Figure 1B) and response to treatment (Prat and Perou 2011; Eroles et al. 2012). HER2+/basal-like tumors have the worst prognosis, differing from luminal A tumors, with the best prognosis.

The main features of each of the intrinsic subtypes can be found in Table 1 (Perou et al. 2000; Prat and Perou 2011; Eroles et al. 2012).

Table 1. Main features of the breast cancer intrinsic subtypes.

Luminal A	• 50–60% of all breast cancers. • Expression of genes activated by the ER transcription factor, typically expressed in the luminal epithelium lining the mammary ducts. • Low expression of genes related to cell proliferation. • Expression of ER (ER+), PgR (PgR+), Bcl-2 (B-Cell Lymphoma 2) and cytokeratin (CK) 8/18, absence of HER2 expression (HER2-), low Ki-67 (<14%) and low histological grade.
Luminal B	• 10-20% of all breast cancers. • Compared to the luminal A, they have a more aggressive phenotype, higher histological grade and proliferative index (Ki-67) and worse prognosis. • ER+. Increased expression of proliferation genes, such as *MKI67* (Ki-67 gene) and cyclin B1; also often expresses EGFR (epidermal growth factor receptor 1) and HER2. • Has tumors with ER+/HER2- and high Ki-67 or ER+/HER2+; up to 6% are clinically ER-/HER2-.
HER2+	• 15-20% of all breast cancers. • High expression of the HER2 gene and other genes associated with the HER2 pathway and/or HER2 amplicon located in the 17q12 chromosome. Over-expression of proliferation genes. Lack of expression of the basal cluster and low expression of the luminal cluster, compared to Luminal A and B tumors. • Highly proliferative, 75% have a high histological grade and more than 40% have p53 mutations. Poor prognosis. • Although ≈30% of HER2-enriched tumors are clinically HER2-, they might be driven by a similar functional event such as HER2 mutation or mutation of some downstream pathway component that phenocopies HER2 amplification

Basal-like	• 10–20% of all breast carcinomas. • Expression of genes usually present in normal breast myoepithelial/basal cells, including high molecular weight cytokeratins CK5/6 and CK17, P-cadherin, caveolin 1 and 2 and EGFR. • High histological grade and high frequency of LN involvement. These tend to be infiltrating/invasive ductal carcinomas (IDC) with a high mitotic index and tumor necrosis. • Absence of expression of the three key receptors in breast cancer: ER, PgR and HER2. Therefore, in clinical practice the terms basal-like and Triple Negative (TN) are often interchanged. • Worse prognosis than luminal tumors, with a higher relapse rate in the first 3 years despite them presenting a high response to chemotherapy. High rate of p53 mutations.

After the initial molecular classification, a new intrinsic subtype was identified by Herschkowitz et al. (2007). It is characterized by a low expression of genes involved in tight junctions and cell-cell adhesion, including claudin-3, -4 and -7 and E-cadherin, hence the name **claudin-low**. It shares some specific gene expression with the basal-like tumors, such as low expression of HER2 and luminal gene cluster. In contrast to the basal-like subtype, this group overexpresses a set of genes related to immune response, indicating a high infiltration of tumor immune cells. Claudin-low tumors have a poor prognosis, despite presenting a low expression of genes related to cell proliferation. Besides that, they overexpress a subset of genes closely linked to mesenchymal differentiation, epithelial–mesenchymal transition (EMT) and tumor initiating cells (TIC). It is a relatively rare subset of tumors (12–14%), clinically corresponding to high grade IDC and characterized by immunohistochemistry (IHC) as normally TN; however, as the basal-like tumors, the concordance TN/claudin-low is not 100% and about 15% of these tumors are positive for hormone receptors (HR+). These tumors show an insufficient response to neoadjuvant chemotherapy, with intermediate values between basal-like and luminal tumors (Herschkowitz et al. 2007; Prat and Perou 2011; Eroles et al. 2012).

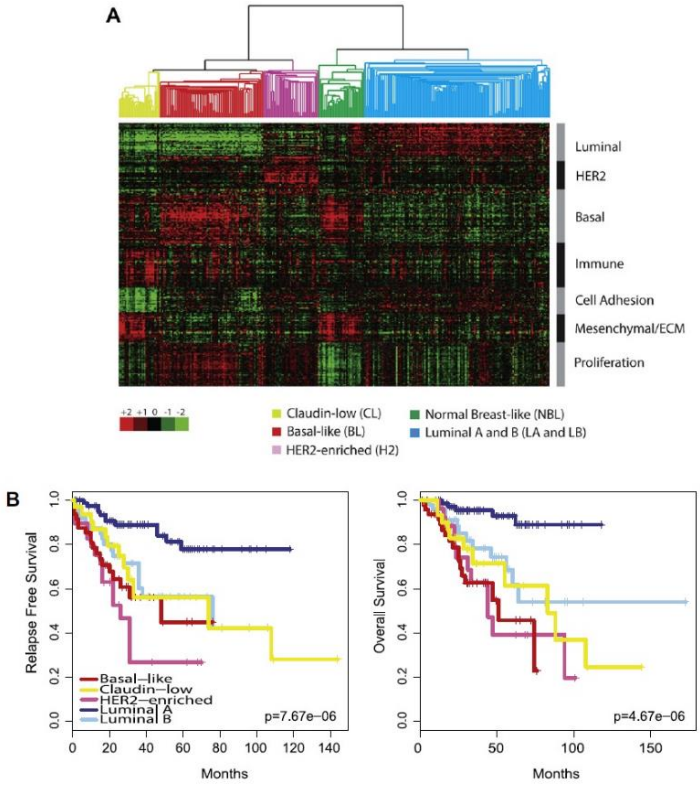

Figure 1. (A) Intrinsic hierarchical clustering and selected gene expression patterns. (B) Kaplan-Meier relapse-free survival and overall survival curves (adapted from (Prat and Perou 2011))

Noteworthy, the information made available by the several studies on the breast cancer intrinsic subtypes complements and expands the information provided by the classical clinical-pathological markers.

The St. Gallen International Breast Cancer Conference Expert Panel 2011 recognized, for the first time, the utility of the breast cancer intrinsic subtype's classification (by means of gene expression profiles) in the therapeutic decision process. However, that year's panel and the subsequent one (2013) have considered the use of clinical-pathological markers as suitable surrogates for subtype definition, in clinical practice, despite them not fully recapitulate the intrinsic subtypes. The considerable economic investment as well as the lack of sufficient validation and standardization might have contributed to this decision (Goldhirsch et al. 2011; Goldhirsch et al. 2013; Eroles et al. 2012).

Regarding therapeutic strategies, it has been established that luminal A disease generally requires only endocrine therapy, which is also an option for the luminal B subtype. Chemotherapy is considered the recommended treatment for most luminal B, HER2+ and TN (basal-like and claudin-low) diseases, with the addition of trastuzumab in HER2+ disease (in combination or sequentially after chemotherapy) (Prat and Perou 2011; Eroles et al. 2012; Goldhirsch et al. 2013). In general, systemic therapies have been shown to be

beneficial or to have a direct effect in approximately 90% of primary breast tumors and 50% of metastatic cases. In clinical practice, a small proportion of breast cancer patients present with locally advanced or metastatic disease, whereas the majority (80-90%) present at early/operable stages (Rakha and Ellis 2011).

Two studies have directly evaluated the response to neoadjuvant chemotherapy (NACT) of the intrinsic subtypes. Rouzier et al. (2005) evaluated several primary breast tumors treated with paclitaxel followed by 5-fluorouracil, doxorubicin and cyclophosphamide (FAC). After surgery, patients were evaluated for pathological complete response (pCR). Among the patients with basal-like tumors and HER2-enriched tumors, the pCR rates were both 45%, whereas only 7% of Luminal A/B tumors achieved a pCR (Rouzier et al. 2005). On another study, Parker et al. (2009) evaluated the ability of the molecular subtypes to predict pCR to anthracycline/taxane-based chemotherapy, using a combined cohort of patients from three different neoadjuvant studies. Basal-like and HER2-enriched tumors showed the highest response rate, with 43% and 36% pCR rates, respectively, whereas Luminal A and B tumors showed 7% and 17% pCR rates. These studies highlight the higher chemo-sensitivity of basal-like and HER2-enriched subtypes (mainly ER-negative) and the chemo-insensitivity of the Luminal subtypes (mostly ER-positive), which explains why ER status is such a robust predictor of pCR (Parker et al. 2009). Also, neoadjuvant endocrine therapy (NAET) was highly accepted as a reasonable option in post-menopausal patients with highly endocrine responsive disease, with a therapy duration until maximal response (Goldhirsch et al. 2013).

The St. Gallen Experts Panel's majority voted for the following factors as clear arguments for inclusion of adjuvant chemotherapy into systemic therapy: histological grade 3 tumor, high Ki-67, low HR status, positive HER2 status, TN status, high 21 gene recurrence score (RS; e.g. > 25), 70 gene high risk profile and > 3 positive nodes (Goldhirsch et al. 2013).

The panel considerations, in the 2013 session, concerning adjuvant chemotherapy were as follows (Goldhirsch et al. 2013).:

- Luminal A tumors are less responsive to chemotherapy, thus less intensive chemotherapy is adequate for this subtype.
- Luminal B subtype by itself was considered to be sufficient to advise chemotherapy. Anthracyclines rather than CMF (cyclophosphamide, methotrexate and 5-fluorouracil) and the inclusion of taxanes were preferred.
- For HER2+ disease, there was no preferred chemotherapy regimen and a clear majority voted for the use of anthracyclines and taxanes. Likewise, for the basal-like or TN phenotype, the use of anthracyclines and taxanes was also endorsed.

- A unanimous vote considered trastuzumab therapy (simultaneously or following chemotherapy) over 1 year as standard in HER2+ early breast cancer (EBC). This combination allows for an improvement in recurrence-free survival (RFS) and overall survival (OS).

Still, a challenge remains as to the identification of effective targets for the TN cases, which are basically composed of basal-like and claudin-low tumors. The list of molecular targets that are being evaluated includes: poly(adenosine diphosphate [ADP]-ribose) polymerase 1 (PARP1), vascular endothelial growth factor (VEGF), HER1, mitogen-activated protein kinase (MAPK), phosphatidylinositol-4,5-bisphosphate 3-kinase (PI3K)/mammalian target of rapamicin (mTOR) and the stem cell pathways NOTCH and Hedgehog (Prat and Perou 2011).

Several multigene assays that predict outcome and response to therapy in breast cancer have been developed, an approach pioneered by Van't Veer et al. (2002). The most frequently reported and validated assays are the 21-gene signature Oncotype DX and the 70-gene MammaPrint.

Oncotype DX is a real-time (RT)-PCR assay, which measures the expression of 21 genes in RNA extracted from formalin-fixed samples (Habel et al. 2006). The levels of expression of these genes are handled by an empirically-derived, prospectively defined mathematical algorithm to calculate a recurrence score (RS), which is then used to allocate a patient to 1 of 3 groups by estimated risk of distant metastasis. For instance, a subsequent study have validated the clinical utility of Oncotype DX in LN-positive post-menopausal women treated with endocrine therapy (Dowsett et al. 2010).

MammaPrint is another prognostic multigene assay composed of 70 genes. This test is approved by Food and Drug Administration (FDA) for use in the US, for LN-negative breast cancer patients < 61 years of age, with tumors < 5 cm in size. However, this test, which uses oligonucleotide microarrays, requires a fresh sample of tissue that is composed of a minimum of 30% malignant cells. This assay was first validated in untreated LN-negative patients (Veer et al. 2002).

Routine clinical management of breast cancer relies on the availability of robust prognostic and predictive factors. Overall, the information provided by the intrinsic subtypes, when combined with the current clinical-pathological markers, helps not only to further explain the biological complexity of breast cancer, but also to increase the efficacy of current and novel therapies and, ultimately, improve outcomes for breast cancer patients.

1.2. HORMONE-DEPENDENT BREAST CANCER

Hormone-dependent breast cancer comprises both luminal A and B intrinsic subtypes.

The **luminal A** breast cancer is the most common subtype, representing 50–60% of the total. It is characterized by the expression of genes activated by the ER. It also presents a low expression of genes related to cell proliferation. Based on their molecular profile, all cases of lobular carcinoma in situ (LCIS) are luminal A tumors, as are most of the infiltrating lobular carcinomas (ILC). The luminal A IHC profile is characterized by the expression of ER, PgR, Bcl-2 and cytokeratins CK8/18, absence of HER2 expression, a low rate of proliferation measured by Ki-67 and a low histological grade. Patients with this subtype of cancer have a good prognosis; the relapse rate is 27.8%, being significantly lower than that for other subtypes. They have a distinct pattern of recurrence with a higher incidence of bone metastases (18.7%); other locations such as central nervous system, liver and lung represent less than 10%. The treatment of this subgroup of breast cancer is mainly based on third-generation aromatase inhibitors (AIs) in post-menopausal patients, selective estrogen receptor modulators (SERMs) like tamoxifen and pure selective regulators of ER like fulvestrant (Eroles et al. 2012). These tumors frequently exhibit abrogation of stress-induced apoptotic kinase JNK signaling, either through loss-of-function mutations in the *MAP3K1* or *MAP2K4* genes or through activating mutations in the genes in the PI3K/AKT pathway and this abrogation has been associated with reduced response to chemotherapy compared with patients with normal JNK signaling (Small et al. 2007).

Tumors with the **luminal B** molecular profile constitute 10% to 20% of all breast cancers. As already mentioned, compared to luminal A, they have a more aggressive phenotype, higher histological grade and proliferative index and worse prognosis. The pattern of distant relapse also differs and although the bone is still the most common site of recurrence (30%), this subtype has a higher recurrence rate in sites such as the liver (13.8%) (Eroles et al. 2012).

Luminal A and B are both HR+. The main biological difference between the two subtypes is an increased expression of proliferation genes, such as *MKI67* and cyclin B1 in the luminal B subtype, which also often expresses EGFR and HER2 (Eroles et al. 2012). As referred before, luminal B tumors respond better to neoadjuvant chemotherapy than luminal A, despite them not achieving the same response rate as HER2+ and basal-like tumors (Parker et al. 2009).

Patients with a low-risk of relapse are found almost exclusively in the luminal A subtype (Figure 1). Distinction between luminal A and luminal B tumors has been made possible using the proliferation signature, namely the protein expression of Ki-67, which has higher

expression in luminal B tumors than in luminal A tumors. Thus, the luminal A subtype was defined as being ER+/HER2- and low for Ki-67, whereas the luminal B subtype as being ER+/HER2- and high Ki-67 or ER+/HER2+ (Prat and Perou 2011; Goldhirsch et al. 2011). Nevertheless, this definition does not include all luminal B tumors, since up to 7% of these are clinically ER-/HER2- (Figure 2). The technique used to determine Ki-67, with a cut-off point set at 14%, at the St. Gallen Experts Panel 2011 (Goldhirsch et al. 2011), has not been standardized, which adds a variability factor in the assessment of this marker. Moreover, the St. Gallen Experts Panel 2013 considered a cut-off for Ki-67 between 20% and 25% more appropriate (Goldhirsch et al. 2013).

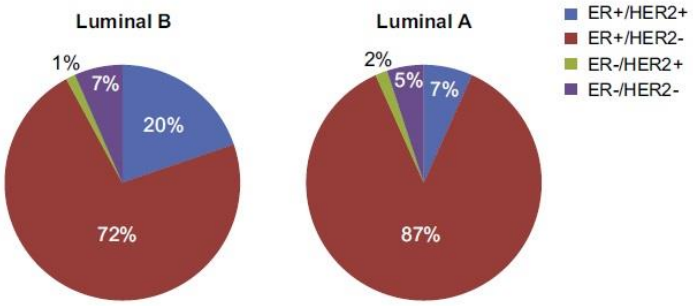

Figure 2. Distribution of ER and HER2 in the luminal subtypes of breast cancer based on mRNA expression (adapted from (Eroles et al. 2012))

1.2.1. Estrogen Synthesis and Aromatase

The steroid hormone estrogen is vital to normal female physiology, namely cell proliferation, inflammatory response, cardiovascular health, immunity, bone density, cognition and behaviour, maintenance of reproductive functions and lipid and cholesterol homeostasis (Castoria et al. 2010; Osborne et al. 2000; To et al. 2014).

There are three main natural estrogens in women: estrone (E1), estradiol (E2) and estriol (E3). Estradiol or 17β-estradiol is a major form of estrogens in women of reproductive age. Estrone is the form of estrogens predominantly found in post-menopausal women and estriol is formed primarily during pregnancy (Chumsri et al. 2011)

Whereas in pre-menopausal women, the ovaries are the main source of estrogen, in post-menopausal women, when the ovaries cease to produce estrogens, E2 is produced in several extragonadal sites and acts locally at these sites as a paracrine or even intracrine factor (Labrie 2014; Sasano et al. 2009; Simpson 2002). These sites include the mesenchymal cells of adipose tissue, skin fibroblasts, osteoblasts and chondrocytes of bone, the vascular endothelium and numerous sites in the brain (Knower et al. 2013; Sasano et al. 2009; Simpson 2002). In the breast, adipose tissue becomes the major source

of local estrogen production (Knower et al. 2013). Therefore, the total amount of estrogen synthesized by these extragonadal sites may be small, but the local tissue concentrations attained are probably high and exert biological effects (Labrie 2014). In both pre- and post-menopausal states, the vast majority of intracrine steroids are generated locally from precursors rather than taken from the circulation (McNamara and Sasano 2014; Sasano et al. 2009).

An essential trait of intracrinology is that the active steroids are not only produced locally, but they are also inactivated at the same site where synthesis takes place. Approximately 95% of the active estrogens and androgens synthesized are inactivated locally before being released in the blood as inactive metabolites for excretion by the liver and/or kidneys, thus avoiding inappropriate exposure of the other tissues. (Labrie 2014).

In post-menopausal women, estrogen production in the extragonadal sites is dependent on an external source of 19-carbon androgenic precursors of mainly adrenal origin, since these tissues are not able to convert cholesterol to the 19-carbon steroids. Consequently, circulating levels of testosterone (T) and androstenedione (A), as well as dehydroepiandrosterone (DHEA) and dehydroepiandrosterone sulfate (DHEAS), all abundant in circulation, become extremely important in terms of providing adequate substrates for estrogen biosynthesis in these sites (Knower et al. 2013; Sasano et al. 2009; Simpson 2002).

Regarding breast carcinoma, the primary source of estrogen in post-menopausal women is via local production by undifferentiated breast adipose fibroblasts (BAFs) surrounding malignant cells (To et al. 2014). As stated above, a mixture of steroid precursors is secreted by adrenals and ovaries, being DHEAS the dominant steroid in circulation and the one with a pivotal role in intratumoral production of estrogens. Nonetheless, it is also possible that E2 may be derived from circulating levels of E1-sulfate (E1-S) through the removal of the sulfate group and conversion of E1 to E2 (McNamara and Sasano 2014; Sasano et al. 2009).

Steroidogenesis

Steroidogenesis in the adrenals is zone-specific, with the inner zone of the adrenal cortex, zona reticularis, making 19-carbon androgen precursors such as DHEA and DHEAS. Ovaries' steroid metabolism is focused on producing androgens and estrogens, while the corpus luteum of the ovary produces progesterone. The ovaries synthesize primarily androstenedione and convert this 19-carbon steroid into 18-carbon estrogens, as well as variable amounts of testosterone. Steroidogenesis in the ovary is also compartmentalized

in a cell-specific manner, with the theca cells mostly producing androstenedione and the granulosa cells completing the synthesis of estradiol (Ghayee and Auchus 2007).

The entire process of steroid hormone production, action and metabolism can be separated into five basic components, namely (Ghayee and Auchus 2007) (Figure 3):

i. Cholesterol conversion to pregnenolone. Cholesterol is a 27-carbon steroid that is cleaved to 21-carbon pregnenolone, the first steroid product common to all steroidogenesis. This conversion is only possible in certain cells, including testicular Leydig cells, placental trophoblast cells, ovarian theca cells and corpus luteum cells and the adrenal cortex cells, as well as certain neuronal cells in the brain;

ii. Pregnenolone metabolism into various intermediates and active steroid hormones. The enzymes present in a given steroidogenic cell limits which steroids are made from pregnenolone in that cell;

iii. Peripheral organ metabolism of hormone precursors and/or hormones;

iv. Specific metabolic effects at the target tissue. Hormones may potentially become more potent or activated in target tissue. A well-known example is how testosterone is converted to dihydrotestosterone (DHT) in the prostate gland;

v. Degradative metabolism of steroids. Steroids are extensively metabolized, primarily by the liver, through many transformations that generally reduce their activities.

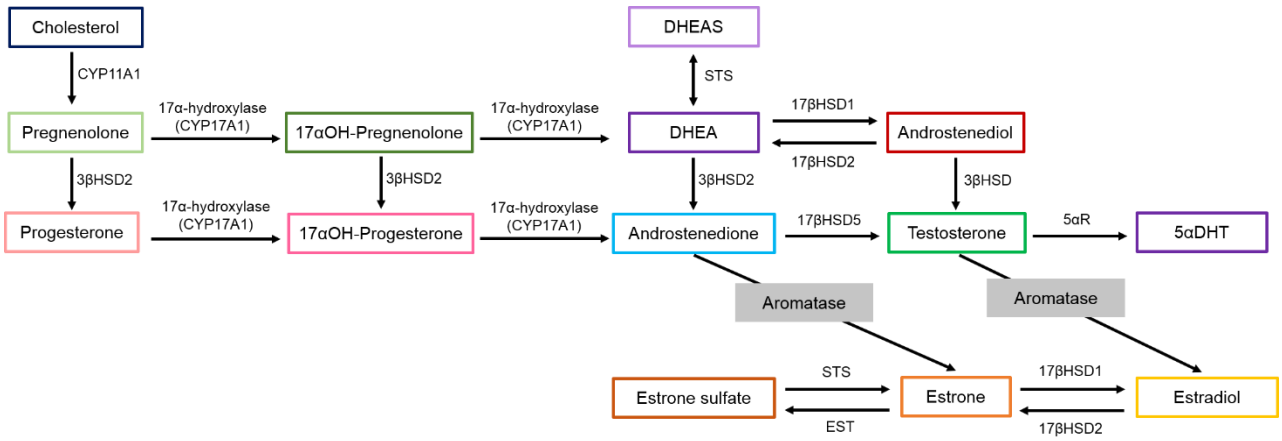

Figure 3. Biosynthesis cascade of estrogen production (adapted from (Ghayee and Auchus, 2007; Knower, To and Clyne, 2013)).

The cytochromes P450 (CYPs) are enzymes whose chemistry is limited to hydroxylation reactions and occasionally carbon-carbon bond cleavage reactions. All cytochromes P450 use molecular oxygen and electrons from NADPH to perform reactions. These enzymes can be described as type I and type II. Type II, specifically, comprises the majority of cytochromes P450 and are located in the smooth endoplasmic reticulum. They use cytochrome P450 reductase (CPR), which contains two flavins, to both oxidize NADPH and reduce the P450 directly. Steroidogenic type II enzymes include CYP11A1 (P450scc), CYP17A1 (P450c17) and CYP19A1 (aromatase, P450aro).

The other major class of enzymes in steroidogenesis includes hydroxysteroid dehydrogenases (HSDs) and reductases. In general, the HSDs exist in one or more isoforms, which regulate the proportions of a given ketosteroid and its cognate hydroxysteroid in a given cell or in plasma and this simple redox reaction greatly alters the potency of that steroid. These HSD isoforms are encoded by separate genes with tissue-specific expression. Functionally, oxidative HSDs use nicotinamide adenine dinucleotide (NAD^+) as a cofactor to convert hydroxysteroids to ketosteroids, whereas reductive HSDs use nicotinamide adenine dinucleotide phosphate (NADPH) to reduce ketosteroids to hydroxysteroids (Ghayee and Auchus 2007).

De novo synthesis of all steroid hormones (Figure 3) starts with the conversion of cholesterol to pregnenolone by CYP11A1 (cholesterol side-chain cleavage enzyme), which is bound to the inner membrane of the mitochondria. Pregnenolone is converted to progesterone by 3β-hydroxysteroid dehydrogenase (3β-HSD) and both these steroids form the precursors for all other steroid hormones (Sanderson 2006).

After obtaining the hydroxylated form of pregnenolone, CYP17A1 (17α-hydroxylase/17,20-lyase) cleaves 17α-hydroxypregnenolone to DHEA in the zona reticularis of the adrenal cortex (Ghayee and Auchus 2007).

Considering now the context of intracrinology and since DHEAS is the predominant precursor in circulation, the first step in using it as a template for estrogen production is the de-sulfation of the conjugated sulfate moiety by steroid sulfatase (STS), which is reported to be expressed in up to 90% of breast carcinomas. Following this and prior to aromatization, there's the conversion to androstenedione by 3β-HSD, which moves the double bond from the second carbon ring to the first one in an irreversible manner (McNamara and Sasano, 2014).The synthesis of estrogens from androstenedione (and testosterone) is accomplished by the aromatase enzyme, which will be further focused on during this section.

Other enzymes, such as 17β-hydroxysteroid dehydrogenase (17β-HSD) isozymes, steroid sulfatase (STS) and estrogen sulfotransferase (EST) also play key roles in obtaining bioactive E2. 17β-HSD enzymes act by altering the functional group at the carbon-17 position of the steroid back-bone structure (Simpson 2002). For both androgens and estrogens, the presence of a hydroxyl group (-OH) is generally associated with a more potent steroid and the presence of a ketone group (=O) with a less potent one. Type 1 leads to the potentiation of estrogens and type 5 to that of androgens. Type 2 is associated with the de-potentiation of both androgens and estrogens. 17βHSD1 was reported in up to 60% of breast cancer cases and associated with adverse clinical outcome for the patients (McNamara and Sasano, 2014; Sasano *et al.*, 2009). It is also important to note that the great majority of circulating E1 is in a sulfated form (E1-S) and is hydrolysed by STS to E1, while EST sulfonates estrogens to biologically inactive estrogen sulfates (Knower et al. 2013; McNamara and Sasano 2014).

Increased intra-tumoral expression of the enzymes involved in estrogen synthesis is considered to result in increased tissue concentrations of estrogens in clinical settings of breast carcinoma (Sasano et al. 2009).

Aromatase

Aromatase catalyses the final and rate-limiting step of estrogen biosynthesis and is localized in the endoplasmic reticulum of estrogen-producing cells. The main sites of aromatase expression in women are the ovarian granulosa cells, placental syncytiotrophoblast, adipose and skin fibroblasts, bone (osteoblasts and chondrocytes) and brain (Bulun et al. 2009; Nelson and Bulun 2001; Sanderson 2006).

Aromatase is encoded by the *CYP19A1* gene, located on chromosome 15, band q21 of the human genome. The full length of *CYP19A1* is 123 kilo-bases (kb), of which the coding region accounts for approximately 30 kb. The upstream 93 kb contains nine tissue-specific promoters that control the highly tissue-specific expression of *CYP19A1* in sites of estrogen production in a signaling pathway-specific manner (Figure 4). Promoters are transcribed and spliced into a common linkage immediately upstream of the ATG translational start site, resulting in the same aromatase protein. In normal human breast tissue, up to 50% of aromatase transcripts are derived from the distal promoter I.4 (PI.4). The remaining transcripts are derived from the combined contribution of promoter I.3 (PI.3) and promoter II (PII). However, in the presence of a tumor, there is a significant up-regulation of PI.3 and PII *CYP19A1* transcripts, accounting for up to 80% of total transcripts. Transcripts of promoter I.7 (PI.7) are also detected in tumor tissue. This promoter switching results in an

overall 3 to 4-fold increase in aromatase transcripts in the tumor-bearing breast (Bulun et al. 2009; Richards and Brueggemeier 2003; To et al. 2014).

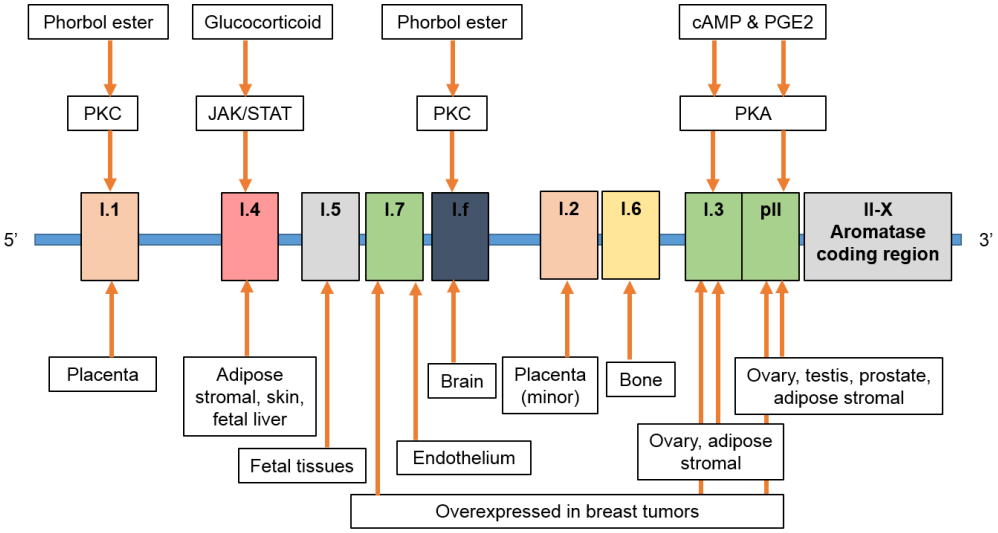

Figure 4. Promoters and signaling pathways involved in the tissue-specific regulation of human aromatase expression (adapted from (Sanderson 2006; To et al. 2014)).

Previous IHC studies have detected aromatase in both stromal (fibroblasts and adipocytes) and carcinoma cells, with biochemical studies showing that expression of the enzyme is greater in the stromal compartment (Richards and Brueggemeier 2003; Sasano et al. 2009). Also, aromatase activity of breast adipose tissue was higher in tissue obtained from sites close to the tumor than in tissue isolated from sites distal to the tumor (Nelson and Bulun 2001).

In adipose stromal cells, glucocorticoids, together with interleukin-6 (IL-6), give rise to activation of promoter I.4, whereas treatment with cyclic adenosine monophosphate (cAMP) analogues or prostaglandin E2 (PGE2) switches the promoter use to I.3 and II (Nelson and Bulun 2001). Besides, activity of PI.4 in *in vitro* BAFs can also be induced by the effects of other cytokines such as tumor necrosis factor α (TNF-α), oncostatin M (OSM) and IL-11, alongside the synthetic glucocorticoid dexamethasone (DEX), via the Jak/STAT pathway (To et al. 2014).

Previous studies demonstrated that breast carcinoma cells secrete various factors, which are known to induce aromatase expression in adipocytes and/or fibroblasts, thus establishing a particular carcinoma-stromal interaction. Several key regulatory elements have been identified within the PI.3/PII region and the hypothesized major tumor-derived factor is PGE2. PGE2, produced by the cyclooxygenase (COX) isozymes, binds to four G-protein coupled receptors EP1-4, all of which have been linked to various aspects of breast cancer pathology. Their activation leads to an increase in cAMP levels and consequent

activation of the protein kinase A (PKA) and C (PKC) pathways. PKA activation phosphorylates the cAMP-responsive element binding protein 1 (CREB1), allowing it to translocate into the nucleus and bind to both proximal and distal cAMP response elements (CREs) within PI.3/PII (Bulun et al. 2009). Specifically, Richards et al (2002) demonstrated that PGE2 acts in an autocrine and paracrine way to increase aromatase expression and, later on, the same authors established this effect as dependent on PGE2 receptors EP1 and EP2 (Richards and Brueggemeier 2003).

This carcinoma-stromal interaction goes even further. Both aromatase activity and mRNA levels in breast adipose tissue primarily reside in undifferentiated fibroblasts, rather than in mature adipocytes (Bulun et al. 2009; Nelson and Bulun 2001). Malignant epithelial cells secrete large amounts of the anti-adipogenic cytokines TNF and IL-11, which inhibit the differentiation of fibroblasts to mature adipocytes, at the same time that they stimulate aromatase expression in these cells via IL-6 and PGE2 (Figure 5). Thus, large numbers of estrogen-producing adipose fibroblasts are maintained proximal to malignant cells, allowing the creation of a vicious cycle of intra-tumoral estrogen overproduction in the breast (Sanderson 2006; Sasano et al. 2009; Bulun et al. 2009).

Expression via PI.3/PII is also significantly higher in the breast adipose tissue of women carrying mutations of BRCA1, suggesting that BRCA1 has a repressive effect on aromatase expression and higher aromatase levels contribute to the increased risk of breast cancer development in these women (Bulun et al. 2009; To et al. 2014).

Epigenetic mechanisms also seem to play a role in modulating aromatase expression. For instance, Demura et al (2008) showed that CpG methylation status within the cAMP response element (CRE) of PII modulates *CYP19A1* expression in human skin adipose fibroblasts (Demura and Bulun 2008).

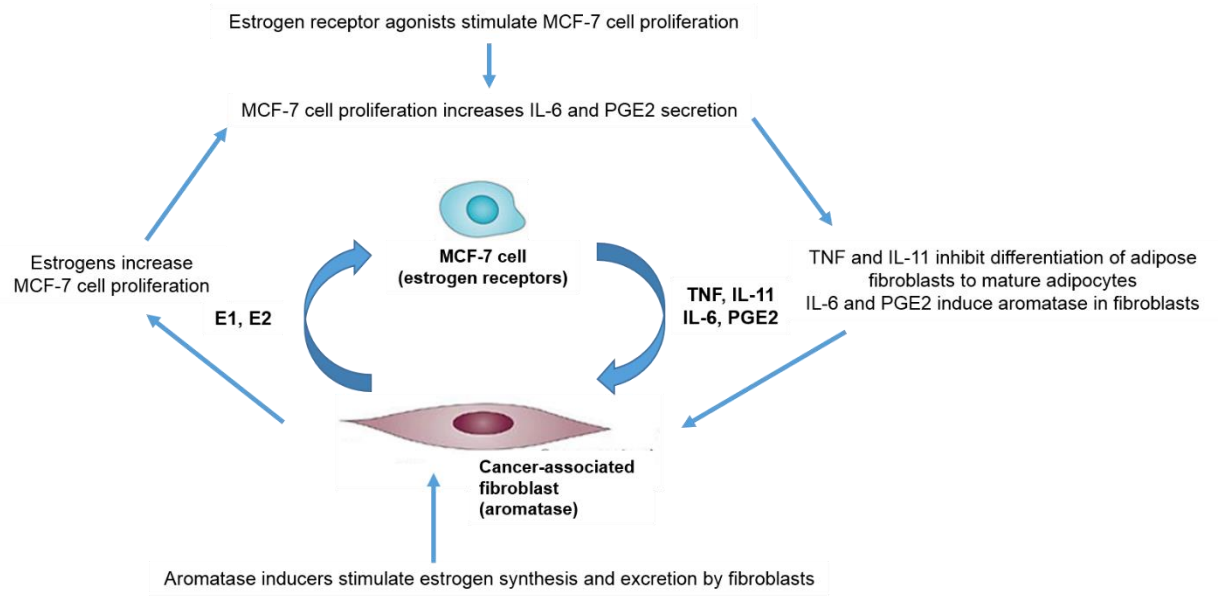

Figure 5. A simplified representation of the interaction between aromatase inducers and estrogen receptor agonists in a co-culture of MCF-7 cancer cells and primary human mammary fibroblasts (adapted from (Sanderson 2006; Bulun et al. 2009))

The aromatase enzyme complex is comprised of two polypeptides: aromatase cytochrome P450 (P450arom) and a flavoprotein, NADPH-cytochrome P450 reductase (CPR). The catalytic portion of P450arom contains a heme group as well as a steroid binding site. This complex catalyses the rate-limiting and final step of estrogen biosynthesis, the aromatization of androgens to estrogens, leading to the formation of the phenolic A ring which is characteristic of biological estrogens. It does so via three oxidation reactions of the androgens A ring, following electron transfer from CPR to aromatase. The first and second hydroxylations occur at the 19-methyl group of androgens, while the third hydroxylation results in the cleavage of the C10−C19 bond and the aromatization of the A ring. This last step is unique to aromatase, while the others are common to all cytochromes P450 (Chumsri et al. 2011; Hong et al. 2009; To et al. 2014).

Several laboratories have reported the purification of aromatase from human placenta and recombinant expression systems. However, attempts to crystallize either form of aromatase turned out unsuccessful. Only in 2009 did Ghosh et al successfully crystallize the aromatase enzyme (purified from term human placenta) (Figure 6) and provided a structural basis for the specificity to androgens (Ghosh et al. 2009).

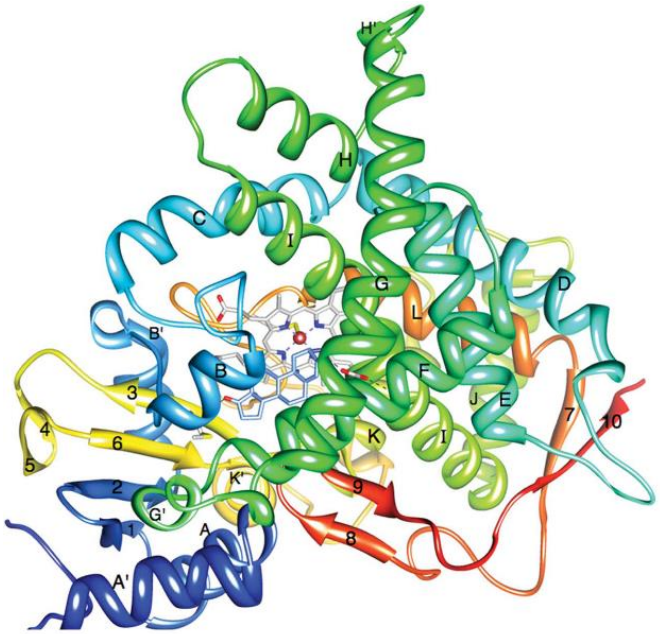

Figure 6. The structure of aromatase. A ribbon diagram showing the overall structure. The N terminus, starting at residue 45, is coloured dark blue and the C terminus ending at residue 496 is coloured red. The α-helices are labelled from A to L and β-strands are numbered from 1 to 10. The haem group, the bound androstenedione molecule at the active site and its polar interactions are shown (Ghosh et al. 2009).

Intratumoral production of estrogen in breast cancer is actually an intricate system that can be modulated at many different levels, including (1) the availability of potent circulating steroid templates, such as DHEA, for the generation of estrogens; (2) the expression levels of enzymes required to make these modifications; (3) the interplay of both stromal and epithelial components and (4) the interaction of steroid pathways with others involved in cancer progression (McNamara and Sasano 2014).

Hence, a number of diverse mechanisms, for instance, decreased adipogenic differentiation leading to accumulation of adipose fibroblasts surrounding breast carcinomas, increased production of PGE2 that stimulates aromatase expression in these fibroblasts or deficiency of a transcriptional suppressor of an aromatase promoter, can cause local or systemic estrogen excess, contributing to tumor growth and pathology (Bulun et al. 2009).

1.2.2. Estrogen Receptor (ER) Signaling Pathway

ER belongs to a superfamily of nuclear receptors that work as transcription factors. ERα and ERβ are produced by distinct genes located on chromosomes 6 and 14, respectively. Both receptors are present in normal breast tissue, but only ERα is associated with tumorigenesis and tumor progression, while ERβ function in breast cancer is still unclear.

Despite this, some studies have described ERβ as presenting an opposite effect to ERα, inhibiting the ability of estrogens to stimulate proliferation. The relative expression levels of these receptors will affect cellular responsiveness to estrogens (Garcia-Becerra et al. 2012; Riggs and Hartmann 2003). Both receptors share a common structural architecture, being composed of six domains, designated A–F (Figure 7). The A/B domain contains the activation function 1 (AF-1), responsible for the ligand-independent transcriptional activity of ER; the C domain, known as the DNA-binding domain (DBD), plays an important role in receptor dimerization and binding to specific DNA sequences; the D domain includes a nuclear localization signal; the E domain, referred to as ligand-binding domain (LBD), consists of a second nuclear localization signal, a dimerization site and a twelve-helix region involved in ligand binding, at the same time it harbors the activation function 2 (AF-2), responsible for the ligand-dependent activation of ER; lastly, the F domain, located at the C-terminal, is a small region that modulates both AF-1 and AF-2, although it is unnecessary for transcriptional activation (Garcia-Becerra et al. 2012; Musgrove and Sutherland 2009; Osborne et al. 2000; Osborne and Schiff 2005).

Estradiol controls proliferation and survival of breast cancer cells. This action is attributed to regulation of gene transcription, as well as to extra-nuclear and membrane-mediated signaling events (Castoria et al. 2010; Musgrove and Sutherland 2009).

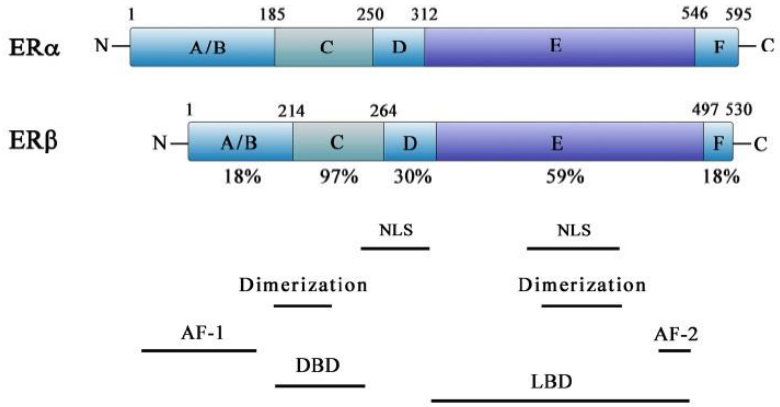

Figure 7. Schematic representation of functional domains of human ERα and ERβ (Garcia-Becerra et al. 2012).

ERα is associated to cell proliferation and survival through two distinct mechanisms: genomic and non-genomic signaling pathways. ER signaling pathway is initiated by ligand binding to the receptor. The binding induces a conformational change and dissociation of its chaperon proteins, leading to receptor dimerization and translocation to the nucleus. This ligand-ER complex binds to the consensus sequence estrogen-response element (ERE),

directly (classical genomic pathway) or indirectly (non-classical genomic pathway) through protein-protein interactions with activator protein 1 (AP-1) or specificity protein 1 (SP-1) sites in the promoter region of target genes (via Fos and Jun transcription factors), resulting in recruitment of co-regulatory proteins (co-activators or co-repressors), which can either enhance or repress ER transcriptional activity depending on the specificity of the ligand (Figure 8) (Arpino et al. 2008; Garcia-Becerra et al. 2012; Osborne et al. 2000; Jordan 2004). Proteins encoded by this later group of genes include insulin-like growth factor receptor 1 (IGFR1), cyclin D1, myc and the anti-apoptotic factor Bcl-2 (Arpino et al. 2008; Osborne and Schiff 2005). In particular, the transcriptional activity of ER is enhanced by the binding of co-activators such as members of the p160 family of nuclear receptor co-activators (e.g., nuclear receptor co-activator 1 [NCOA1 or SRC-1], NCOA2 and NCOA3 [AIB1/SRC-3]). These proteins enhance ER-driven transcription by different mechanisms, including recruitment of histone acetiltransferases that modulate the chromatin structure at the promoter site (Arpino et al. 2008).

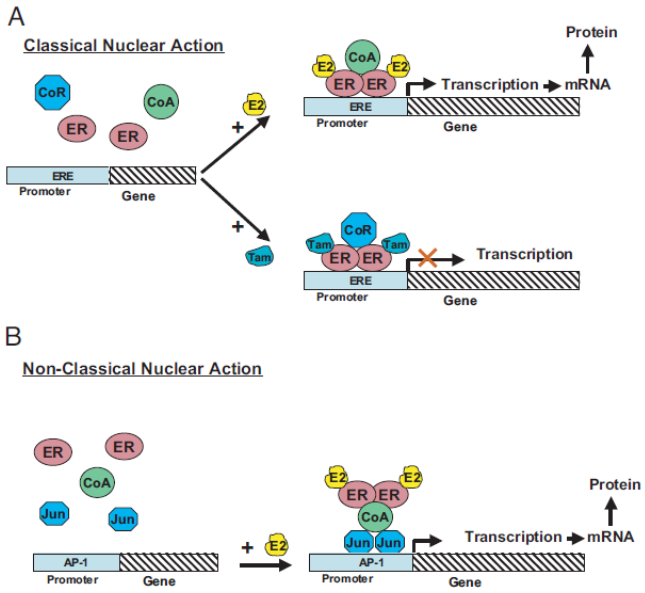

Figure 8. Nuclear genomic ER activity (Arpino et al. 2008).

Estrogens can also produce quick responses that are often non-genomic. These are mediated via ERs localized either near or at the plasma membrane. The plasma membrane ER may interact with many other proteins, including adaptor proteins, G-proteins, Src, growth factor receptors (EGFR, IGFR1, HER2), cytoplasmic kinases (MAPKs, PI3K, AKT), and signaling enzymes (adenylyl cyclase, nitric-oxide synthase), mediating mechanisms of cell survival and proliferation (Figure 9) (Garcia-Becerra et al. 2012; Osborne and Schiff 2005)

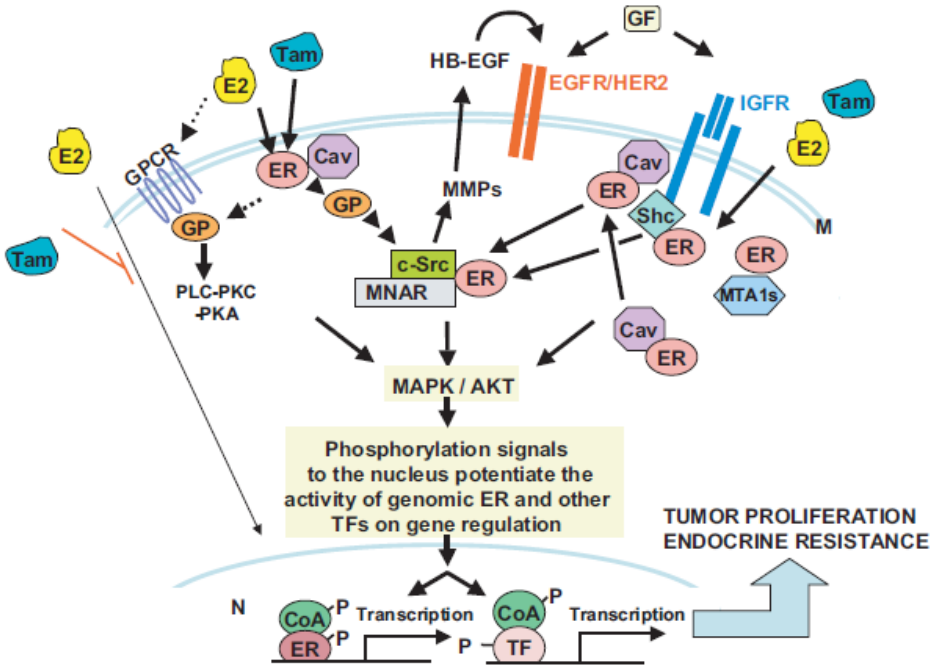

Figure 9. Integration of genomic and non-genomic/rapid ER signaling and its crosstalk with growth factor receptor and cell kinase pathways in endocrine resistance: a working model (Arpino et al. 2008).

Both genomic and non-genomic pathways interact with each other. While nuclear ER induces the expression of transforming growth factor α (TGFα) and amphiregulin, both these are able to bind and stimulate EGFR or EGFR/HER2 and, consequently, activate MAPK and AKT. On the other hand, membrane ER can bind to caveolin 1 and activate specific G proteins and Src, which activates matrix metaloproteinases that cleave transmembrane precursors of heparin binding-EGF (HB-EGF), an EGFR ligand. In addition, several cytokines, growth factors, EGFR ligands, IGF1R and pathways such as MAPK/ERK, PI3K/AKT and p38 MAPK phosphorylate ER at key positions in the AF-1 and other domains, leading to ligand-independent activation and eliciting ER genomic pathway (Figure 9) (Arpino et al. 2008; Garcia-Becerra et al. 2012; Osborne et al. 2000; Osborne and Schiff 2005).

1.3. ENDOCRINE THERAPIES

Endocrine treatment is the first and oldest targeted therapy in breast cancer and considered a standard adjuvant therapy in all patients with endocrine-responsive tumors. The introduction and subsequent evolution of many endocrine agents since the 1970s (Table 2) has transformed the treatment of women with breast cancer, leading to a more favourable prognosis and improved patient's quality of life (Sainsbury 2013). Current endocrine therapies include tamoxifen, fulvestrant and aromatase inhibitors (AIs) (Palmieri et al. 2014).

Table 2. Overview of the main milestones in the development of endocrine therapy for breast cancer since the 1970s (adapted from Sainsbury, 2013)

1977	Tamoxifen approved for treatment of post-menopausal women with advanced breast cancer (ABC)
1985-1990	Tamoxifen approved as adjuvant treatment for post-menopausal women with early breast cancer (EBC)
1989	Tamoxifen approved for pre-menopausal women with ABC
1995	Anastrozole approved for treatment of post-menopausal women with ABC after progression following tamoxifen
1997	Letrozole approved for treatment of post-menopausal women with ABC after progression following anti-estrogens
1998-2007	Tamoxifen approved for reduction of contralateral breast cancer/prevention
2000	Anastrozole approved as first-line treatment of post-menopausal women with ABC or metastatic breast cancer (MBC)
2001	Letrozole approved as first-line treatment of post-menopausal women with MBC
2002	Fulvestrant approved for treatment of post-menopausal women with MBC and progression following anti-estrogens. Approval of 500 mg fulvestrant by EMA and FDA.
2004	Exemestane shown superior to tamoxifen for first-line treatment of ABC
2002 onwards	Benefits of AIs vs. tamoxifen as adjuvant therapy for post-menopausal women with EBC
2004 onwards	Benefits of switching from tamoxifen to an AI and from a non-steroidal AI to a steroidal AI in post-menopausal women with EBC
2005 onwards	Extended adjuvant therapy compared with no treatment reduces the risk of recurrence

In the St. Gallen consensus conference, the majority of the panel members rated tamoxifen as minimal standard in endocrine adjuvant therapy for pre-menopausal women. On the other hand, the panelists spoke for the combination of ovarian function suppression (OFS) with aromatase inhibition as a valid option in case of contraindication for tamoxifen.

As for post-menopausal patients, some of these can be adequately treated with tamoxifen alone. If AIs are preferred, they need to be started upfront, at least in high-risk patients. A majority of the panelists argued for replacing upfront AIs by tamoxifen after 2 years (Goldhirsch et al. 2013).

In ER+ tumors, late recurrences can occur up to 20 years or more after diagnosis despite adjuvant endocrine treatment (Ignatiadis and Sotiriou 2013). These are largely incurable disease states, but responses can be achieved with first-line endocrine therapies in around 30% and clinical benefit (response or stable disease for at least 6 months) in around 50% of patients (Schiavon and Smith 2013). In this context, chemotherapy is added on the basis of the estimated risk for relapse. According to the St. Gallen consensus conference, adding chemotherapy should be considered in patients with an intermediate or high risk for recurrence. Regarding patients previously treated with endocrine therapy, apart from the type used, the disease-free interval (DFI) as well as the site of relapse are essential in determining the choice of first-line therapy, at the time of relapse. In cases of a long DFI, no or limited visceral relapse and slowly progressive disease, first-line hormonal therapy should be offered. In cases of post-menopausal patients treated with adjuvant tamoxifen, a third-generation AI or fulvestrant can be recommended. Contrarily, if DFI<2 years and there are visceral metastases, chemotherapy can be recommended as first-line therapy. (Guarneri and Conte 2009)

1.3.1. Selective Estrogen Receptor Modulators (SERM) and Down-regulators (SERD)

Tamoxifen (Figure 10), a selective estrogen receptor modulator (SERM), is converted by cytochrome P450 enzymes to active metabolites (including N-desmethyltamoxifen and 4-hydroxytamoxifen), which bind to the ER, thus inhibiting the expression of many estrogen-regulated genes required for tumor growth (Sainsbury 2013). Results of *in vitro* studies have implicated multiple CYP isoforms, such as CYP3A and CYP2D6, in the biotransformation of tamoxifen to its primary metabolites (Jin et al. 2005).

The essential structural determinant of the SERM molecule is a correctly positioned alkylaminoethoxyphenyl side chain that interacts with asp351 in ERα to modulate anti-estrogenic action through co-repressor binding to the SERM-receptor complex. This

interaction allosterically modulates the estrogenic and anti-estrogenic action of tamoxifen. The net response of SERMs in a cell depends, however, on the particular balance of co-activators and co-repressors present in cells (Osborne et al. 2000).

Tamoxifen only blocks the transcriptional activating function 2 (AF-2) of the ER. This allows activation of AF-1, ER dimerization and ER binding to estrogen-regulated genes (Figure 11b). Therefore, tamoxifen only partially inactivates ER-regulated transcription (Dowsett et al. 2005).

Tamoxifen is mainly cytostatic and slows the proliferation of breast cancer cells by inhibiting their progression from the G1 phase of the cell cycle; it also induces apoptosis *in vitro* (Riggs and Hartmann 2003).

Although tamoxifen therapy is related to secondary benefits, such as improvement in lipid profiles and increases in bone mineral density in post-menopausal women, it is also associated with several adverse events, including rare venous thrombosis and higher risk for endometrial cancer and, more commonly, hot flashes (Jin et al. 2005).

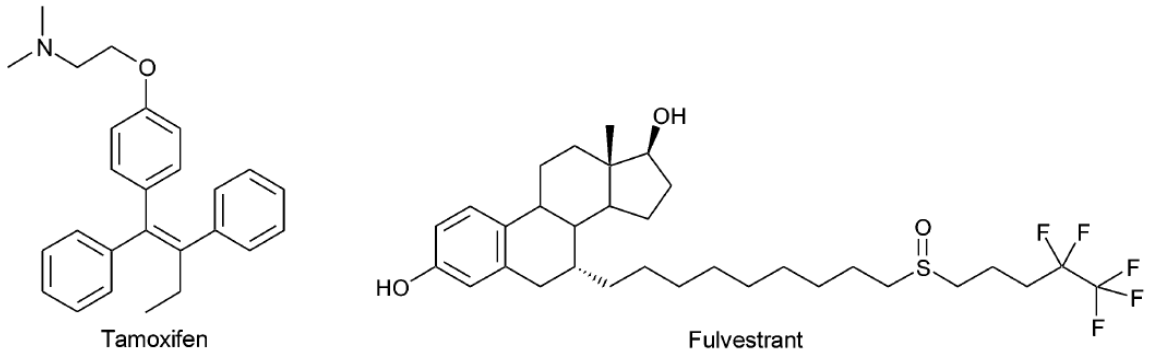

Figure 10. Chemical structures of tamoxifen and fulvestrant (adapted from (Salvador et al. 2013)).

Fulvestrant (Figure 10) is a 7α-alkylsulphinyl analogue of 17β-estradiol (E2) that acts as an ER antagonist, competitively inhibiting binding of E2 to the ER (Dowsett et al. 2005; Krell et al. 2011). In contrast to estradiol (Figure 11a) and tamoxifen (Figure 11b), fulvestrant binding to the ER induces a conformational change within the receptor, which results in inhibition of receptor dimerization, reduced nuclear uptake of the drug-receptor complex and prevention of ER binding to estrogen-responsive genes. The half-life of the protein is reduced and the receptor is rapidly degraded by ubiquitin-proteosome complex, resulting in down-regulation of cellular ER levels. Furthermore, contrarily to tamoxifen, any fulvestrant–ER complex that enters the nucleus is transcriptionally inactive, because both AF-1 and AF-2 functions of ER are inactivated, resulting in complete abrogation of the transcription of ER-regulated genes (Figure 11c). Consequently, fulvestrant is not associated with estrogen

agonist activity, unlike tamoxifen (Ciruelos et al. 2014; Dowsett et al. 2005; Krell et al. 2011). Fulvestrant presents anti-proliferative activity, being able to increase the proportion of cells in the G0/G1 phase of the cell cycle and induce apoptosis (Ciruelos et al. 2014; Krell et al. 2011). Importantly, fulvestrant lacks cross-resistance with tamoxifen.

Fulvestrant is an option for the treatment of post-menopausal women with locally advanced or metastatic ER+ breast cancer, who relapse or develop progression on or after adjuvant endocrine therapy and it is a well-tolerated drug (Ciruelos et al. 2014; Krell et al. 2011). Prolonged exposure to fulvestrant via chronic administration is necessary for activity and, thus, several studies led to the development of a long-acting, intramuscular formulation of fulvestrant that gives adequate bioavailability and controlled release of the drug (Krell et al. 2011).

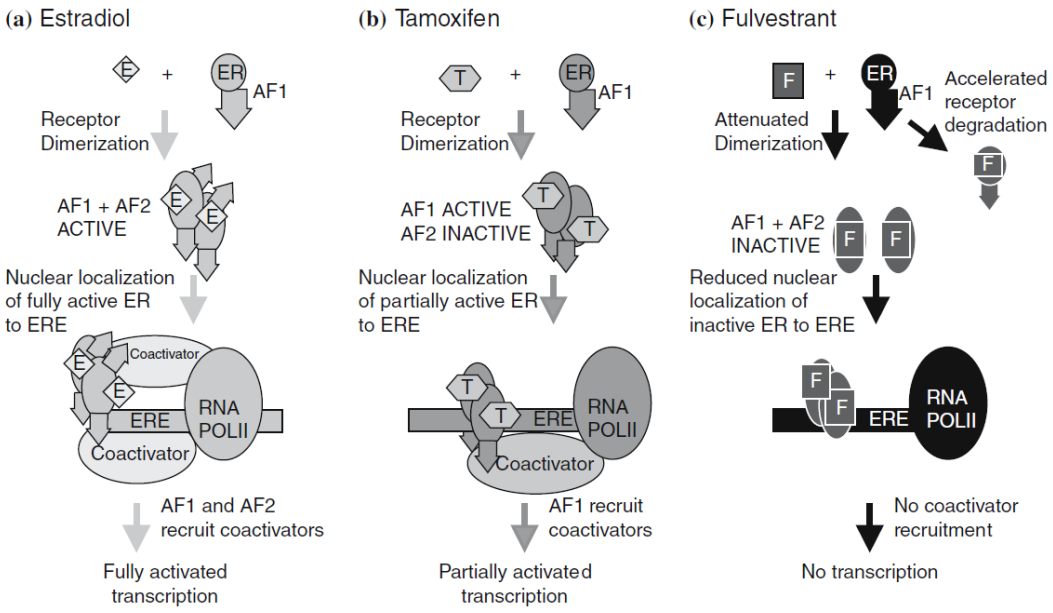

Figure 11. Mechanism of action of estradiol, tamoxifen and fulvestrant at the level of transcriptional regulation (Dowsett et al. 2005).

1.3.2. Aromatase Inhibitors (AIs)

Aromatase inhibitors (AIs) bind competitively to the aromatase enzyme, thus preventing the conversion of androgens to estrogen in peripheral tissues. The first-generation AI, aminoglutethimide, was effective in post-menopausal women with ABC, but it was used infrequently due to lack of selectivity and inhibition of other steroidogenic cytochrome P450-dependent enzymes (Hong and Chen 2006). Following first-generation AIs, second-generation AIs such as fadrozole and formestane showed promise, but they also influenced other steroidogenic pathways and required intramuscular administration, respectively. Thus, they have been surpassed by the development of third-generation AIs with increased potency, greater specificity and reduced toxicity (Figure 12) (Choueiri *et al.*, 2004; Hong and Chen, 2006; Sainsbury, 2013).

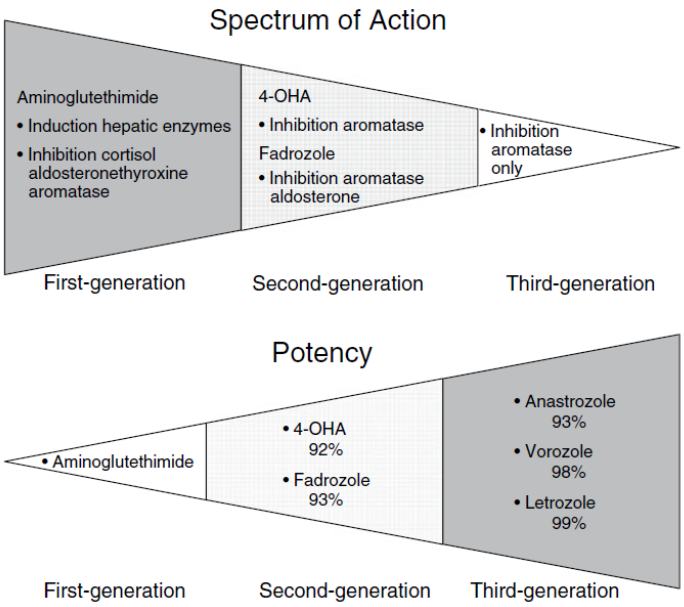

Figure 12. Spectrum of action of first- through third-generation AIs. The development of aromatase inhibitors (AIs) has culminated in agents with high specificity and potency for aromatase (Bhatnagar 2007).

Third-generation AIs (Figure 13) are orally administered and can be subdivided into steroidal agents (exemestane) and non-steroidal agents (anastrozole and letrozole). The improved efficacy and favourable tolerability profiles of the third-generation AIs compared with tamoxifen has resulted in their widespread use in the management of post-menopausal women with hormone-sensitive breast cancer in the advanced and adjuvant setting (Sainsbury 2013).

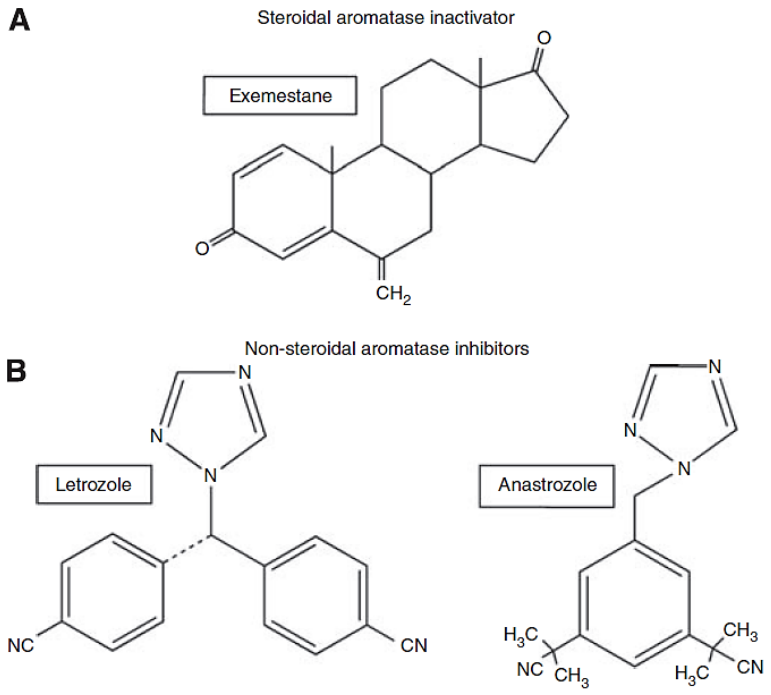

Figure 13. Chemical structures of currently used anti-aromatase compounds. (A) Steroidal aromatase inhibitors, exemestane. (B) Non-steroidal aromatase inhibitors, letrozole and anastrozole (Geisler 2011).

Anastrozole and Letrozole

Anastrozole is a potent and selective non-steroidal AI that binds reversibly to aromatase and fits into the substrate-binding site, such that azole nitrogens interact with heme prosthetic group. It is completely absorbed from the gastrointestinal tract and has a half-life, with 1 mg dose, of ca. 40.6 h. The drug is metabolized in the liver via *N*-dealkylation, hydroxylation and glucuronidation (Figure 14). Functional UGT1A4 polymorphisms might play a role in anastrozole metabolism (Turkistani and Marsh 2012). Anastrozole inhibits several CYP enzymes, but it does not cause clinically significant interactions with other CYP-metabolized drugs. A dosage of 1 mg/day is shown to inhibit *in vivo* aromatization by a mean of 96.7%. It has also been shown to suppress plasma E1, E2 and E1-S by ≥ 86.5%, ≥ 83.5% and ≥ 93.5%, respectively. The maximal suppression of plasma estrogens happens after 3-4 days of administration. The most common adverse effects include hot flashes, weakness, arthralgias/arthritis, generalized pain and headaches; mean serum total cholesterol can also increase; musculoskeletal disorders and fractures can also occur (Choueiri et al. 2004).

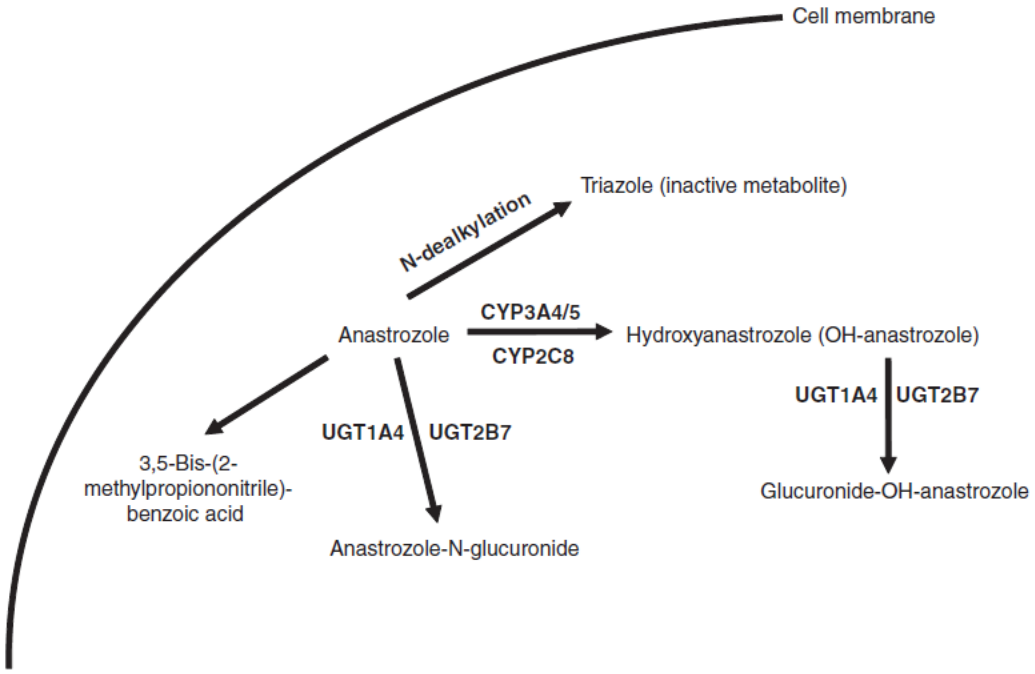

Figure 14. Summary of anastrozole metabolism (Turkistani and Marsh 2012).

Letrozole is the other non-steroidal AI. Like anastrozole, it binds reversibly to the heme group of aromatase and is able to decrease estrogen synthesis by > 98%. It has a minor effect on mineralocorticoid or glucocorticoid synthesis, unlike the first- and second-generation AIs. It is rapidly absorbed in the gastrointestinal tract and has a half-life of ca. 48 h. The major pathway for letrozole clearance is through renal excretion of its inactive metabolite (Figure 15). CYP2A6 genetic variants showed an 8.5-fold difference in letrozole metabolism, resulting in significantly higher plasma concentrations for patients with the slow or intermediate genotypes versus patients with the normal metabolizer genotype (Turkistani and Marsh 2012). Doses of 0.5 mg or higher were shown to suppress E2 and E1 below the limit of detection of several assays. Letrozole has been demonstrated to be a more potent suppressor of total-body aromatization and plasma estrogen levels compared to anastrozole. Its adverse effects are similar to anastrozole's (Bhatnagar 2007; Choueiri et al. 2004). MCF-7aro xenograft models demonstrate that both non-steroidal AIs are better than fulvestrant and tamoxifen in suppressing tumor growth, while letrozole is the only able to induce tumor regression (Bhatnagar 2007).

As to their biological effects, both anastrozole and letrozole have been shown to induce apoptosis of MCF-7aro cells via down-regulation of Bcl-2, up-regulation of Bax and activation of caspase-9, caspase-6 and caspase-7. Moreover, they can cause a cell cycle arrest, blocking the G1-S phase transition, following up-regulation of p53 and p21 proteins

and mRNA levels, alongside down-regulation of cyclin D1 and c-myc mRNA (Thiantanawat et al. 2003).

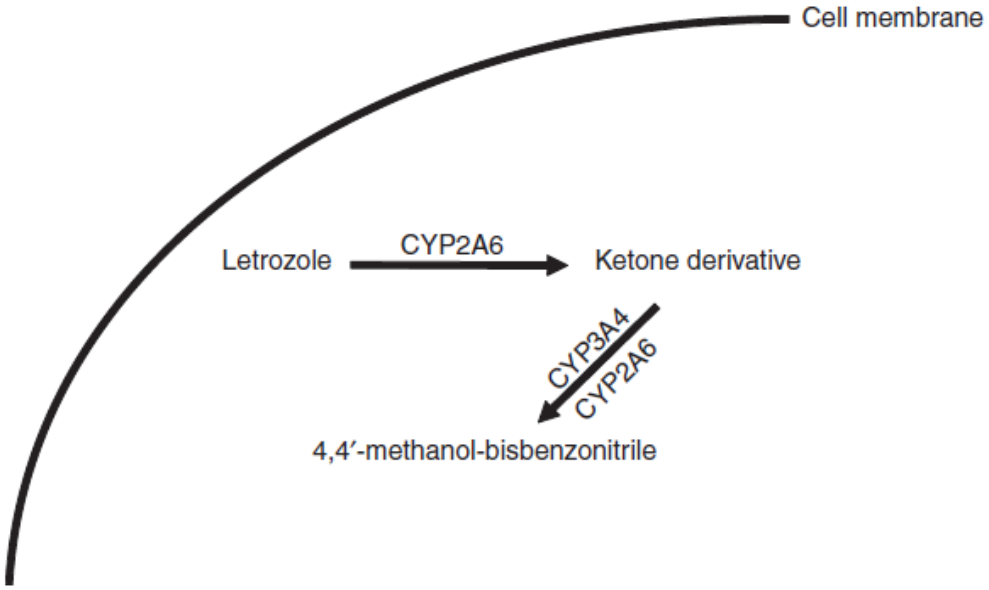

Figure 15. Summary of letrozole metabolism (Turkistani and Marsh 2012).

Exemestane

Exemestane is a unique steroidal AI, structurally related to androstenedione, which irreversibly inhibits aromatase, through a mechanism-based action. In the MCF-7aro cells, exemestane destabilizes aromatase, thus leading to its degradation by proteosomic enzymes (Miller et al. 2008). It is rapidly absorbed and is equally metabolized by the kidneys and the liver (Figure 16). UGT2B17 has an entire gene deletion polymorphism, which was reported to decrease exemestane glucuronidation process by 14-fold, resulting in altered metabolism and excretion (Turkistani and Marsh 2012). Doses of 25 mg/day have been shown to reduce whole-body aromatization by 98%, a value comparable to both anastrozole and letrozole. Its adverse effects are similar to those previously mentioned for the non-steroidal AIs (Choueiri et al. 2004).

This steroidal AI presents androgenic properties, since its main metabolite, 17-hydroxyexemestane binds with high affinity to the androgen receptor. Some pre-clinical studies might suggest that estrogen depletion following AIs treatment might sensitize cancer cells to the anti-proliferative effects of androgens (Miller et al. 2008). On the other hand, exemestane has been demonstrated to possess weak estrogen-like properties, which can possibly explain certain differences observed clinically between steroidal and non-steroidal AIs (Masri et al. 2009).

The biological effects of exemestane in breast cancer cells were described for the first time by Amaral et al. (2012). Exemestane was shown to induce a decrease in cell viability, mainly due to cell cycle arrest in G0/G1 and G2/M phases. Furthermore, autophagy and mitochondrial-mediated apoptosis occurred simultaneously; autophagy, in particular, was found to be a mechanism of cell survival (Amaral et al. 2012).

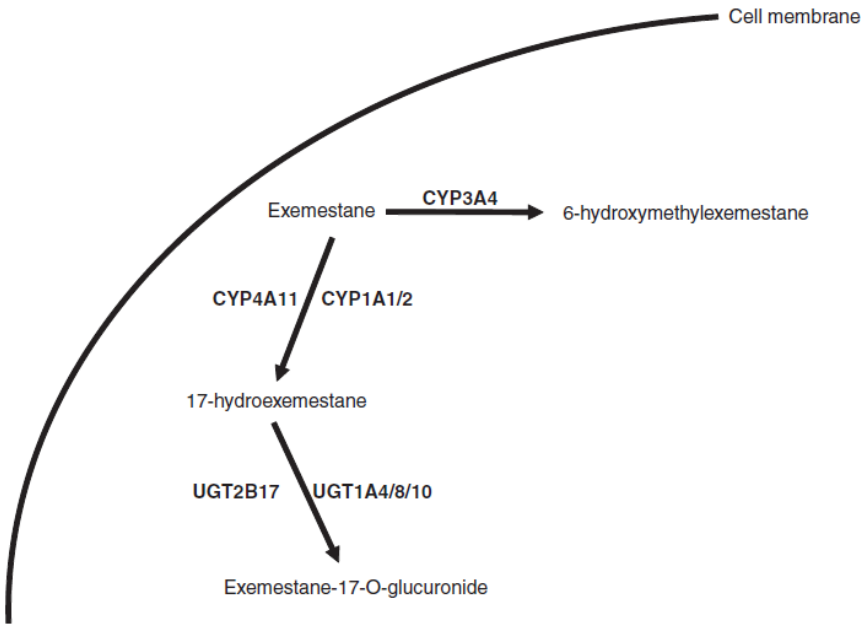

Figure 16. Summary of exemestane metabolism (Turkistani and Marsh 2012).

Exemestane was compared with tamoxifen in a randomized control trial conducted by the European Organization for Research and Treatment of Cancer (EORTC) Breast Cancer Cooperative Group (Paridaens et al. 2008). Median progression-free survival (PFS) was longer with exemestane (9.9 months) than with tamoxifen (5.8 months), but these early differences did not translate to a longer-term benefit in PFS, the primary study end point or OS.

The NCIC Clinical Trials Group (NCIC CTG) MA.27 study is the only one to date that has reported data regarding the efficacy and tolerability of 5 years of non-steroidal aromatase inhibition (NSAI) vs steroidal aromatase inhibition (SAI). In this open-label trial, 7576 women were randomized to either anastrozole or exemestane (Goss et al. 2013). At a median follow-up of 4.1 years, there was no difference in the primary end-point of event free-survival, 91% for exemestane and 91.2% for anastrozole (stratified hazard ratio, 1.02). Distant disease-free survival and disease-specific survival were also similar.

The Intergroup Exemestane Study (IES) was a switch study with women randomized after 2–3 years of tamoxifen to further tamoxifen or 2–3 years of exemestane. At a median follow-up of 91 months, the primary end-point disease-free survival (DFS) favoured the switch to exemestane (HR; 0.81). An improvement in overall survival (OS) was also demonstrated, again favouring the switch (HR, 0.86) (Bliss et al. 2012).

Finally, a phase II study evaluated exemestane in 241 patients who had progressed after treatment with a nonsteroidal AI (Lønning et al. 2000). A clinical complete response (CR) was observed in 3 (1.2%) patients and partial response (PR) in 13 (5.4%), giving an objective response rate (ORR) of 6.6%. Stable disease (SD) for at least 6 months was seen in 101 (41.9%) patients and the median time-to-progression (TTP) was 14.7 months.

1.4. MECHANISMS OF RESISTANCE TO ENDOCRINE THERAPIES

Despite the success in the management of ER+ breast cancer, using endocrine therapies, their efficacy is still limited by intrinsic or acquired therapeutic resistance. Therefore, there are two main aspects concerning this context: the establishment of biomarkers that are able to predict therapeutic response and the identification of novel therapeutic targets that allow to overcome endocrine resistance.

Figure 17 illustrates several mechanisms that can contribute to the onset of endocrine resistance, including deregulation of ER signaling and co-regulators associated with it, regulation of signal transduction pathways, increased receptor tyrosine kinase signaling, which leads to activation of ERK and PI3K pathways and deregulation of apoptotic machinery.

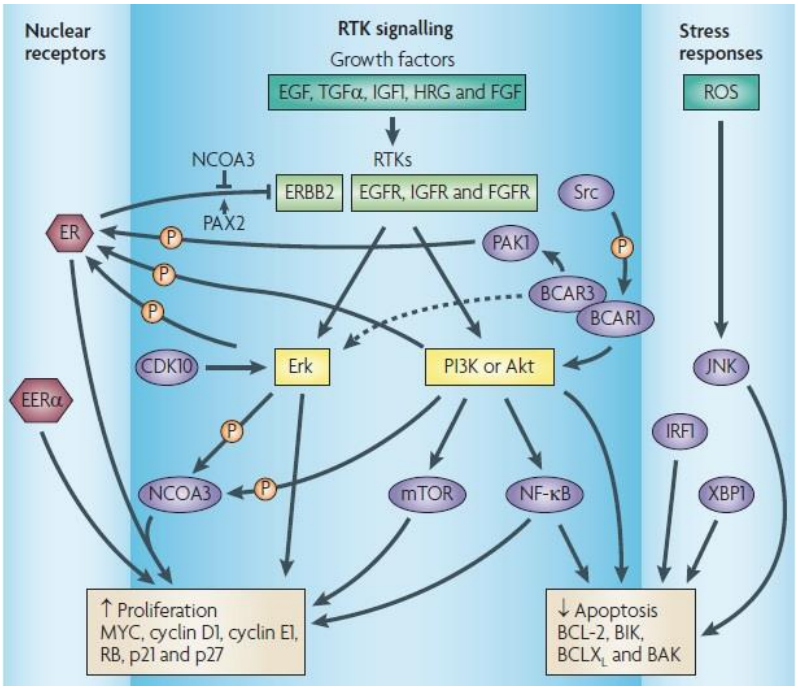

Figure 17. Molecular mechanisms of endocrine resistance (Musgrove and Sutherland 2009).

1.4.1. ER Signaling and Co-Regulators

ER co-activator AIB1, also known as SRC-3/NCOA3, is considered a proto-oncogene, being over-expressed in more than 30% of breast cancers and amplified in 5-10%. High levels of this protein, together with HER-2 over-expression, can stimulate tamoxifen's agonistic effects and contribute to endocrine resistance (Garcia-Becerra et al. 2012).

Harigopal et al. (2009) demonstrated that an up-regulation of AIB1 is correlated with a worse overall survival of patients. The authors also showed that breast cancer cell lines MCF7,

BT-474 and T47D exhibit an interaction between AIB1 and ER and a co-localization of both in the nuclei (Harigopal et al. 2009).

Additionally, Osborne et al. (2003) noticed that high levels of AIB1 were correlated with a worse disease-free survival in patients treated with tamoxifen in the adjuvant setting. More, a correlation between the protein and mRNA levels of AIB1 and HER-2 was identified and the authors believe there must be an increase in AIB1 protein levels so that HER-2 over-expression can have a meaningful impact in endocrine resistance (Osborne et al. 2003).

Yet, in another study, O'Hara et al. (2012) established a relationship between ER/AIB1 interaction and letrozole resistance. Their data supported the hypothesis that ligand-independent transactivation of target genes can contribute to tumor progression in AI resistance. Specifically, they found pS2 and Myc, ER target genes involved in tumor cell proliferation, to be up-regulated in this context; also, AIB1 expression was associated with enhanced growth factor signaling proteins, p-Src and p-ERK1/2 (O'Hara et al. 2012).

1.4.2. Crosstalk between ER and Growth Factor Receptors

As seen before, ER can be associated with a non-genomic pathway, where the receptor interacts with other proteins, namely receptor tyrosine kinases (RTK) (Figure 18).

Hurtado et al. (2008) evaluated the impact of the transcription factor PAX2, a repressor of *ErbB2* expression, in cell lines and primary tumors. In fact, previous analysis showed that the use of estrogens and tamoxifen induced a decrease in HER-2 expression. Therefore, the authors used a short interfering RNA (siRNA) specific to PAX2 gene to silence its transcription, which, together with tamoxifen or estrogen treatment, led to the loss of HER-2 repression and, thus, an increase in its levels at the cell membrane. On the other hand, if PAX2 was present, again, in the cells, after tamoxifen treatment, HER-2 levels would decrease. In primary tumors positive for PAX2, the relapse-free survival (RFS) was higher than for tumors negative for PAX2. Moreover, there's also a correlation between PAX2 and AIB1, since absence of PAX2 allows AIB1 to interact with the ER and, thus, induce expression of HER-2 (Hurtado et al. 2008).

Regarding another study, by Brodie et al. (2010), the use of MEK1/2 inhibitors and MAPK inhibitors can inhibit growth in long-term letrozole treated cells (LTLT cells), thus providing evidence that MAPK pathway has a functional role in letrozole resistance and in enhancing LTLT cell proliferation. Furthermore, ER expression was reinstated after inhibition of the MAPK pathway, suggesting a return to hormone sensitivity could be achieved by inhibiting MAPK pathway. The use of trastuzumab was able to also inhibit growth of LTLT cells, as well as pHER-2 and p-MAPK expression, which was accompanied by up-regulation of ERα.

Altogether, these data suggest that mechanisms of resistance to AIs include activation of RTK such as HER-2 and IGFR, which, in turn, suppresses ERα (Brodie et al. 2010).

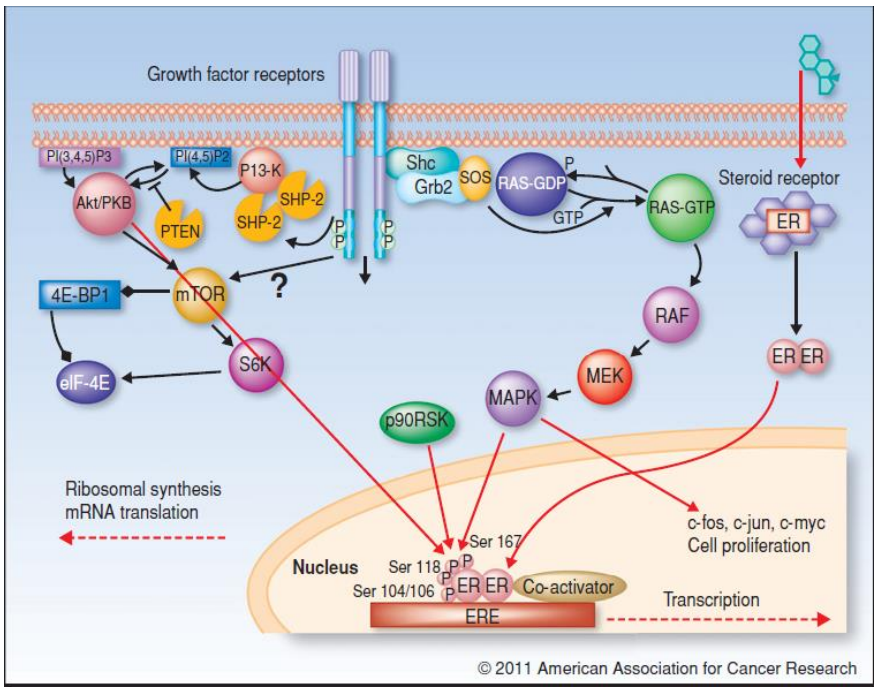

Figure 18. Signaling pathways that drive the growth of hormone therapy refractory cells (Brodie and Sabnis 2011).

1.4.3. Apoptosis and cell survival

As tumor growth reflects the balance between cell proliferation and cell death, deregulation of this balance can contribute to a change in the clinical setting.

There is cumulative evidence for the increased expression of anti-apoptotic molecules, namely Bcl-2 and Bcl-X_L and decreased expression of pro-apoptotic molecules, such as BAK, BIK and caspase-9, in weakened responses to tamoxifen. This can be a consequence of over-expression of RTK and increased non-genomic signaling from cytoplasmic ER (Musgrove and Sutherland 2009). Activation of the TNFα/Fas cell surface receptors leads to activation of caspase-8, which cleaves cytosolic BID, whose translocation to the mitochondria enables cytochrome *c* release and activation of Apaf-1 and caspase-9 (Figure 19). Cell survival signals, on the other hand, lead to phosphorylation of BAD, which is sequestered in the cytosol, preventing apoptosis (Gross et al. 1999; Parrish et al. 2013).

Cannings et al. (2007) have shown that patients whose tumors presented high levels of BAD had a significantly higher relapse-free survival, which is in line with the fact that high

levels of BAD promote blockade of Bcl-2/Bcl-X_L, allowing the formation of Bax-Bax homodimers and an enhanced apoptotic pathway (Cannings et al. 2007).

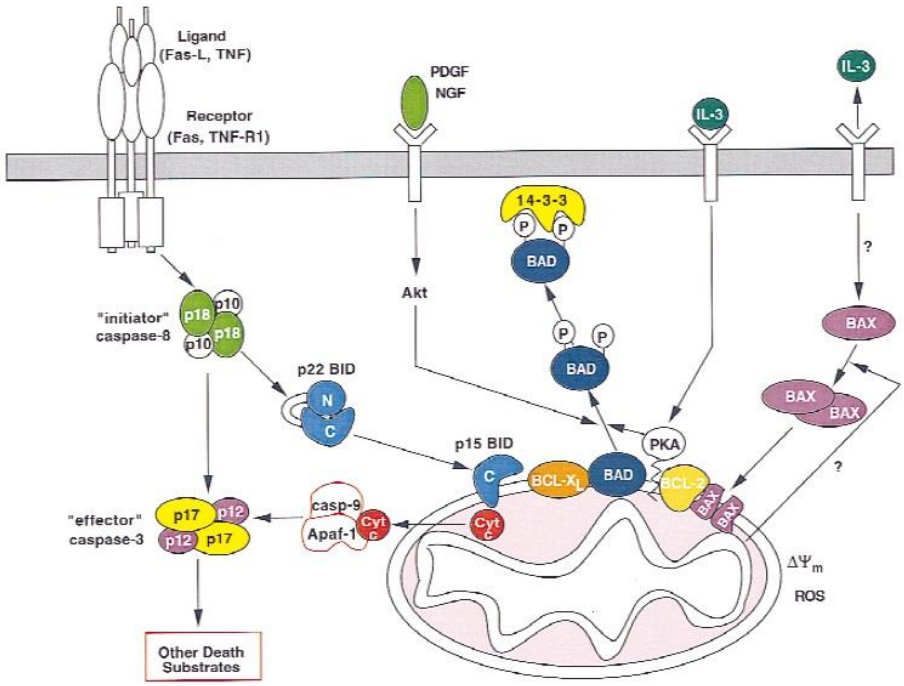

Figure 19. Model of apoptotic and survival signaling pathways involving the Bcl-2 family members (Gross et al. 1999).

1.4.4. Autophagy and Apoptosis

Autophagy is a homeostatic and evolutionary conserved process designed for degradation of cellular organelles and proteins and to maintain cellular biosynthesis during nutrient deprivation or metabolic stress. This process starts with the formation of double-membrane vesicles (autophagosomes), which fuse with lysosomes, where the sequestered content undergoes degradation and recycling (Figure 20). Autophagy can play a dual role, either as tumor suppressor or promoter of tumor cell survival. Complexes including the proteins from the Atg family start autophagy, integrating stress signals from mTOR complex 1. PI3K class III protein Vps34 forms a complex with Beclin-1, allowing the recruitment of other autophagy-related gene (Atg) products critical for autophagosome formation. In general, cellular stress leads to down-regulation of mTOR1 activity, thus triggering autophagy (Yang et al. 2011).

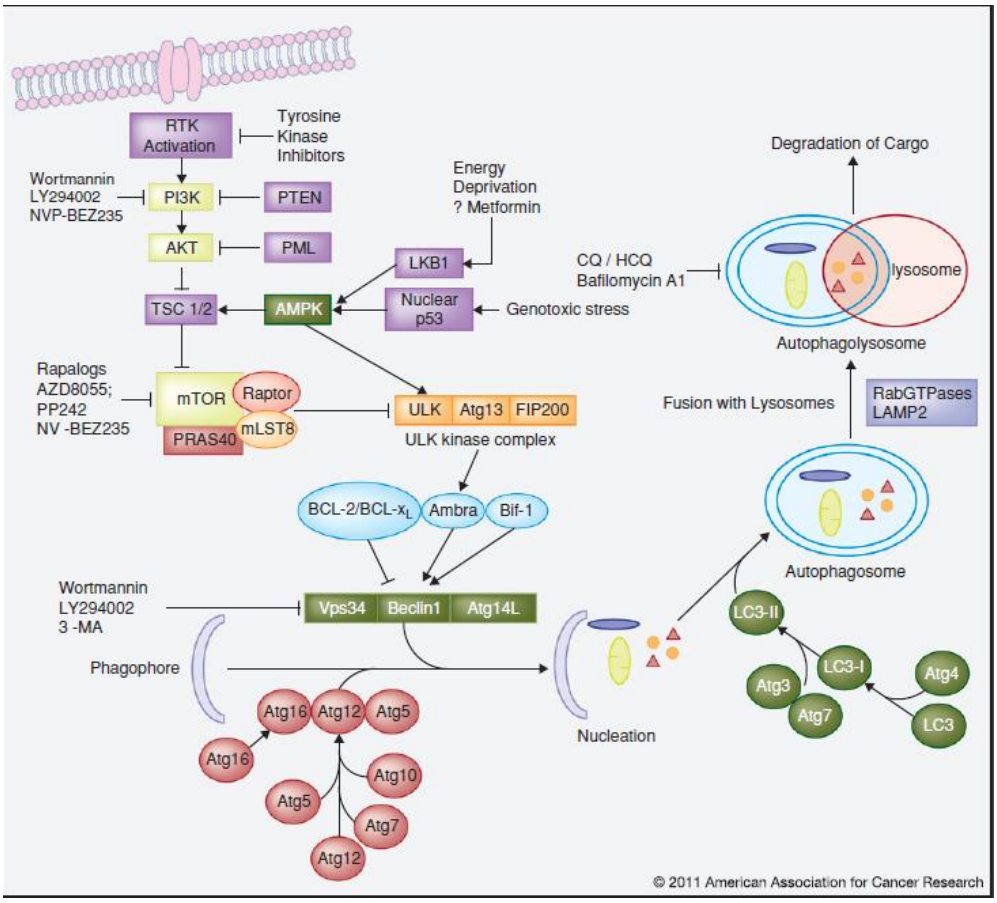

Figure 20. Overview of the autophagy pathway (Yang et al. 2011)

As a tumor suppressor mechanism, autophagy removes damaged organelles/proteins and limits cell growth and genomic instability. However, it can also act as a tumor cell survival pathway, conferring stress tolerance. Cytotoxic and metabolic stresses, including hypoxia and nutrient deprivation, can activate autophagy for recycling of ATP and maintenance of cellular biosynthesis and survival (Yang et al. 2011). In breast cancer cells subjected to exemestane treatment, autophagy has been shown to play a role as promoter of cell survival (Amaral et al. 2012). Thus, the concomitant use of autophagic inhibitors, such as 3-methyladenine (3-MA), allows for the suppression of the autophagic process and enhancement of apoptosis. The interplay between autophagy and apoptosis can be mediated, for example, by p62/SQSTM1, which bind to caspase-8, enabling its aggregation and activation and enhancing TRAIL-mediated apoptosis. On the other hand and since anti-apoptotic Bcl-2 family members are often over-expressed in a multitude of tumors, these can disrupt the autophagic function of Beclin-1, thus preventing autophagy (Yang et al. 2011). This interplay and mutual regulation of apoptosis and autophagy is a rather complex mechanism and its modulation may be the key to circumvent certain events in tumor cell behaviour.

AIMS

Despite the AIs efficacy in hormone-dependent breast cancer, they present two major drawbacks, namely acquired resistance and the side effect of bone loss, which emphasises the importance for searching for new potent AIs.

In addition, it is important not only to understand the cellular mechanisms by which AIs exert their effects, but also to identify the mechanisms of resistance associated. Therefore, the main aims of the present work can be listed as follows:

1) Discovery of new potent AIs in an ER+ breast cancer cell line, MCF-7aro.
2) Evaluate the biological effects and mechanisms associated, in MCF-7aro cells, namely analysis of apoptosis and cell cycle progression.
3) Evaluate the response of the cell line LTEDaro, which mimics a late-stage acquired resistance to endocrine therapies, to the new AIs and investigate the effect of autophagy, since it was described as being involved in cell resistance to exemestane treatment.

Chapter II

Materials and Methods

2.1. Materials

Eagles' minimum essential medium (MEM), fetal bovine serum (FBS), L-glutamine, antibiotic–antimycotic (10,000 units/ml penicillin G sodium, 10,000 mg/ml streptomycin sulphate and 25 mg/ml amphotericin B), Geneticin (G418), sodium pyruvate, trypsin and 3,3-dihexyloxacarbocyanine iodide [$DiOC_6(3)$] were supplied by Gibco Invitrogen Co. (Paisley, Scotland, UK). Testosterone (T), estradiol (E2), ethylenediaminetetraacetic acid (EDTA), dimethylsulfoxide (DMSO), paraformaldehyde, tetrazolium salt [3-(4,5-dimethylthiazol-2-yl)-2,5-difenyltetrazolium (MTT)], 3-methyladenine (3-MA), Hoëchst 33258, propidium iodide (PI), Triton X-100, DNase-free RNase A, staurosporine (STA), activated charcoal, dextran, carbonyl cyanide *m*-chlorophenylhydrazone (CCCP), 2',7'-dichlorodihydrofluorescein diacetate ($DCFH_2$-DA), phorbol 12-myristate 13-acetate (PMA) and acridine orange (AO) were from Sigma-Aldrich Co. (Saint Louis, USA). Cyto-Tox 96 nonradioactive cytotoxicity assay kit, Reporter Lysis buffer, Caspase-Glo® 9, Caspase-Glo® 8, Caspase-Glo® 3/7 luminometric assays were from Promega Corporation (Madison, WI, USA). [1β-^{3}H] androstenedione was obtained from Perkin-Elmer (Boston, MA, USA) and liquid scintillation cocktail Universol from ICN Radiochemicals (Irvine, CA, USA). Giemsa was from Merck Millipore (©Merck KGaA, Darmstadt, Germany).

2.2. Compounds under study

In this work, it was studied four steroidal AIs (Figure 21), 7α-allylandrost-4-ene-3,17-dione (**6**), 7α-allylandrost-4-en-17-one (**9**), 7α-allyl-3-oxoandrosta-1,4-dien-17β-ol (**10**) and 7α-allylandrosta-1,4-diene-3,17-dione (**12**), which were synthesized by the Centre for Pharmaceutical Studies (Pharmaceutical Chemistry group), Faculty of Pharmacy, University of Coimbra, according to what was previously reported (Varela et al. 2013). This series of compounds presents a common allyl substituent at the C7 position. Besides that, they all present a carbonyl at C3, except for AI **9** and a carbonyl at C17, except for AI **10**, which has a hydroxyl. Both AIs **6** and **9** have a double bond at C4-C5 and AIs **10** and **12** have two double bonds, at C1-C2 and C4-C5.

The stock solution of each steroid (20 mM) was prepared in 100% DMSO and stored at −20ºC. The stock solution of testosterone (T) and estradiol (E2) (10 mM) was prepared in absolute ethanol and stored at −20ºC. Appropriate dilutions were freshly prepared with medium, immediately prior to the assays and the final concentration of DMSO and ethanol in culture medium was less than 0.05% and 0.01%, respectively.

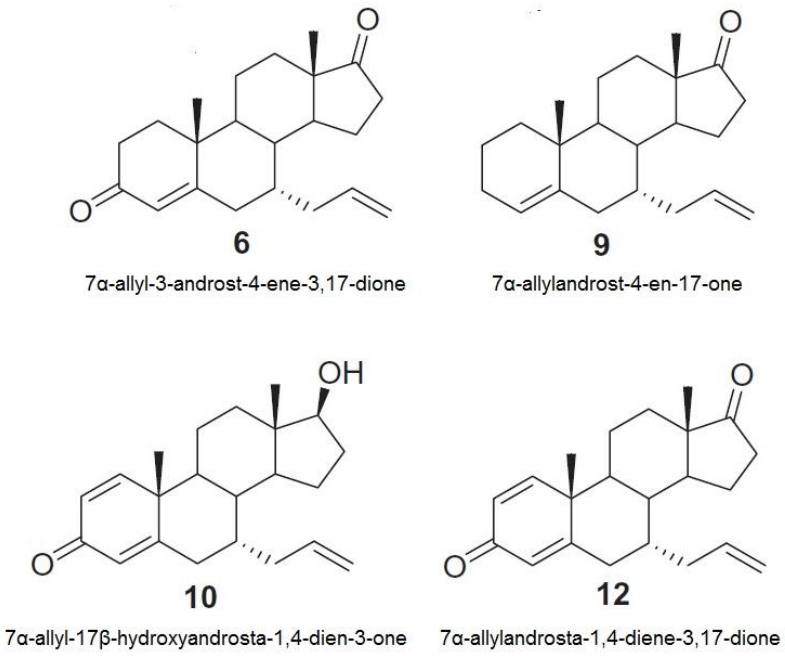

Figure 21. Compounds under study.

2.3. Cell culture

It was used an ER-positive aromatase-overexpressing human breast cancer cell line, **MCF-7aro**. This cell line was obtained from MCF-7 cells via a stable transfection with the human placental aromatase gene and Geneticin selection, as previously described (Zhou et al. 1990). The cells were maintained in Eagles' minimum essential medium (MEM) with phenol red, containing Earle's salts, 1 mmol/L sodium pyruvate, 1% penicillin–streptomycin-amphotericin B, 700 ng/ml Geneticin (G418) and 10% heat-inactivated FBS. In order to evaluate the biological effects of each steroid, 3 days before starting the experiments, cells were cultured in an estrogen-free MEM medium without phenol red, containing 5% charcoal pre-treated heat-inactivated fetal bovine serum (CFBS) plus 1 mmol/L sodium pyruvate, 2 mmol/L L-glutamine and 1% penicillin–streptomycin-amphotericin B, in order to avoid the interference of the estrogenic effects of phenol red and the steroids present in FBS (Berthois et al. 1986). MCF-7aro cells were treated with each steroidal AI and 1 nM of T, which was used as an aromatase substrate and proliferation inducing agent. As control, MCF-7aro cells were incubated with 1 nM of T.

The ER-negative human breast cancer cell line, **SK-BR-3**, was maintained in MEM with phenol red and Earl's salts, supplemented with 1 mmol/L sodium pyruvate, 1% penicillin–streptomycin-amphotericin B and 10% heat-inactivated FBS. Assays were carried out using the same medium and cells were treated with each AI. SK-BR-3 cells incubated without any of the AIs were used as control.

The long-term estrogen deprivation cells, **LTEDaro** cells, were generated by prolonged culture of parental MCF-7aro cells in steroid-depleted medium, as previously described (Masri et al. 2008). They were cultured in MEM without phenol red, supplemented with 10% charcoal pre-treated heat-inactivated fetal bovine serum (CFBS), 1 mmol/L sodium pyruvate, 2 mmol/L L-glutamine, 1% penicillin–streptomycin-amphotericin B and 700 ng/ml Geneticin (G418). Assays were carried out using the same medium and cells were treated with each AI. LTEDaro cells incubated without any of the AIs were used as control. MCF-7aro and LTEDaro cells were kindly provided by Dr. Shiuan Chen from the Beckman Research Institute, City of Hope, Duarte, CA, U.S.A.

The human foreskin fibroblasts cell line, **HFF-1**, was maintained in phenol red-free Dulbecco's Modified Eagle Medium (DMEM), supplemented with 10% heat-inactivated FBS, 1 mmol/L sodium pyruvate and 1% penicillin–streptomycin-amphotericin B. Assays were carried out using the same medium and cells were treated with each AI. HFF-1 cells incubated without any of the AIs were used as control.

All cell lines were regularly grown at 37ºC in 5% CO_2 atmosphere and medium plus compounds were changed every three days.

2.4. In cell aromatase assay

Aromatase activity and IC_{50} of each compound, **6**, **9**, **10** and **12**, in MCF-7aro cells, were determined by a modification of the method of Thompson and Siiteri (Thompson and Siiteri 1974) and Zhou et al. (Zhou et al. 1990). This assay uses [1β-^{3}H] androstenedione as substrate for the aromatase. When the aromatization reaction takes place, tritium is released into the medium as tritiated water (^3H_2O) and its quantification is a direct measure of estrogen synthesis and, thus, aromatase activity.

Briefly, MCF-7aro cells were cultured in 24-well plates (density of 5.0×10^5 cells/ml) with serum-free MEM with phenol red, until confluence. Then, the cells were cultured with the compounds at 10 µM, for aromatase activity screening, or at various concentrations (0.01–10 µM) for IC_{50} determination, plus 50 nM of androstenedione (30 nM of [1β-^{3}H] androstenedione and 20 nM of non-labelled androstenedione) and 500 nM of progesterone, at 37ºC during 1 h. The latter hormone allows the suppression of the 5α-reductase activity, which also uses androgens as substrates. Formestane at 1 µM was used as reference AI. After the incubation, the reaction was stopped by adding 100 µL of trichloroacetic acid 20%. The sample is collected into activated charcoal/dextran-containing tubes, resting for 1 h, at room temperature, to allow the sequestering of non-metabolized androstenedione and other steroid metabolites. Finished this period, samples were centrifuged (14,000 x g, for 10 min)

and each supernatant (ca. 500 µL) was transferred to new tubes containing activated charcoal/dextran, resting for 10 min. After new centrifugation (14,000 x g, for 10 min), the supernatant (ca. 300 µL) was transferred into tubes containing 3 mL of scintillation cocktail. The quantification of tritiated water was performed in a scintillation counter (LS 6500, Beckman Instruments, CA, USA), an instrument that detects and measures ionizing radiation. All experiments were carried out in triplicate in three independent experiments.

The cells contained in the 24-well plates were lysed, overnight, at room temperature, using 500 µL of NaOH 0.5 N, in order to determine the protein content, using the Bradford method.

2.5. Cell viability

To evaluate the effects of each steroid, **6**, **9**, **10** and **12**, in MCF-7aro, SK-BR-3, HFF-1 and LTEDaro cells' viability, 3-(4,5-dimethylthiazol-2-yl)-2,5-difenyltetrazolium (MTT) and lactate dehydrogenase (LDH) release assays were performed. MTT is a tetrazolium salt, which is reduced by mitochondrial reductases to a blue precipitate of formazan. Since only viable cells have functioning mitochondria, formazan is directly correlated with cell viability. On the other hand, LDH release assay relies on another enzymatic reaction, where a tetrazolium salt is converted by LDH to a red formazan product. The amount of colour formed is proportional to the number of lysed cells. LDH is a cytosolic enzyme that is released upon cell lysis; thus, this assay measures the cytotoxicity of compounds.

Cells were cultured in 96-well plates at a cellular density of 2.5×10^4 cells/ml (3 days) and 1×10^4 cells/ml (6 days), for all the cell lines, with different concentrations of each compound (1 – 50 µM).

MCF-7aro cells cultured in MEM without phenol red, containing 5% CFBS, were treated with 1 nM of testosterone (T), the aromatase substrate and proliferation inducing agent or with 1 nM of estradiol (E2), the product of aromatase.

LTEDaro cells were cultured in MEM without phenol red, containing 10% CFBS. MCF-7aro cells and LTEDaro cells treated with or without compounds **9**, **10** and **12** were also treated with the autophagic inhibitor 3-methyladenine (3-MA), at 1 mM.

SK-BR-3 cells were cultured in MEM with phenol red and HFF-1 cells in DMEM without phenol red, containing 10% FBS.

After each incubation, 20 µL of MTT (0.5 mg/ml) were added to each well and cells were incubated for 2 h 30 min, at 37ºC, in 5% CO_2. Following this, formazan was dissolved by adding 200 µL of DMSO:isopropanol mixture (3:1) and quantified spectrophotometrically at 540 nm.

LDH release was measured using CytoTox 96 nonradioactive cytotoxicity assay kit, according to the manufacturer's protocol.

All the assays were performed in triplicate in three independent experiments and results are expressed as a percentage of the untreated control cells. Absorbance was read in BioTek Power Wave XS.

2.6. Morphological studies

MCF-7aro cells were cultured in 24-well plates with 1 nM of T and 10 and 25 µM of each AI for 3 and 6 days (cellular density of 2.0×10^5 cells/ml and 1.0×10^5 cells/ml, respectively). After this incubation, cell morphology was evaluated by phase contrast microscopy, Giemsa and Hoëchst stainings. After AI treatment, cells were fixed with methanol (Giemsa staining) or 4% paraformaldehyde (Hoëchst staining).

For Giemsa staining, after treatment, cells were washed with PBS and fixed with 500 µL of methanol, for 25 min, in the cold. Following this, cells were washed with PBS and incubated with 500 µL Giemsa (dilution 1/10 in water), for 30 min; finished this, cells were washed with tap water, mounted with DPX mounting medium and observed under the microscope Eclipse E400, Nikon, Japan, equipped with image analysis software LeicaQwin.

For Hoechst staining, after the incubation, cells were washed with PBS and fixed with 500 µL of 4% fresh paraformaldehyde, for 30 min, in the cold. Following this, cells were washed with PBS and incubated with 600 µL of 0.5 mg/ml Hoechst 33258, for 20 min; after this, cells were washed with PBS and mounted with vectastain and nuclear morphology was examined under a fluorescence microscope (Eclipse Ci, Nikon, Japan), equipped with a blue excitation filter of 490 nm and a maximum transmission at 360/400 nm and processed by Nikon NIS Elements v4.0 image software.

2.7. Cell cycle analysis

The effects of each AI in cell cycle progression were evaluated by flow cytometry, using cell DNA content as basis.

MCF-7aro cells were cultured in 6-well plates (7×10^5 cells/ml) for 3 days in MEM without phenol red, with T and different concentrations of AIs (10 and 25 µM). After treatment, the non-adherent cells were collected to a tube and the attached cells were trypsinized and added to the content of the tube. Cells were then centrifuged (1200 x g, 5 min, 4ºC); following this, cells were ressuspended in PBS and fixed with ethanol 70%. Fixed cells were

centrifuged (1200 x g, 5 min, 4ºC), washed with PBS and stained with 0.5 mL of DNA staining solution (5 µg/mL propidium iodide (PI), 0.1% Triton X-100 and 200 µg/ml DNase-free RNase A in PBS), during 30 min, at room temperature. DNA content was analysed by flow cytometry, based on the acquisition of 20,000 events in a Becton–Dickinson FACS Calibur (San Jose, CA, U.S.A) equipped with CELLQuest Pro software. Detectors for the three fluorescence channels (FL-1, FL-2 and FL-3) and for forward (FSC) and side (SSC) scatter were set on a linear scale. Debris, cell doublets and aggregates were gated out using a two parameter plot of FL-2-Area versus FL-2-Width of PI fluorescence. Data were analysed using FlowJo Software (Tree Star, Inc). The anti-proliferative effects of each AI were indicated by the percentage of cells in G0/G1, S and G2/M phases of cell cycle. Assays were performed in triplicate in three independent experiments.

2.8. Analysis of apoptosis

In order to study the effects of AIs on cell death, the mitochondrial transmembrane potential ($\Delta\Psi_m$) and caspases activation were investigated, as well as the production of reactive oxygen species (ROS).

The $\Delta\Psi_m$ loss was studied by flow cytometry using 3,3'-dihexyloxacarbocyanine iodide [$DiOC_6(3)$]. This is a cell permeable cationic dye that is able to bind to mitochondria, since $\Delta\Psi_m$ is negative.

MCF-7aro cells were cultured in 6-well plates (7.0×10^5 cells/ml) and treated with each AI (10 µM) during 3 days. Adherent cells were trypsinized and, together with non-adherent cells, collected into tubes. Cells were centrifuged and washed with PBS. Following this, cells were incubated with 10 nM of $DiOC_6(3)$, for 30 min, at 37ºC. As a positive control, the mitochondrial depolarizing agent, carbonyl cyanide *m*-chlorophenylhydrazone (CCCP), was incubated with cells (10 µM), 5 min before adding $DiOC_6(3)$. After staining, cells were centrifuged and resuspended in 1 mL of PBS. PI at 5 µg/ml was added prior to FACS analysis, allowing the discrimination between live cells ($DiOC_6(3)^+/PI^-$), early apoptotic cells ($DiOC_6(3)^-/PI^-$) and late apoptotic/necrotic cells (PI^+). Detectors for FSC and SSC light scatter were set on a linear scale, whereas logarithmic detectors were used to measure $DiOC_6(3)$ at green fluorescence (FL-1) and PI at red fluorescence (FL-2 and FL-3). Flow cytometric analysis was carried out in a BD Accuri™ C6 (Becton–Dickinson, San Jose, CA, USA), equipped with BD Accuri C6 software, based on the acquisition of 20,000 events. Data were analysed using FlowJo Software (Tree Star, Inc).

Caspases activities were evaluated by luminescent assays with Caspase-Glo® 9, Caspase-Glo® 8 and Caspase-Glo® 3/7, according to the manufacturer's instructions. These kits rely

on the use of a caspase-specific substrate, which is cleaved, releasing a substrate for luciferase and resulting in the luciferase reaction and production of light.

MCF-7aro cells (2.0×10^4 cells/ml) were incubated with each AI (10 µM), with or without 3-MA (1 mM, in the case of caspase-7 assay), during 3 days, in white-walled 96-well plates. As a positive control, cells were incubated with staurosporine (STA) at 10 µM for 3 h, prior to adding the caspase's kit substrate. The luminescence, presented as relative light units (RLU), was measured after 1 h 30 min, in a 96-well Microplate Luminometer (BioTek Instruments). It must be noted that, as MCF-7aro cells are known to be caspase-3 deficient (Kurokawa et al. 1999), the use of Caspase-Glo® 3/7 kit only evaluates the activation of caspase-7. Caspase assays were performed in triplicate, in three independent experiments.

To determine the levels of intracellular ROS, it was used the 2',7'-dichlorodihydrofluorescein diacetate ($DCFH_2$-DA) method. $DCFH_2$-DA is a lipophilic non-fluorescent compound that crosses cell membrane and is oxidized to the fluorescent compound 2',7'-dichlorofluorescein (DCF) (Gomes et al. 2005). MCF-7aro cells (2.0×10^4 cells/ml) were cultured in black-walled 96-well plates and incubated with each AI (10 µM), with or without 3-MA (1 mM), during 3 days. Cells were labelled with $DCFH_2$-DA (50 µM), for 1 h, at 37ºC. As positive control, cells were incubated with phorbol 12-myristate 13-acetate (PMA) at 25 ng/ml, for 2 h or with H_2O_2 at 200 µM, for 14-16h, prior to adding the dye. The fluorescence, presented as mean fluorescence intensity (MFI), was measured using an excitation wavelength of 480 nm and an emission filter of 530 nm, in a 96-well Microplate Luminometer (BioTek Instruments). Assays were performed in triplicate in three independent experiments.

2.9. Detection of acid vesicular organelles

Acridine orange (AO) was used to evaluate the formation of acid vesicular organelles (AVOs), by fluorescence microscopy. AO is an acidotropic fluorescent dye that stains DNA and cytoplasm bright green (AO^-) and, when protonated in the presence of acid compartments, it fluoresces bright yellow/orange/red (AO^+). MCF-7aro and LTEDaro were cultured in 24-well plates at a cellular density of 1.75×10^5 cells/ml and 2.0×10^5 cells/ml for 3 days, respectively and 1.0×10^5 cells/ml for 6 days, for both cell lines and treated with each AI (10 and 25 µM). Then, cells were stained with AO at 0.1 mg/ml, during 15 min, at 37ºC and 5% CO_2. Following this, media was rejected and cells washed with PBS. Finally, cells were mounted in aqueous media and the presence of AVOs was indicated by the yellow/orange/red fluorescence, analysed in the fluorescence microscope (Eclipse Ci,

Nikon, Japan), equipped with a blue excitation filter of 490 nm and a maximum transmission at 360/400 nm and processed by Nikon NIS Elements v4.0 image software.

2.11. Statistical analysis

The data presented are expressed as the mean ± SEM. Statistical analysis, using GraphPad Prism 5 software, was performed using analysis of variance (ANOVA) followed by Bonferroni and Tukey post-hoc tests for multiple comparisons (Two-way and One-way ANOVA, respectively). Values of $p < 0.05$ were considered as statistically significant.

Chapter III

Results

3.1. In cell aromatase assay

From a series of synthesized A-, B- and D-ring modified steroidal AIs synthesized by our group, four of them, which presented, in human placental microsomes, an anti-aromatase activity higher than 70%, were selected for studying their inhibition of aromatase in MCF-7aro cells (Varela et al. 2013). The anti-aromatase activity of steroids **6**, **9**, **10** and **12** was evaluated by a radiometric assay, using [1β-^{3}H] androstenedione as substrate. AIs **6**, **9**, **10** and **12** (at 10 µM) induced an aromatase inhibition of 92.67%, 74.74%, 96.37% and 97.18%, respectively. Formestane (1 µM), used as a reference AI, presented an aromatase inhibition of 92.67%. Compound **12** was the most potent inhibitor with an IC_{50} of 0.3 µM. Compound **10** was de second most potent, with an IC_{50} of 0.5 µM, while compounds **6** and **9** had an IC_{50} of 3.5 µM and 3.1 µM, respectively (Figure 22).

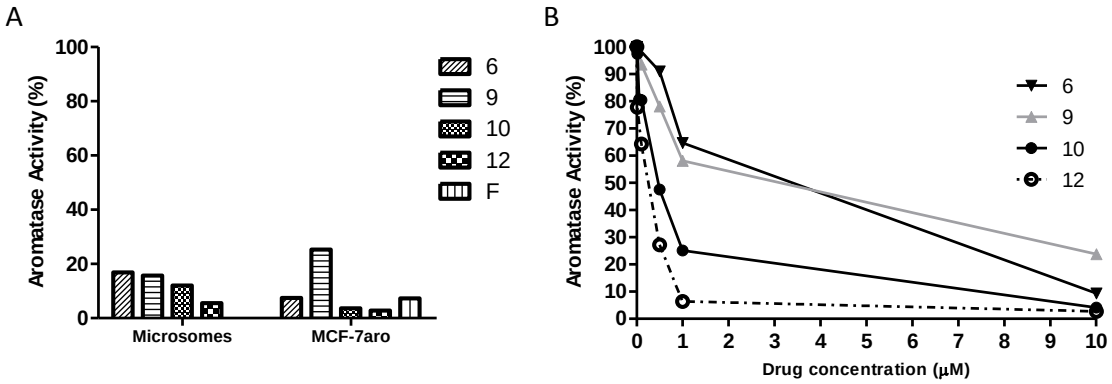

C

AIs	IC_{50} (µM) MCF-7aro
6	3.5
9	3.1
10	0.5
12	0.3

Figure 22. Anti-aromatase activity of AIs **6**, **9**, **10** and **12** in MCF-7aro cells. (A) Aromatase activity of AIs, at 10µM, in placental microsomes* and in intact MCF-7aro cells. (B) The IC_{50} (µM) values were determined by the in-cell aromatase assay in MCF-7aro cells incubated with different concentrations (0–10 µM) of AIs and 50 nM of [1β-^{3}H] androstenedione. (C) IC_{50} (µM) values for the steroids under study in MCF-7aro cells. Formestane (F) was used as a reference AI. Data are presented as a percentage of the tritiated water control and correspond to three independent experiments carried out in triplicate.

* Data previously published in Varela et al. (2013)

3.2. Cell viability in MCF-7aro cells

The effects of steroids **6**, **9**, **10** and **12** (1–50 µM) in MCF-7aro cells' viability and their putative cytotoxicity were studied by MTT and LDH release assays, after 3 and 6 days of treatment. Cells only treated with testosterone (T) were considered as control. As observed in Figure 23, all the compounds induced a similar decrease in cell viability in a dose- and time-dependent manner. However, for the lowest concentration (1 µM) and after 3 days of treatment, compound **9** ($p < 0.001$) caused a significant increase in cell viability, suggesting an estrogenic effect. Despite that, all compounds induced a significant decrease ($p < 0.01$; $p < 0.001$) in cell viability for all times of incubation and for the higher concentrations (10–50 µM). Compound **10** is the most efficient in decreasing cell viability, after 6 days of treatment (Figure 23F). After 3 days of treatment, no effects were observed in LDH release for all compounds, except for compound **9**, at the highest concentration, which suggests that this compound, at this concentration, is cytotoxic (Figure 23E). Thus, for all the other assays the highest concentration used for steroid **9** was 25 µM. In addition, as it was detected that compound **6** induced the appearance of crystals, its study was abandoned from this point forward.

To address the question whether decrease of cell viability was due to aromatase inhibition, it was evaluated the effects of compounds on estradiol (E2)-treated MCF-7aro cells for the same times as for T-treated cells. In these conditions, all compounds induced a decrease in cell viability (Figure 24A-C), with compound **10** being, again, the most efficient one (Figure 24D). As shown in Figure 25, by comparing T and E2-treated cells, a similar reduction in cell viability is observed, suggesting that the AIs effects are independent of aromatase inhibition.

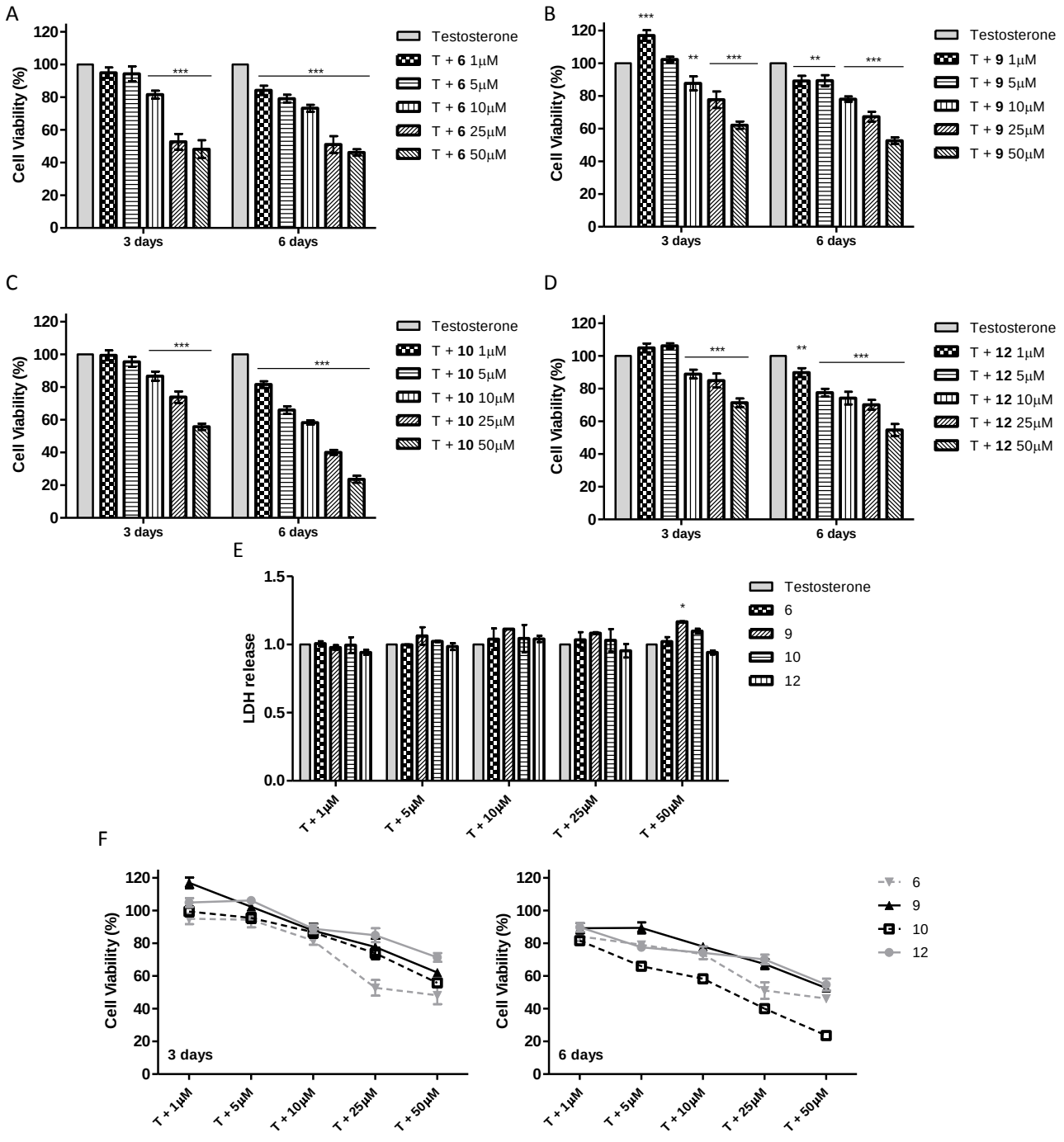

Figure 23. Effects of AIs **6** (A), **9** (B), **10** (C) and **12** (D) in viability of MCF-7aro cells, evaluated by MTT assay and LDH release (E). (F) Comparison of the effects of all AIs. MCF-7aro cells were cultured with different concentrations of each AI (1–50 μM) and testosterone (T) at 1 nM, during 3 and 6 days. Cells cultured with T represent the maximum of cell viability and were considered as control. Results are the mean ± SEM of three independent experiments, performed in triplicate. Significant differences between the control and cells with each AI are denoted by *p < 0.05, **p < 0.01 and ***p < 0.001.

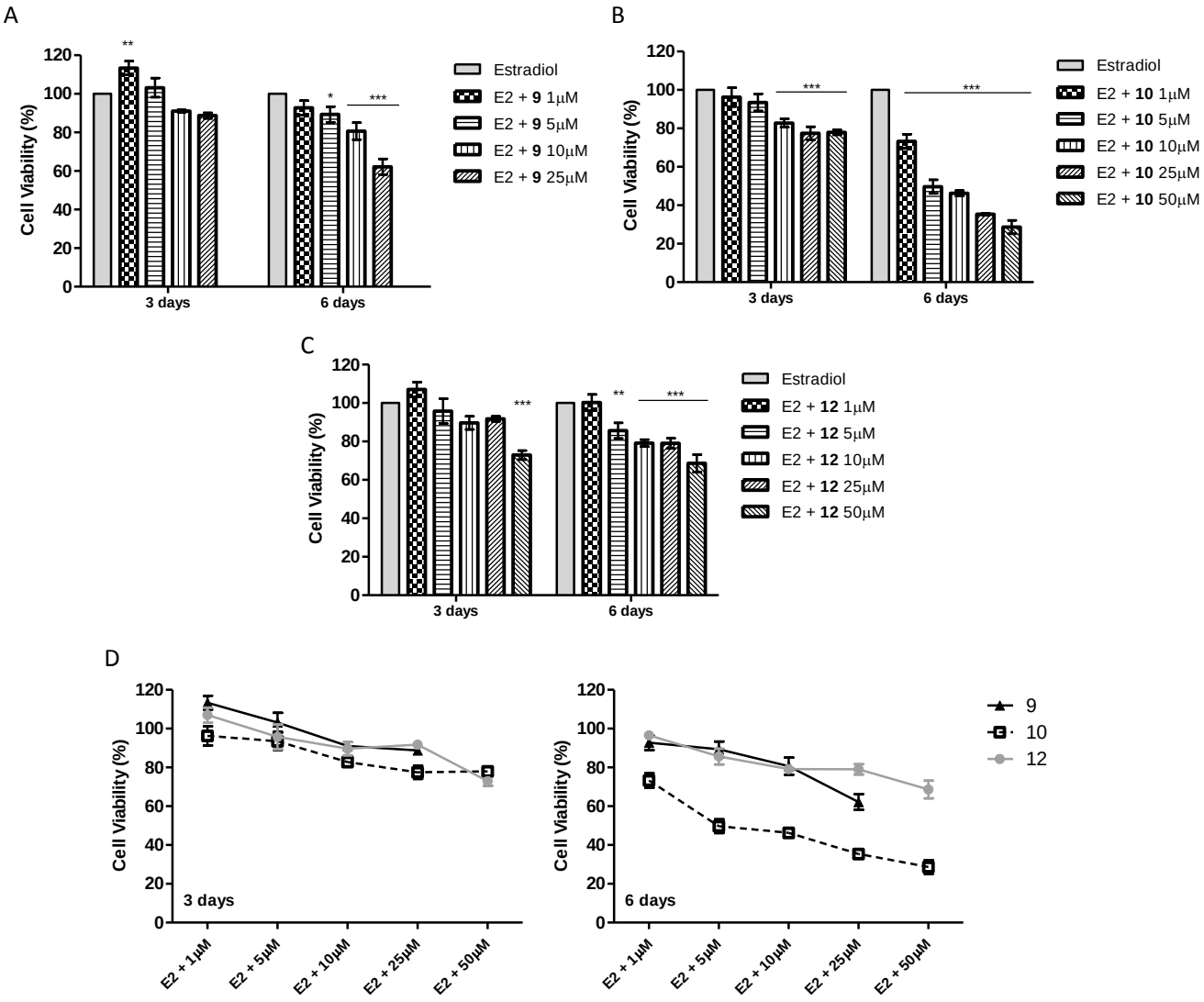

Figure 24. Effects of AIs **9** (A), **10** (B) and **12** (C) in viability of MCF-7aro cells in the presence of estradiol (E2), evaluated by MTT assay. (D) Comparison of the effects of all AIs. MCF-7aro cells were cultured with different concentrations of each AI (1–50 μM) and E2 at 1 nM during 3 and 6 days. Cells cultured with E2 represent the maximum of cell viability and were considered as control. Results are the mean ± SEM of three independent experiments, performed in triplicate. Significant differences between the control and cells with each AI are denoted by **p < 0.01 and ***p < 0.001.

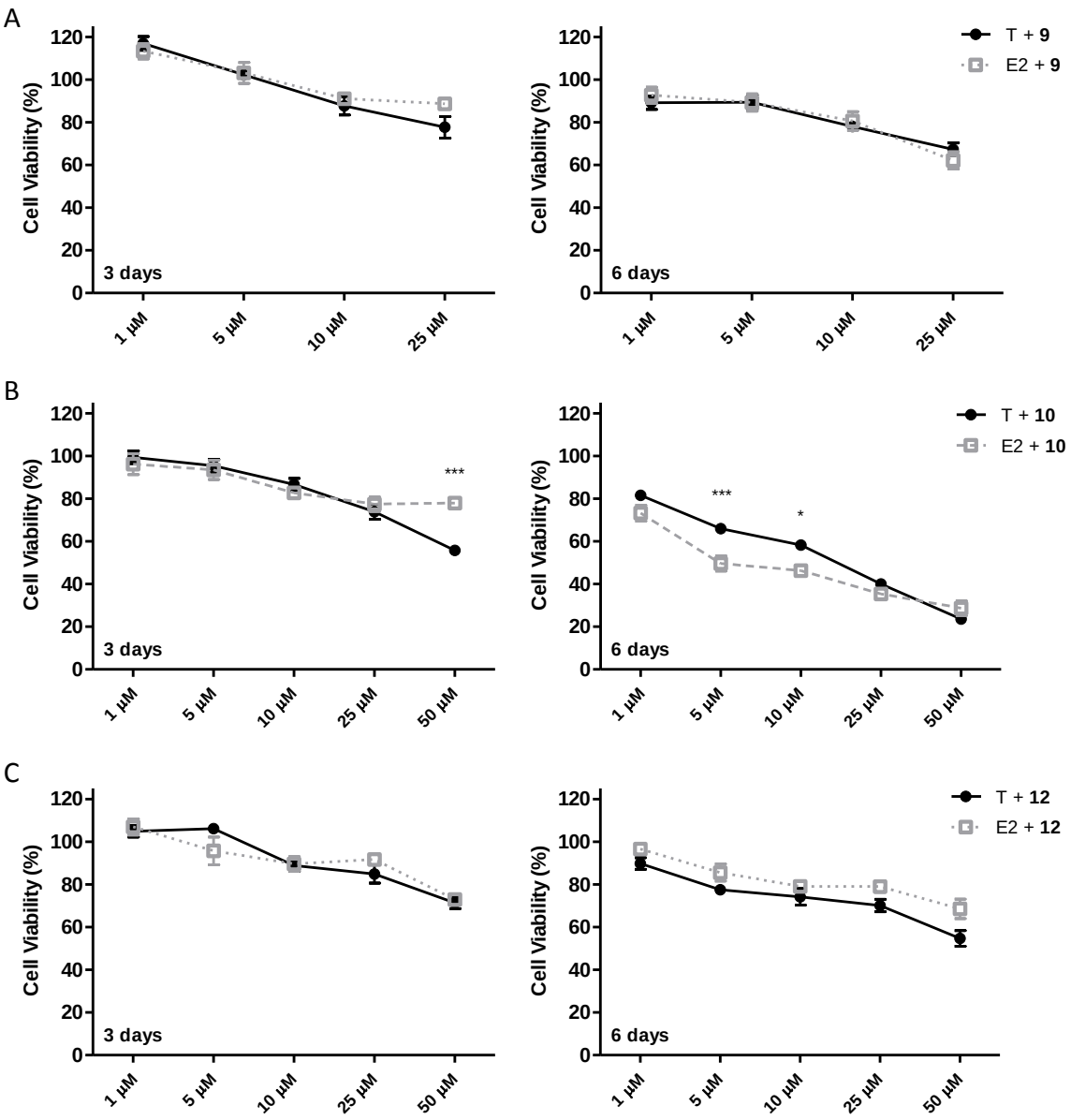

Figure 25. Comparison of the effects of AIs **9** (A), **10** (B) and **12** (C) in viability of MCF-7aro cells cultured with T or E2, evaluated by MTT assay. MCF-7aro cells were cultured with different concentrations of each AI (1–50 µM) and T/E2 at 1 nM during 3 and 6 days. Results are the mean ± SEM of three independent experiments, performed in triplicate. Significant differences between T-treated MCF-7aro cells plus AI versus E2-treated MCF-7aro cells plus AI are denoted by *$p < 0.05$ and ***$p < 0.001$.

3.3. Cell viability in SK-BR-3 cells

To evaluate if the biological effects of the different steroids in MCF-7aro cells were dependent on ER, it was also studied the effects of these compounds in an ER^- human breast cancer cell line, SK-BR-3, during the same periods of time (Figure 26). All the studied AIs induced a similar decrease in the viability of SK-BR-3 cells (Figure 26D). These effects were similar to the ones observed in E2-treated MCF-7aro cells for all compounds, at 3 days of treatment (Figure 27A-C). Nonetheless, compound **10** presented a more marked

decrease in cell viability in the E2-treated cells, at 6 days of treatment and for all the concentrations.

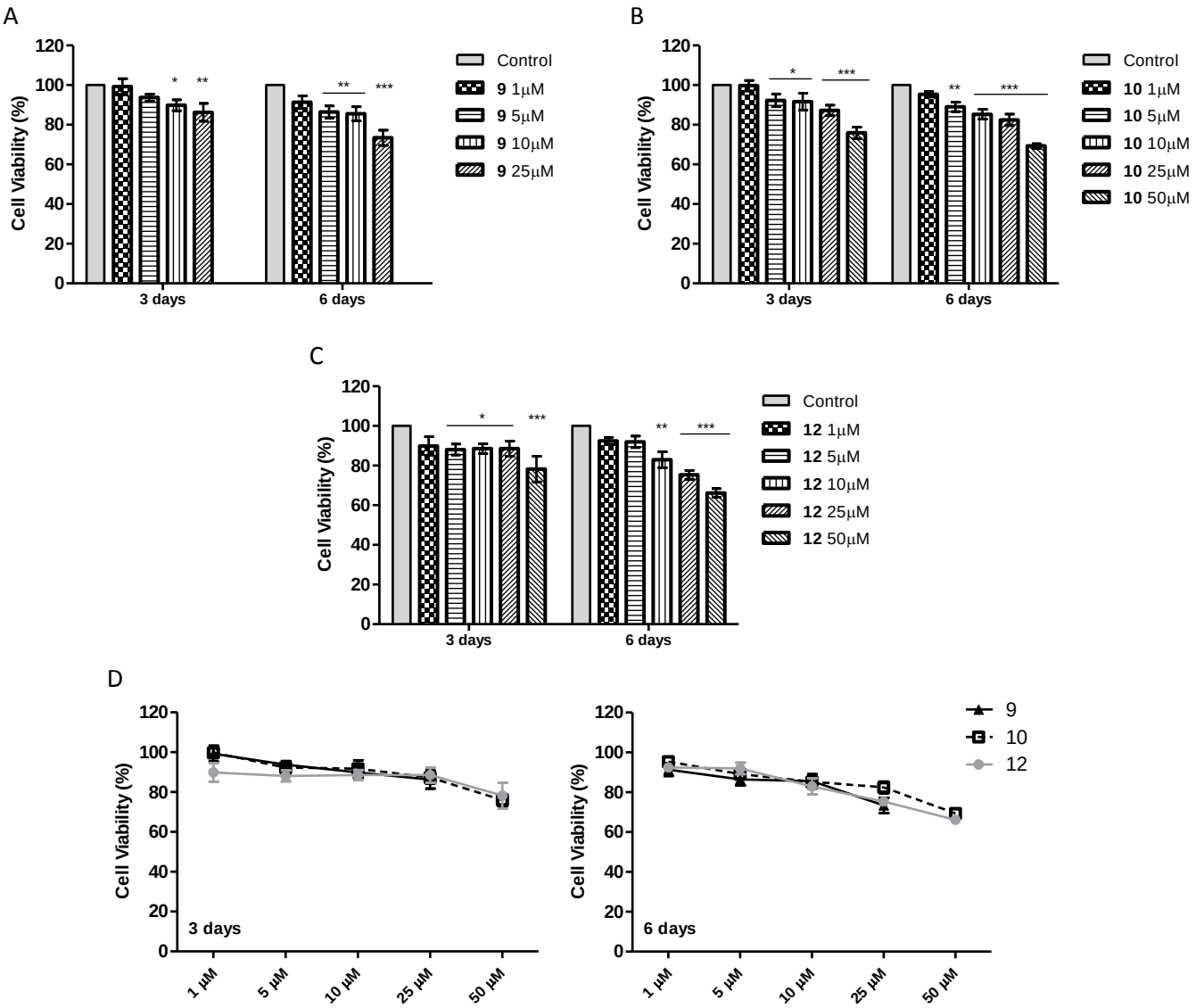

Figure 26. Effects of AIs **9** (A), **10** (B) and **12** (C) in viability of SK-BR-3 cells, evaluated by MTT assay. (D) Comparison of the effects of all AIs. SK-BR-3 cells were cultured with different concentrations of each AI (1–50 μM) during 3 and 6 days. Cells cultured without any AI represent the maximum of cell viability and were considered as control. Results are the mean ± SEM of three independent experiments, performed in triplicate. Significant differences between the control and cells with each AI are denoted by *p < 0.05, **p < 0.01 and ***p < 0.001.

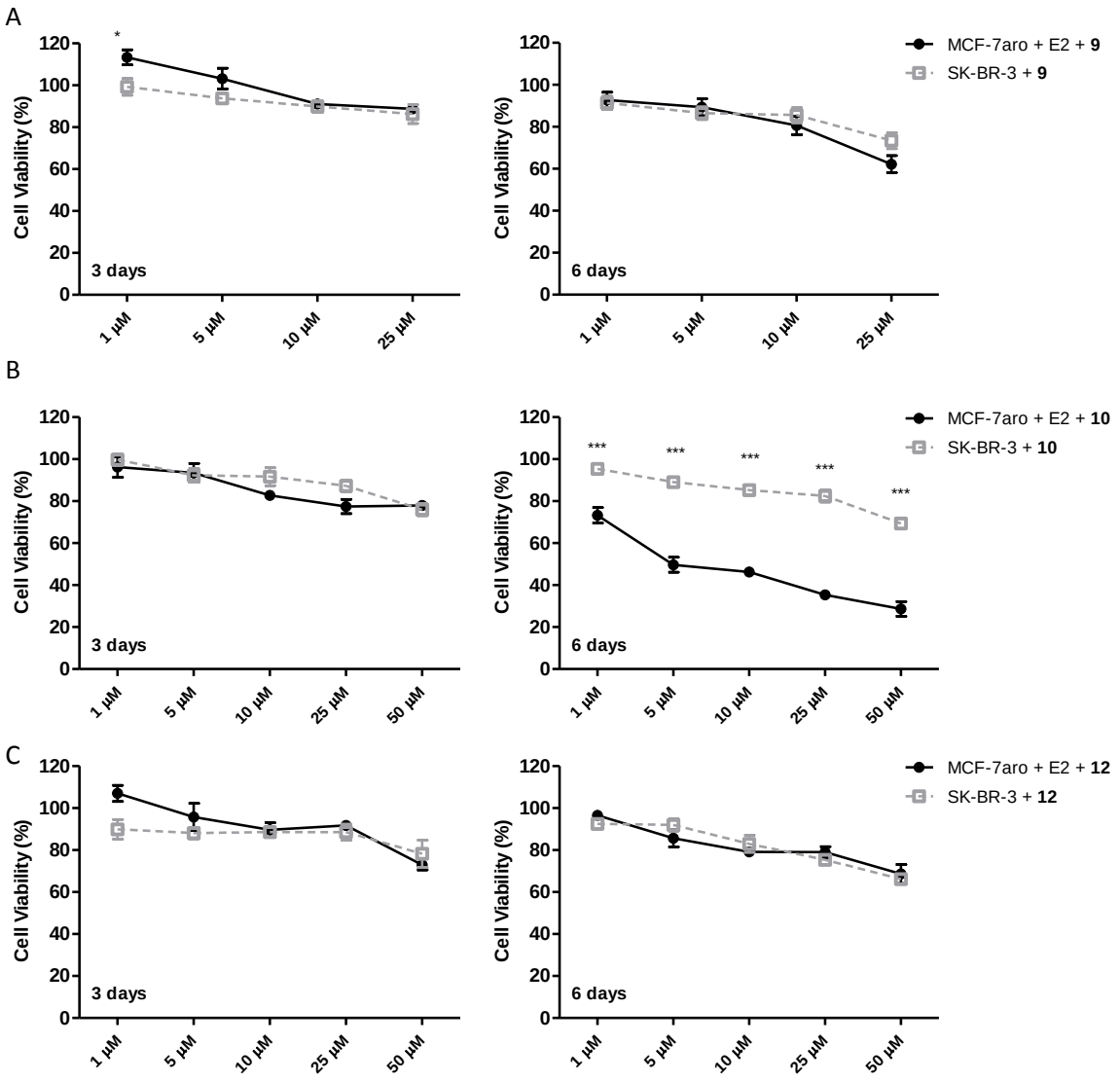

Figure 27. Comparison of the effects of AIs **9** (A), **10** (B) and **12** (C) in viability of MCF-7aro cells cultured with E2 and of SK-BR-3 cells, evaluated by MTT assay. Cells were cultured with different concentrations of each AI (1–50 µM) during 3 and 6 days. Results are the mean ± SEM of three independent experiments, performed in triplicate. Significant differences between E2-treated MCF-7aro cells plus AI versus SK-BR-3 cells plus AI are denoted by *$p < 0.05$ and ***$p < 0.001$.

3.4. Cell viability in HFF-1 cells

In order to investigate the cytotoxicity of the new steroids, their effects were evaluated in a non-tumoral cell line, HFF-1, using MTT. None of the compounds induced a decrease in cell viability. Surprisingly, compounds **10** and **12** induced a significant increase ($p < 0.01$; $p < 0.001$) in mitochondrial metabolic activity for the highest concentrations (25 and 50 µM), at 6 days of treatment (Figure 28).

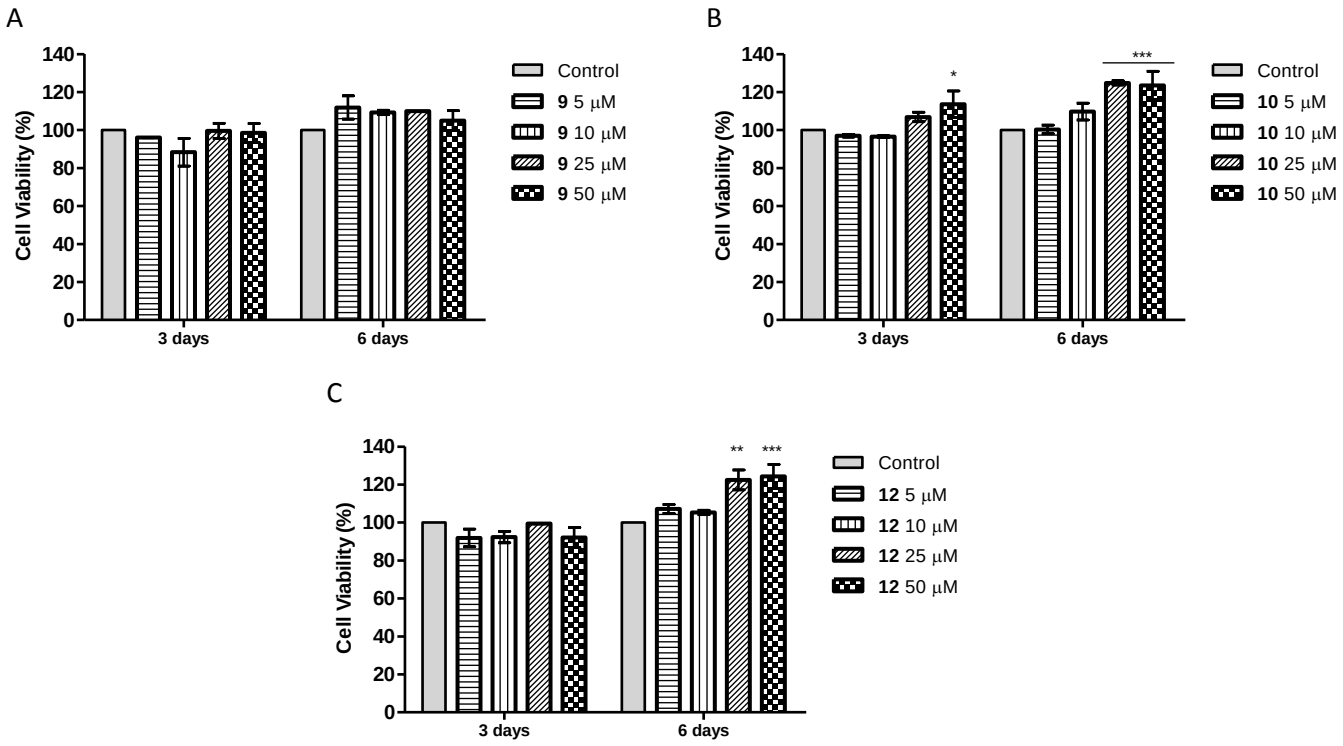

Figure 28. Effects of AIs **9** (A), **10** (B) and **12** (C) in viability of HFF-1 cells, evaluated by MTT assay, after 3 and 6 days. Cells cultured without any AI represent the maximum of cell viability and were considered as control. Results are the mean ± SEM of three independent experiments, performed in triplicate. Significant differences between the control and cells with each AI are denoted by *p < 0.05, **p < 0.01 and ***p < 0.001.

3.5. Morphological studies

To investigate morphological alterations induced by each AI, MCF-7aro cells were examined by phase contrast microscopy, Giemsa and Hoechst staining (Figure 29). Cells treated with the different AIs showed marked morphological alterations such as membrane blebbing, cell shrinkage and chromatin condensation/fragmentation, typical features of apoptotic cell death. In addition, it was observed in some cells the presence of cytoplasmic vacuoles. Except for compound **9**, these alterations were more evident with increasing AI concentrations (10 and 25 μM) and time of exposure. In general, these features were accompanied by a reduction in cell density. Compounds **9** and **12** presented more chromatin condensation and fragmentation, particularly seen by Hoechst staining.

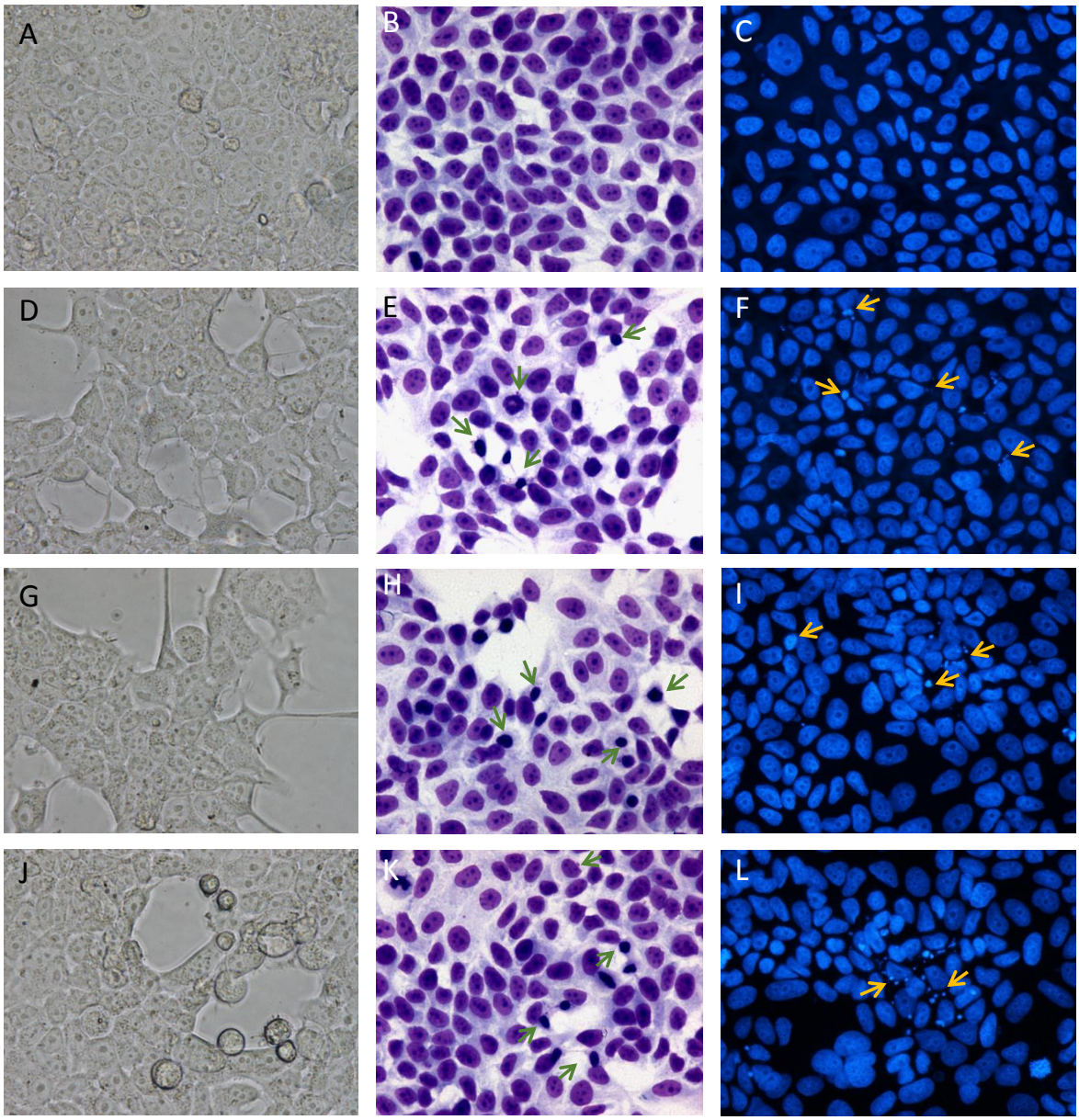

Figure 29. Effects of AIs **9**, **10** and **12** on MCF-7aro cells' morphology, examined by phase contrast microscopy (A, D, G and J), Giemsa staining (B, E, H and K) and Hoechst staining (C, F, I and L), after 3 days of treatment. Cells were cultured in the absence (A, B and C) or in the presence of 10 μM of AIs **9** (D, E and F), **10** (G, H and I) and **12** (J, K and L). Treated cells presented cell shrinkage and membrane blebbing, chromatin condensation (green arrows) and chromatin fragmentation (yellow arrows).

3.6. Cell cycle analysis

In order to explore the cause of the anti-proliferative effects of each AI in MCF-7aro cells, the total cellular DNA content was analysed by flow cytometry, after 3 days, following treatment with 10 and 25 µM of each AI. As shown in Table 3 and in Figure 30, compounds **9** and **10** induced a significant ($p < 0.01$; $p < 0.001$) cell cycle arrest in G0/G1 phase, when compared to control (T). This was accompanied by a significant ($p < 0.05$; $p < 0.01$; $p < 0.001$) decrease of cells in S phase for AI **9** and of cells in S and G2/M phase for AI **10**, for both concentrations. Contrary to the other steroids, compound **12** only induced a significant ($p < 0.01$) cell cycle arrest in G2/M phase, when compared to control (T), at 25 µM.

Table 3. Effects of AIs **9**, **10** and **12** in the different phases of cell cycle progression in MCF-7aro cells incubated with T during 3 days.

Cell cycle	G0/G1	S	G2/M
Testosterone	76,73 ± 0,33	6,62 ± 0,22	15,89 ± 0,31
Steroid 9			
T + 10µM	78,80 ± 0,30 **	4,92 ± 0,43 *	15,90 ± 0,32
T + 25µM	80,12 ± 0,69 ***	4,34 ± 0,32 **	14,40 ± 0,27
Steroid 10			
T + 10µM	84,98 ± 1,07 ***	4,14 ± 0,30 **	11,34 ± 0,77 ***
T + 25µM	88,25 ± 0,65 ***	2,87 ± 0,26 ***	8,94 ± 0,58 ***
Steroid 12			
T + 10µM	75,70 ± 0,72	5,41 ± 0,44	17,13 ± 0,49
T + 25µM	76,05 ± 1,00	5,85 ± 0,15	18,35 ± 1,10 **

Cells were treated with 10 µM and 25 µM of the AIs for 3 days. Treated cells were fixed and their DNA content was evaluated by PI labelling followed by flow cytometry analysis. Data are presented as single cell events in G0/G1, S and the G2/M phases of the cell cycle. The data represents means ± SEM of triplicates and are representative of three independent experiments. Significant differences between the control versus AI-treated cells are indicated by *$p < 0.05$, **$p < 0.01$ and ***$p < 0.001$.

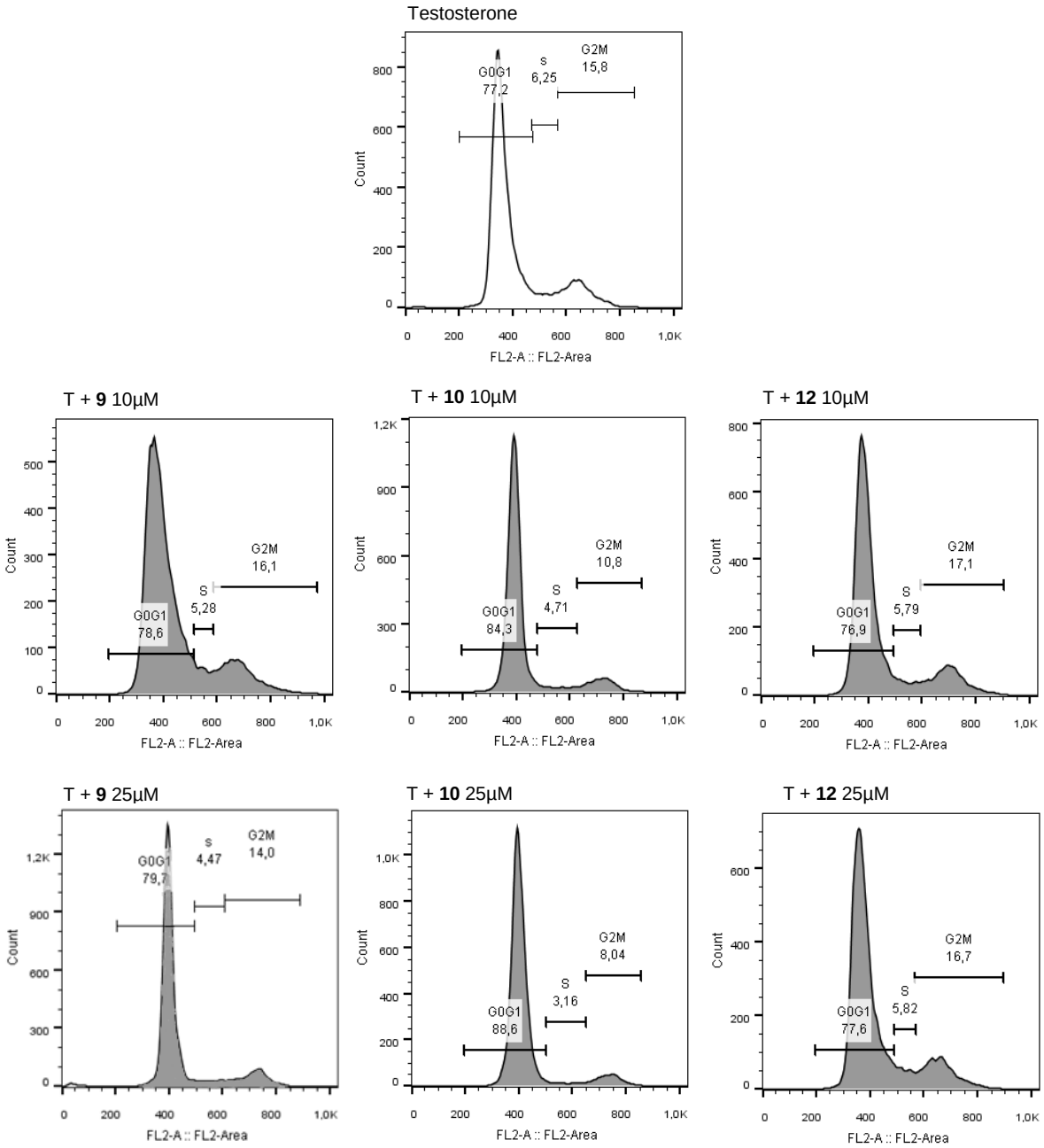

Figure 30. Representative histograms of cell cycle distribution of MCF-7aro cells treated with testosterone (T) and AIs **9**, **10** and **12** at 10 and 25 µM during 3 days. Histograms were obtained with FlowJo Software (Tree Star, Inc) and are representative of one independent assay. The numbers indicate the percentage of cells in each cell cycle phase.

3.7. Analysis of apoptosis

Since treated cells presented morphological features typical of apoptosis and to understand which apoptotic pathway may be associated to cell death, it was evaluated, after 3 days of treatment with the AIs (10 µM), the activity of caspase-9, -8 and -7 (Figure 31), by luminescent assays. All compounds induced a significant ($p < 0.001$) increase in caspase-9 activity (Figure 31A) of 78.48 % (43598 ± 3020 RLU), 69.23 % (41339 ± 1894 RLU) and

81.49 % (44333 ± 3027 RLU), respectively for AI **9**, **10** and **12**, when compared to control (24427 ± 768.9 RLU). No significant differences in caspase-8 activity were observed after treatment with each of the AIs (Figure 31B). Moreover, all compounds induced a significant ($p < 0.01$) increase in caspase-7 activity (Figure 31C) of 22.60 % (28349 ± 695.5 RLU), 18.16 % (27324 ± 747.6 RLU) and 17.84 % (27250 ± 704.8 RLU), respectively for AI **9**, **10** and **12**, when compared to control (23124 ± 486.7 RLU).

As the results obtained for caspase-9 activity showed that mitochondria may be involved in the programmed cell death it was also evaluated mitochondrial transmembrane potential ($\Delta\Psi_m$). The preliminary results for mitochondrial transmembrane potential were not conclusive for any of the compounds. As the production of ROS may be correlated with mitochondria dysfunction, its levels were also evaluated after 3 days of treatment, using $DCFH_2$-DA in a fluorescence assay. No significant production of ROS was observed for any of the AIs studied (Figure 31D).

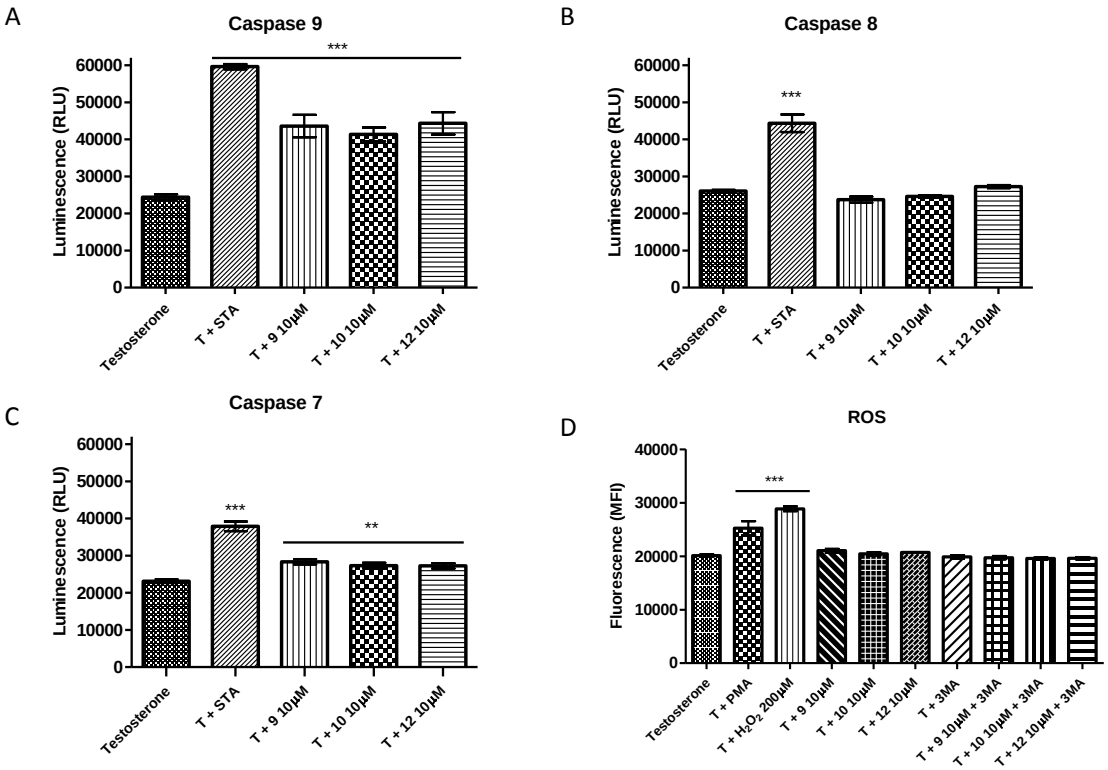

Figure 31. Effects of AIs **9**, **10** and **12** on caspase-9 (A), caspase-8 (B) and caspase-7 (C) activities and on ROS production (D), after 3 days of treatment. MCF-7aro cells cultured with testosterone (T), with or without 3-MA, were considered as control. For caspase assays, cells treated with staurosporine (STA) were considered as positive control, while cells treated with PMA or H_2O_2 were considered as positive control for ROS production. The results are represented as mean fluorescence intensity (MFI) for caspase activities assays and as relative luminescence units (RLU) in ROS production assay. Results are the mean ± SEM of three independent experiments, performed in triplicate. Significant differences between the control versus treated cells are indicated by $^{**}p < 0.01$ and $^{***}p < 0.001$.

3.8. Cell viability in LTEDaro cells

The biological effects of compounds **9**, **10** and **12** were examined in LTEDaro cells, a model for late stage acquired resistance. As shown in Figure 32, compound **10** is the most efficient one, with a dose- and time-dependent decrease in cell viability. Compound **9**, at 3 days of treatment, showed only a significant decrease ($p < 0.05$; $p < 0.001$) for the highest concentrations (25 and 50 µM) and it exerted its effects mainly in a time-dependent manner. Similarly, compound **12** had no effect on LTEDaro cells, at 3 days of treatment, except for its highest concentration ($p < 0.01$) and induced effects in a time-dependent manner.

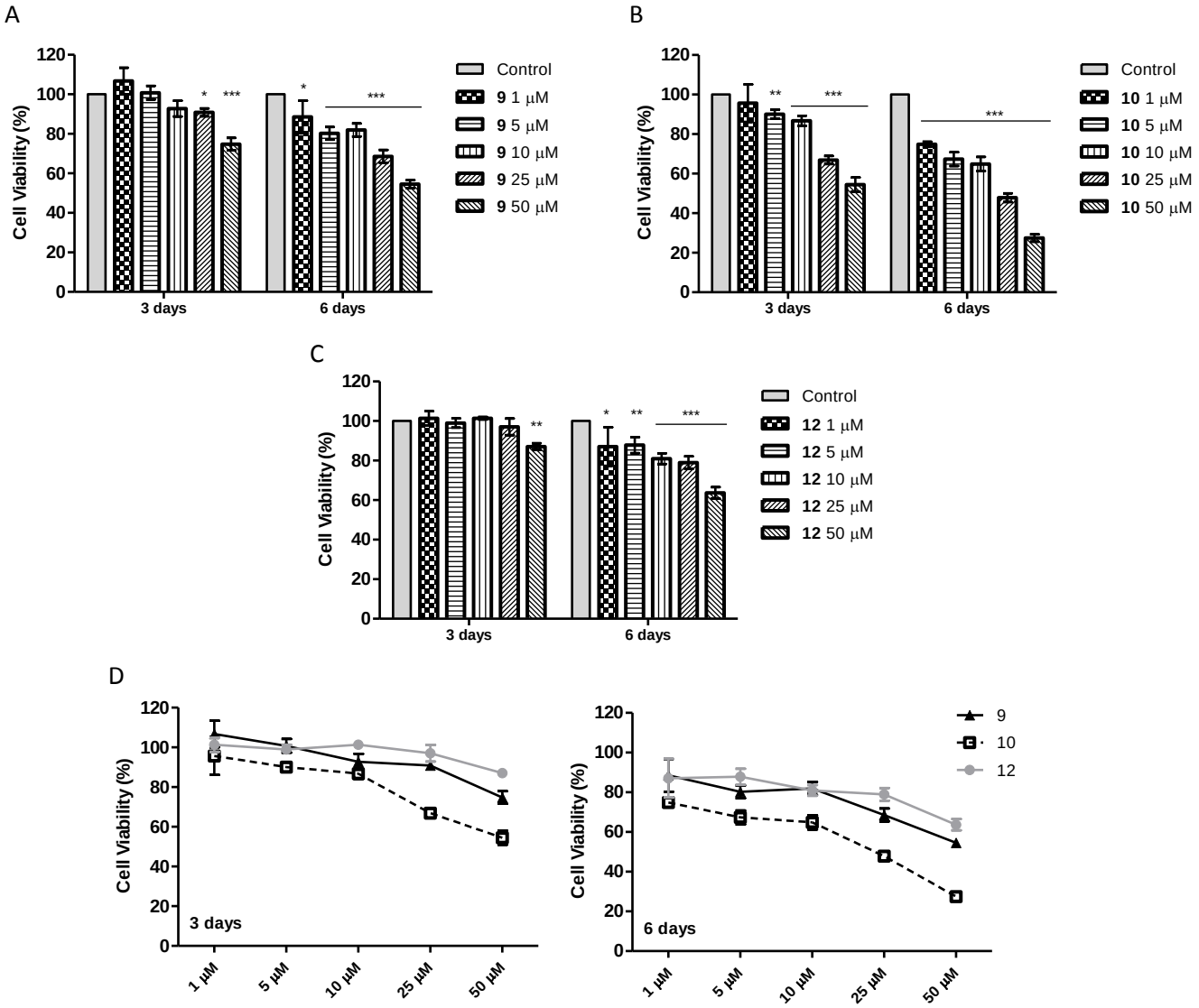

Figure 32. Effects of AIs **9** (A), **10** (B) and **12** (C) in viability of LTEDaro cells, evaluated by MTT assay. (D) Comparison of the effects of all AIs. LTEDaro cells were cultured with different concentrations of each AI (1–50 µM) during 3 and 6 days. Cells cultured without any AI represent the maximum of cell viability and were considered as control. Results are the mean ± SEM of three independent experiments, performed in triplicate. Significant differences between the control and cells with each AI are denoted by *$p < 0.05$, **$p < 0.01$ and ***$p < 0.001$.

3.9. Presence of AVOs in MCF-7aro and LTEDaro cells

In order to clarify the nature of the cytoplasmatic vacuoles observed in Giemsa staining, acridine orange (AO), an acidotropic dye, was used. Using fluorescence microscopy, it was observed alterations in green fluorescence to yellow/orange/red fluorescence for all the compounds, though it did not increase with AI concentration (Figure 33-36). However, the presence of AVOs in MCF-7aro and LTEDaro cells decreases from 3 to 6 days of treatment, for all AIs (Figures 34 and 36). Compound **9** showed higher formation of AVOs than the others, in MCF-7aro cells (Figure 33), whereas, in LTEDaro cells (Figure 35), steroid **10** was the most effective in AVOs formation.

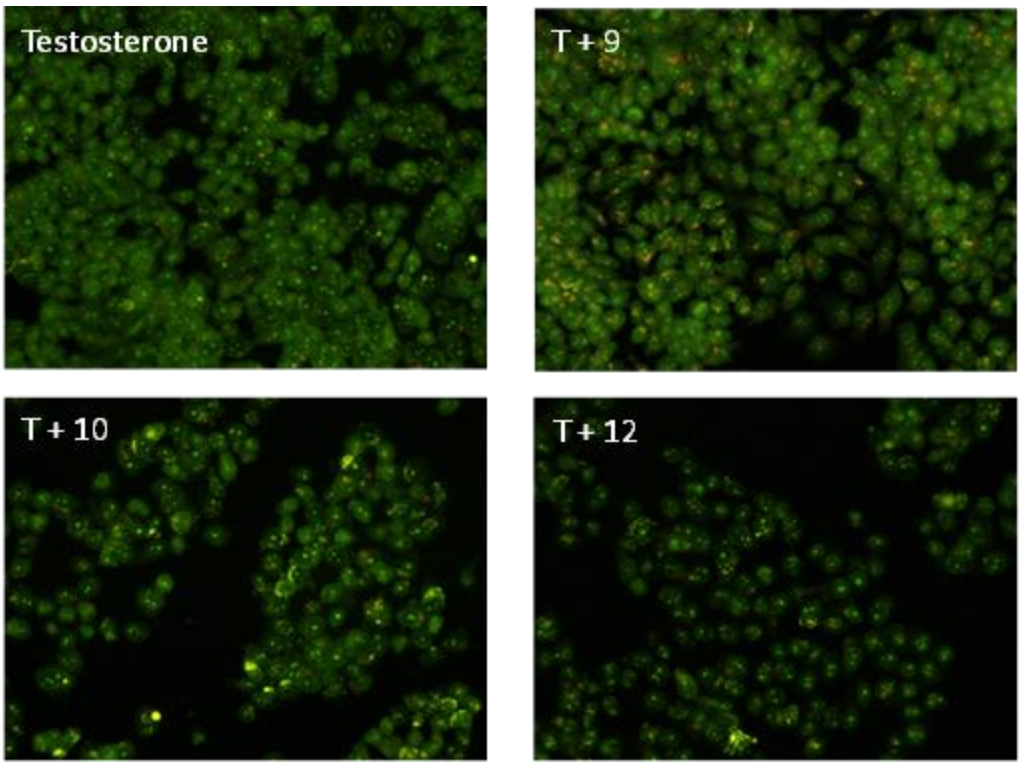

Figure 33. Effects of AIs **9**, **10** and **12** in the formation of AVOs in MCF-7aro cells, after 3 days. Cells were treated with each AI, at 10µM, stained with AO and analyzed by fluorescence microscopy. The presence of AVOs was indicated by the yellow/orange/red fluorescence.

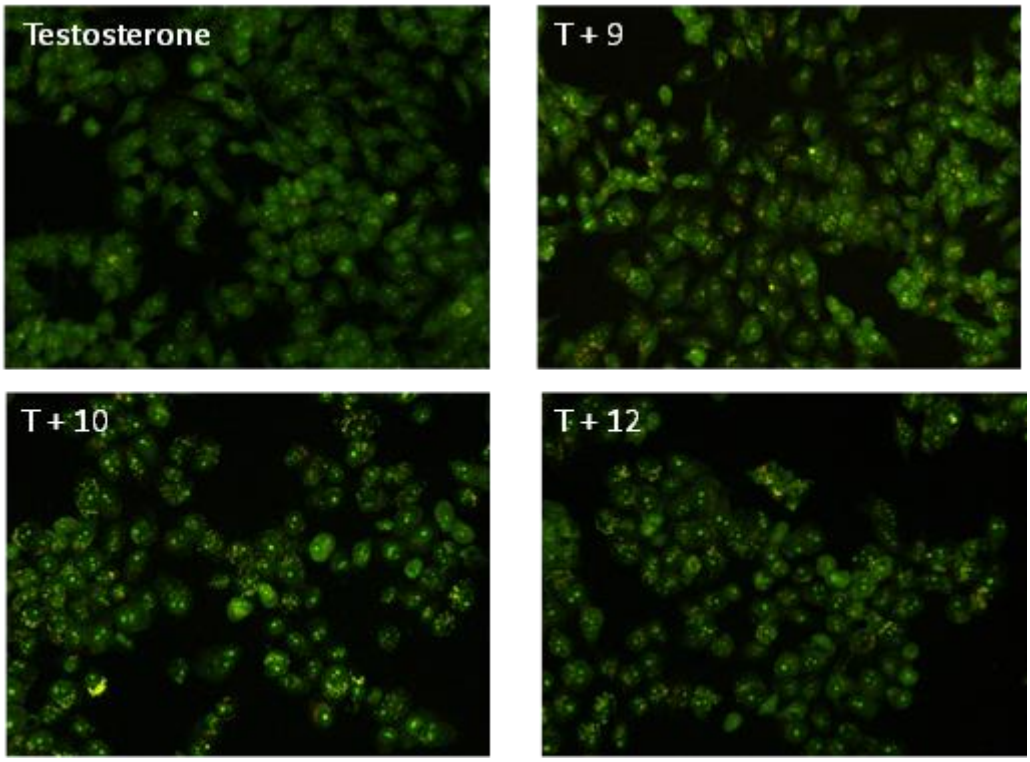

Figure 34. Effects of AIs **9**, **10** and **12** in the formation of AVOs in MCF-7aro cells, after 6 days. Cells were treated with each AI, at 10μM, stained with AO and analyzed by fluorescence microscopy. The presence of AVOs was indicated by the yellow/orange/red fluorescence.

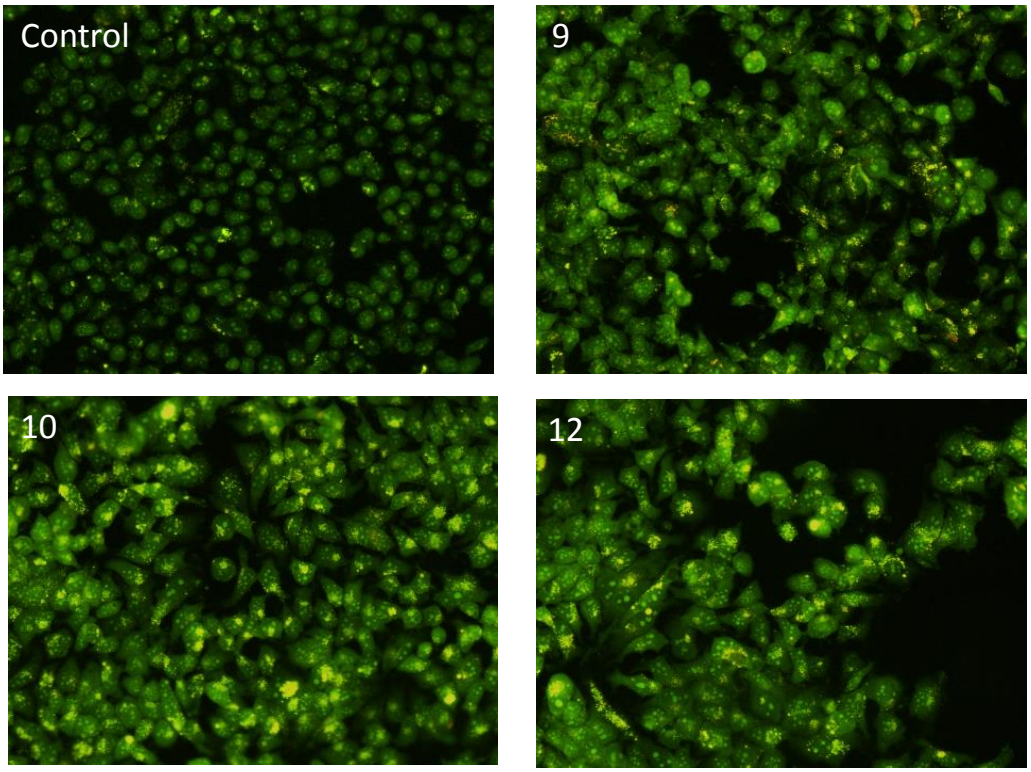

Figure 35. Effects of AIs **9**, **10** and **12** in the formation of AVOs in LTEDaro cells, after 3 days. Cells were treated with each AI, at 10μM, stained with AO and analyzed by fluorescence microscopy. The presence of AVOs was indicated by the yellow/orange/red fluorescence.

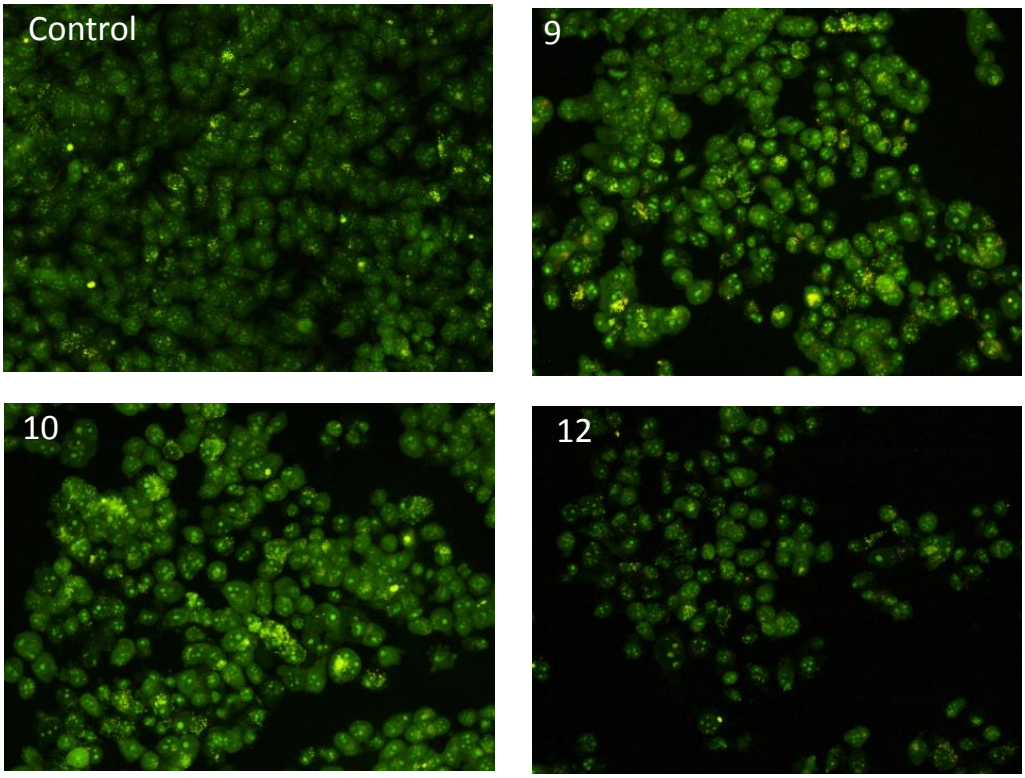

Figure 36. Effects of AIs **9**, **10** and **12** in the formation of AVOs in LTEDaro cells, after 6 days. Cells were treated with each AI, at 10μM, stained with AO and analyzed by fluorescence microscopy. The presence of AVOs was indicated by the yellow/orange/red fluorescence.

3.10. Effects of an inhibitor of autophagy in MCF-7aro and LTEDaro cells

As autophagy is one of the mechanisms described for AI-acquired resistance, it was also evaluated, by MTT assay, the effect of the autophagic inhibitor 3-MA in AI-sensitive and AI-resistant breast cancer cell lines treated with the steroids**,** after 3 and 6 days. Cells treated with 3-MA were considered as control.

As presented in Figure 37, when comparing AI-treated MCF-7aro cells with or without 3-MA, no significant differences in cell viability were observed, except for compound **9** ($p < 0.001$), at the lowest concentration, after 3 days of treatment and for steroids **10** and **12**, at 1 μM ($p < 0.01$) and 50 μM ($p < 0.01$), respectively, after 6 days of treatment. More, the addition of the autophagic inhibitor, 3-MA, did not induce any alteration in ROS production, when compared to the results obtained in the absence of 3-MA (Figure 31D).

When comparing the effects of all the steroids in LTEDaro cells with or without 3-MA, significant differences were observed ($p < 0.05$; $p < 0.01$; $p < 0.001$) for compounds **9** and **10**, at 3 days of treatment, suggesting a cytoprotective role for autophagy (Figure 38). For steroid **12** the decrease in cell viability, though not significant, was slightly enhanced in the presence of the autophagic inhibitor. Comparing, simultaneously, the effects of each AI in

resistant tumor cells, with or without 3-MA, for 3 and 6 days (Figure 39A-C), it was demonstrated that AI treatment plus 3-MA, at 3 days, causes effects similar to those obtained at 6 days of treatment, with or without 3-MA, for steroids **9** and **12**. However, compound **10** caused a higher reduction in cell viability, after 6 days of treatment without the autophagic inhibitor.

Concerning Figure 40, when comparing both MCF-7aro and LTEDaro cells, with or without 3-MA, confirms that the autophagic inhibitor only affects cell viability in resistant tumor cells for short periods of incubation. At 6 days of treatment both cell types have a similar behaviour.

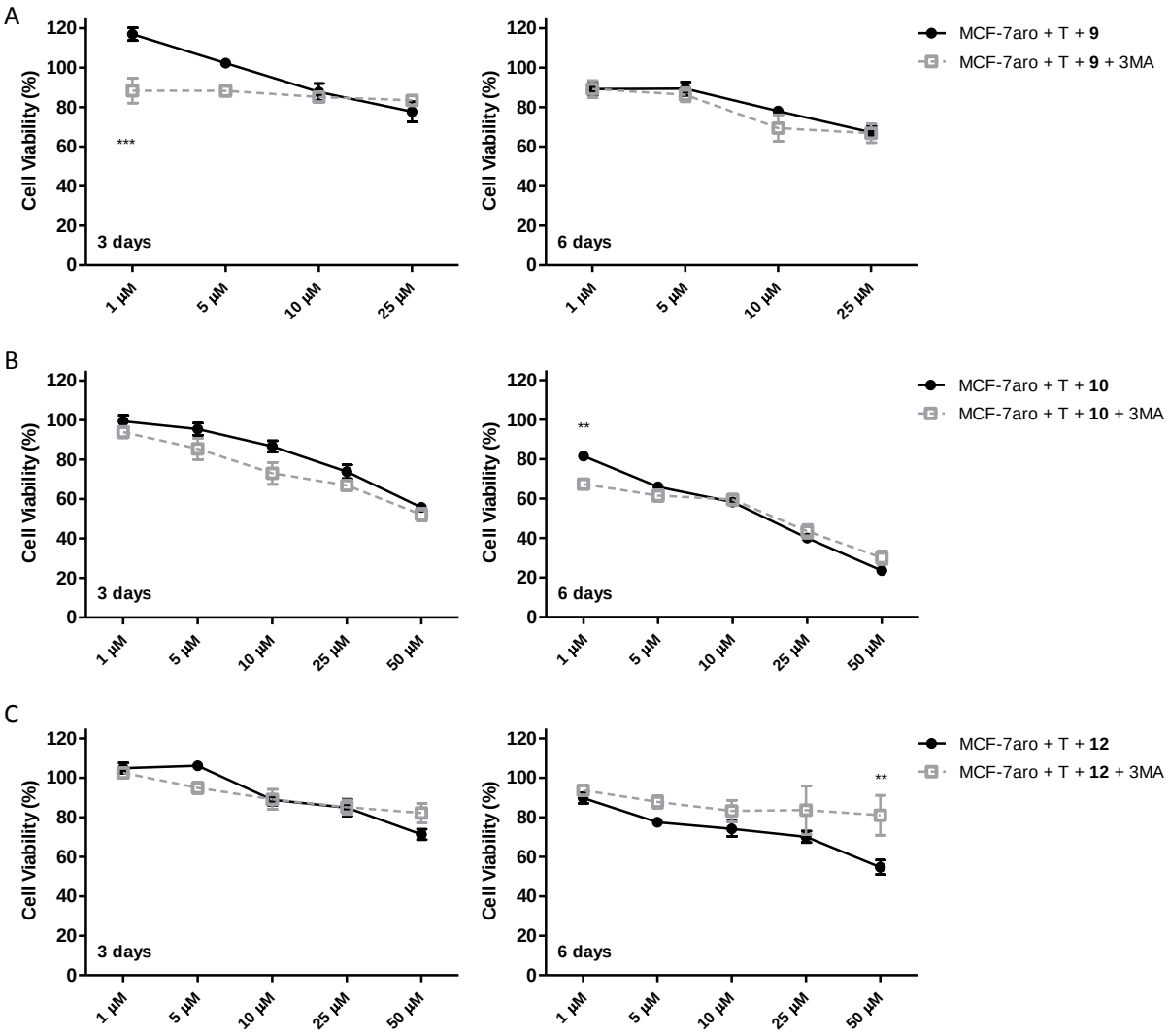

Figure 37. Comparison of the effects of AIs **9** (A), **10** (B) and **12** (C), in the presence or absence of 3-MA, in viability of MCF-7aro cells. Cells were treated with different concentrations of each AI (1–50 µM) and testosterone (T), at 1 nM, during 3 and 6 days. As controls, it was used cells treated with T, with or without 3-MA. Results are the mean ± SEM of three independent experiments, performed in triplicate. Significant differences between MCF-7aro cells with AI versus MCF-7aro cells with AI plus 3-MA are denoted by **$p < 0.01$ and ***$p < 0.001$.

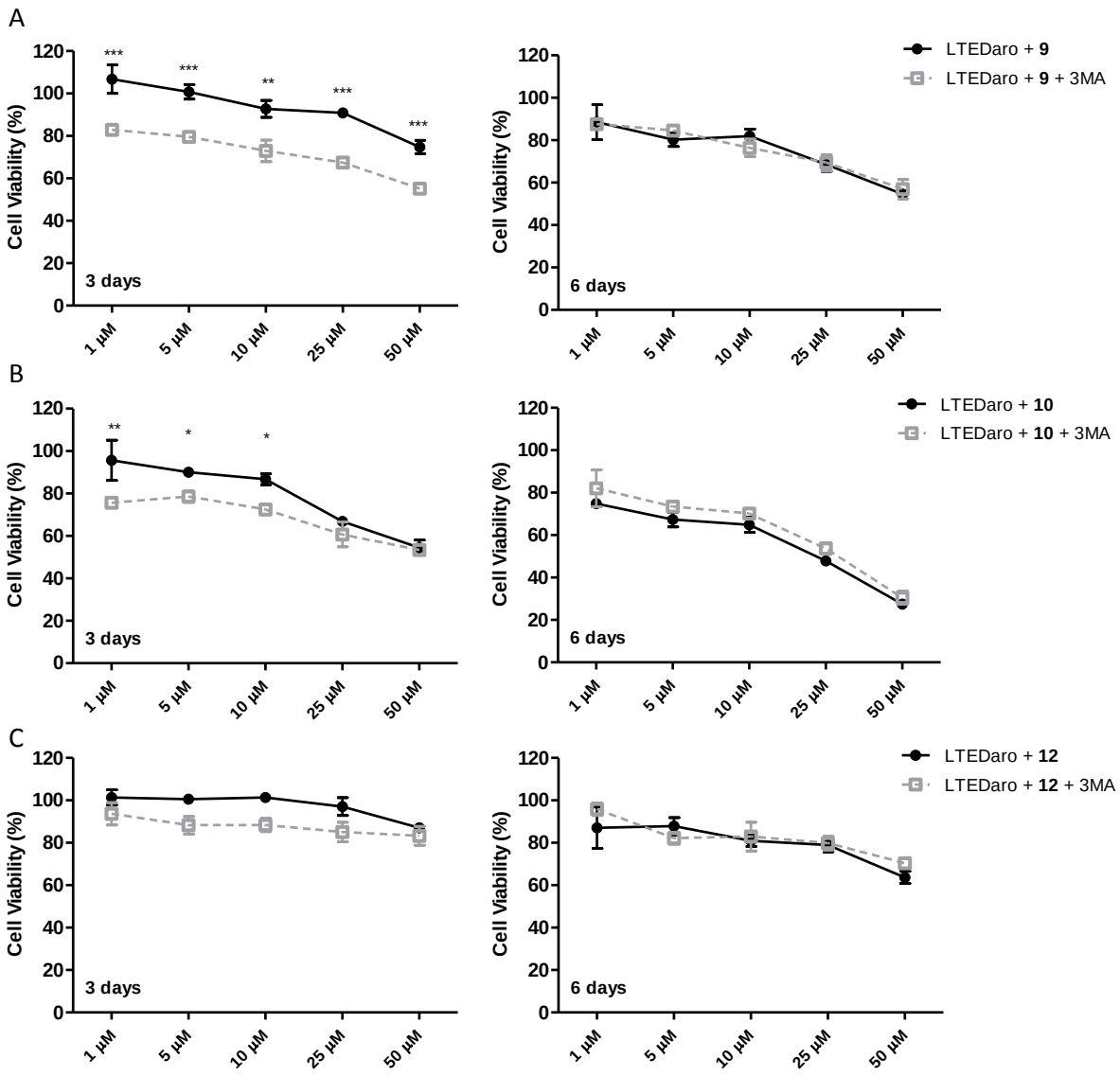

Figure 38. Comparison of the effects of AIs **9** (A), **10** (B) and **12** (C), in the presence or absence of 3-MA, in viability of LTEDaro cells. Cells were treated with different concentrations of each AI (1–50 µM), during 3 and 6 days. As controls, it was used cells treated with or without 3-MA. Results are the mean ± SEM of three independent experiments, performed in triplicate. Significant differences between LTEDaro cells with AI versus LTEDaro cells with AI plus 3-MA are denoted by **p < 0.01 and ***p < 0.001.

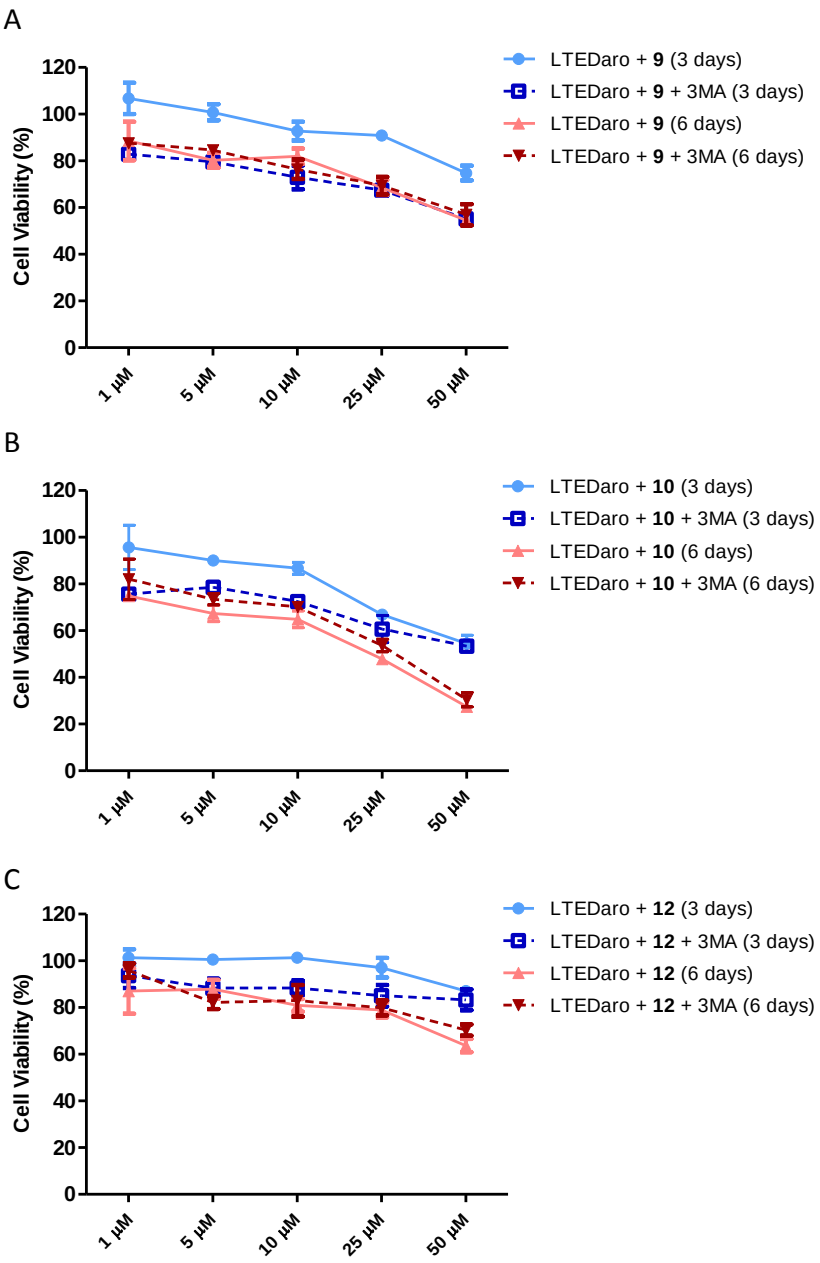

Figure 39. Comparison of the biological effects of AIs **9** (A), **10** (B) and **12** (C) (1–50 µM) in viability of LTEDaro cells with or without 3-MA, after 3 and 6 days of treatment. As controls, it was used cells treated with or without 3-MA. Results are the mean ± SEM of three independent experiments, performed in triplicate.

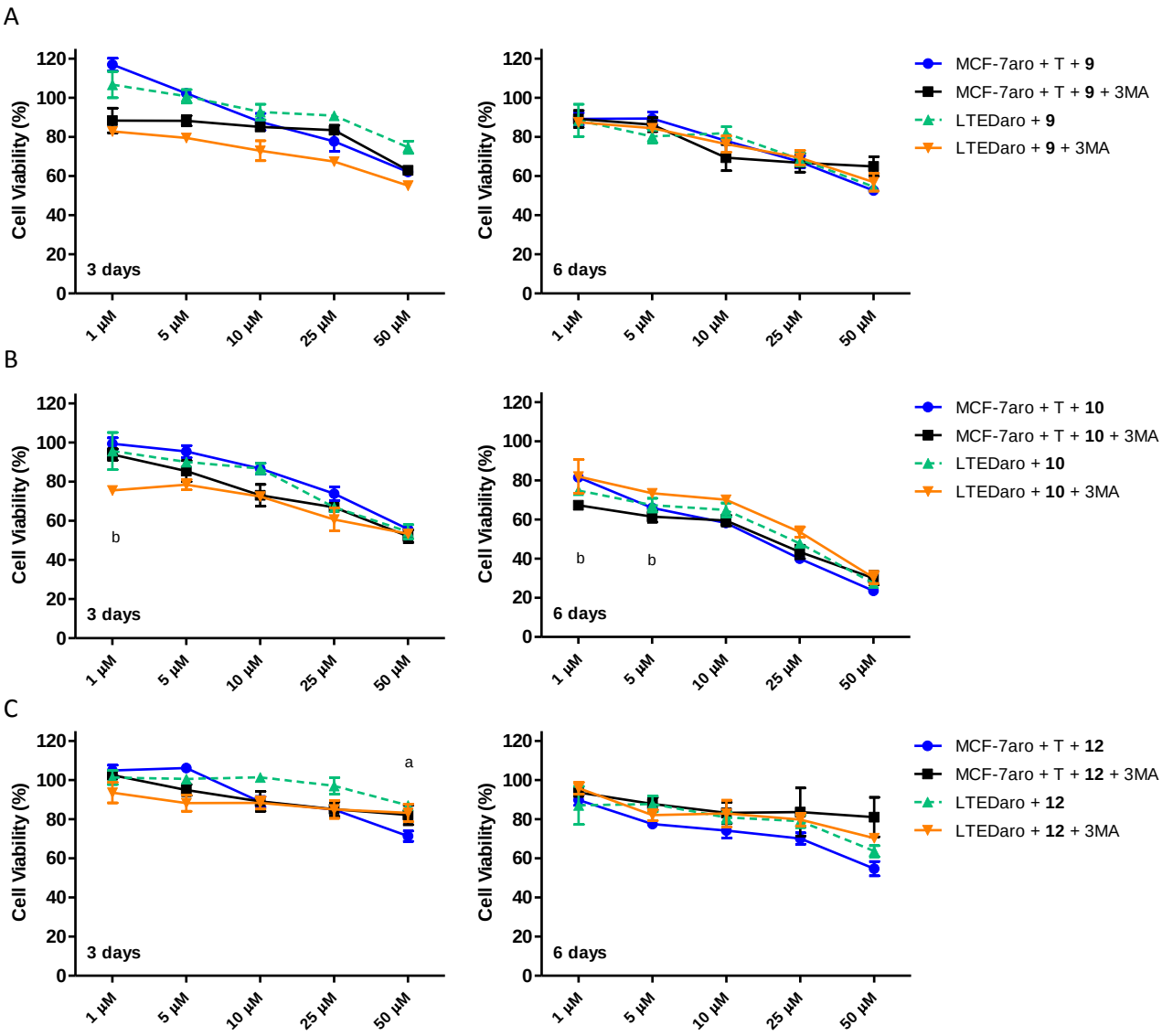

Figure 40. Comparison of the biological effects of AIs **9** (A), **10** (B) and **12** (C) (1–50 μM) in viability of MCF-7aro cells and LTEDaro cells with or without 3-MA, after 3 and 6 days of treatment. As controls, it was used cells treated with or without 3-MA. Results are the mean ± SEM of three independent experiments, performed in triplicate. Significant differences between AI-treated MCF-7aro cells versus AI-treated LTEDaro cells are denoted by [a] $p < 0.05$ and between AI-treated MCF-7aro cells plus 3-MA versus AI-treated LTEDaro cells plus 3-MA are denoted by [b] $p < 0.05$.

Chapter IV

Discussion/Conclusion

The search for new potent AIs by our research group has allowed a better understanding on which chemical features better contribute to this goal. Thus, early structure–activity relationships on competitive aromatase inhibitors highlighted the importance of planarity at the A/B ring junction and the presence of carbonyl groups at positions C3 and C17 (Varela et al. 2012). On the other hand, bulky substituents at the B ring positions C6 and C7 have also been shown to provide potent aromatase inhibitors (Salvador et al. 2013).

The compounds studied in this work were obtained from chemical modifications in the A-, B- and D-rings of the aromatase substrate, androstenedione, as previously described (Varela et al. 2013) and they present the 7α-allyl as a common structural feature at the B-ring. These competitive AIs exhibit, in human placental microsomes, an IC_{50} of 0.59 μM for compound **6**, 0.75 μM for compound **9**, 0.45 μM for compound **10** and 0.47 μM for compound **12** (Varela et al. 2013). In this study, the anti-aromatase activities of the aforementioned steroids were further evaluated in MCF-7aro cells. Steroid **6** presented an IC_{50} of 3.5 μM, compound **9** of 3.1 μM, compound **10** of 0.5 μM and compound **12** of 0.3 μM. Compounds **6** and **9** were not as efficient inhibitors as they were in placental microsomes. This is probably due to a possible interference of cell membrane in the uptake of such compounds. Nevertheless, AIs **10** and **12** presented a similar or even lower IC_{50} values when compared to their counterparts in placental microsomes. Comparing the new steroids with exemestane (IC_{50} of 0.9 μM) (Amaral et al. 2013), steroids **10** and **12** seem to be more effective in inhibiting aromatase. Considering all the data, we can conclude that steroids **10** and **12** are the most potent AIs in both systems and, unlike AIs **6** and **9**, cell membrane does not affect compound uptake.

In order to evaluate the consequences of these compounds upon cell viability, their effects were investigated in MCF-7aro cells, an ER+ breast cancer cell line, stably transfected with the aromatase gene. Our results demonstrated that all the studied AIs induced a significant decrease in cell viability in a dose- and, except for compound **6**, in a time-dependent manner, with no effects on membrane integrity. Compound **9** also induced an estrogenic effect for the lower concentration, after 3 days of treatment. This behavior was already observed for exemestane (Amaral et al. 2012) and for other compounds formerly synthesized and studied by our group (Amaral et al. 2013). Compound **10** was the most efficient in decreasing viability of MCF-7aro cells.

To understand whether these biological effects were dependent on aromatase inhibition, it was also studied the effects of each AI in MCF-7aro cells incubated with E2, the product of the aromatization reaction of testosterone. The AIs induced a decrease in cell viability similar to the T-treated cells' viability, suggesting that their biological effects are aromatase-

independent. Surprisingly, steroid **10** showed a significant difference, at 6 days of treatment, with a more pronounced decrease in E2-treated cells' viability.

In order to understand if the decrease in cell viability was due to an interaction with the estrogen receptor, SK-BR-3 cell line, an ER^- breast cancer cell line, was also used. In fact, in these cells, AI **10** presents a significant difference in cell viability, at 6 days, when compared to E2 or T-treated cells. Thus, this compound might exert some of its effects via an interaction with the ER. The SK-BR-3 cell line, besides expressing all the enzymes required for estrogen biosynthesis, only expresses very low levels of ERβ and has no expression of ERα, indicating that this cell line represents a model for estrogen-independent breast cancers (Ford et al. 2011). Therefore, our data indicate that all compounds induced a decrease in MCF-7aro cells' viability in an aromatase-independent manner, with AI **10** presenting a possible ER-dependent mechanism. This latter finding might explain why AI **10** is the most potent in decreasing cell viability in E2-treated cells, since it might present a synergy between aromatase inhibition and ER modulation. Nevertheless, it cannot be excluded the hypothesis that other mechanisms, independent of ER or aromatase, may also be involved. Further studies should be performed to corroborate the eventual mechanism of interaction with ER.

In addition, to evaluate the cytotoxicity of these steroids, the human foreskin fibroblast cell line, HFF-1, was used. None of the steroids had any effects in the viability of this non-tumoral cell line. Interestingly, compounds **10** and **12** induced cell proliferation, at 6 days of treatment and for the higher concentrations. Which particular signaling pathway is implicated will require further studies.

The reduction on MCF-7aro cells' viability can be due to anti-proliferative effects or induction of cell death. Thus, it was studied the cell cycle progression, by flow cytometry. Results showed that, while compounds **9** and **10** induced a cell cycle arrest in G0/G1 phase, AI **12** caused an arrest in G2/M phase. This is in agreement with what was previously demonstrated for exemestane (Amaral et al. 2012), alongside the non-steroidal AIs, letrozole and anastrozole (Thiantanawat et al. 2003), which suppress proliferation of MCF-7aro cells and induce cell cycle arrest in G0/G1 phase. However, we have also shown that, for longer periods of treatment, exemestane causes retention in G2/M cell cycle phase (Amaral et al. 2012). It has been referred that a cell cycle arrest in G2/M phase, induced by cytotoxic drugs, via regulation of cyclins and cyclin-dependent kinases (CDKs), is associated with enhanced apoptosis (Tyagi et al. 2002).

The anti-proliferative effects and the disruption of cell cycle progression were accompanied by a reduction in cell density and by the presence of morphological alterations, such as

chromatin condensation/fragmentation and membrane blebbing, typical features of apoptosis. In addition, some cells presented cytoplasmic vacuoles. To further investigate the involvement of apoptosis, it was studied the mitochondrial transmembrane potential ($\Delta\Psi_m$), ROS production and the activities of caspases -8, -9 and -7. Concerning caspase activation, all the AIs induced a significant increase in caspase-9 and caspase-7 activities and no effect on caspase-8 activity. Besides this, there was no significant production of ROS, which indicates that cell death is ROS-independent, though other studies must be carried out in order to confirm these results.

In the intrinsic pathway or mitochondrial pathway, the loss of $\Delta\Psi_m$ leads to the release of cytochrome *c* into the cytosol, which interacts with apoptosis protease activating factor-1 (APAF-1), ATP and pro-caspase-9, leading to the formation of apoptosome and activation of pro-caspase-9 (Parrish et al. 2013). On the other hand, caspase-8 can also proteolytically activate Bid, which promotes mitochondrial membrane permeabilization. However and considering all this, a burning question remains: how can caspase-9 be activated? Activation of caspase-9 might be dependent upon different mechanisms. Interestingly, it was reported in the literature that caspase-9 may be activated by caspase-12, a pathway independent of cytochrome *c* release and dependent on endoplasmic reticulum stress (Morishima et al. 2002). This pathway leads to activation of effector caspase-3 (absent in MCF-7aro cells) and a minimum activation of caspase-7, which might explain our results. Furthermore, the findings of the present study, specifically in terms of apoptotic features, might be correlated with a more prominent and assertive apoptotic pathway, i.e., besides caspase-7, effector caspase-6 might also be activated by this axis. Activation of caspase-6 was observed following treatment of MCF-7aro cells with non-steroidal AIs, letrozole and anastrozole (Thiantanawat et al. 2003). Further studies are required to confirm this hypothesis for caspase-9 activation.

In order to evaluate the efficacy of our compounds in acquired endocrine resistance, it was also studied the effects of AIs **9**, **10** and **12** in LTEDaro cells, a good model of late stage acquired resistance that does not respond to AI treatment (Masri et al. 2008). Our data showed that these cells were sensitive to compound **10**, but were resistant to compounds **9** and **12**, after 3 days, except for the highest concentrations. The extension of the treatment allowed the cells to respond to AIs **9** and **12**. Compound **10** was shown, again, to be the most efficient one in decreasing cell viability.

It is known that autophagy is an evolutionary conserved catabolic process of subcellular degradation that may contribute to the modulation of tumor progression, either as a mechanism of cell death or of cell survival and may confer resistance to anti-cancer therapies. Thus, the inhibition of autophagy, by autophagic inhibitors, such as 3-MA, or by

knockdown of autophagy-related genes, may re-sensitize resistant cancer cells and lead to a decrease in tumor growth by enhancing cell death (Yang et al. 2011). In autophagy, the class I PI3K leads to activation of Akt and mTOR, inhibiting autophagy, whereas the class III stimulates autophagic sequestration (Yang et al. 2011). Besides the PI3K role in autophagy, survival and cell-cycle progression, this pathway also interferes with ER directly or indirectly, promoting estrogen-dependent and -independent ER transcriptional activity (Burris 3rd 2013). Our group previously described that autophagy is a cytoprotective mechanism in MCF-7aro cells, when treated with exemestane and may also be involved in exemestane acquired resistance (Amaral et al. 2012). On the other hand, as some AI-treated cells presented cytoplasmic vacuoles, the effects of the autophagic inhibitor 3-MA, that targets class I and class III PI3K, were studied in AI-treated MCF-7aro and LTEDaro cells. In this study, the presence of acid vesicular organelles (AVOs) was observed in both cell lines, at 3 days of treatment, though with prolongation of treatment the presence of AVOs seemed to reduce.

In MCF-7aro cells, the autophagic inhibitor did not induce any alteration in AI-treated cells' viability. However, in LTEDaro cells, the addition of 3-MA, at 3 days, caused a significant reduction in AI-treated cells' viability. This effect is similar to the one obtained after 6 days, regardless of the addition of 3-MA. This data suggests that autophagy has a pro-survival role, though, with prolongation of treatment, it no longer affects cell survival. In addition, both cell lines seem to present the same behavior when exposed to the compounds for 6 days, which means that, regardless of hormone-dependent or –independent microenvironment, these compounds are able to exert their effects.

In summary, steroids **9**, **10** and **12** inhibit aromatase in MCF-7aro cells, causing a decrease in cell viability. Compound **10** is the most potent aromatase inhibitor, being the most effective one in decreasing cell viability in an aromatase-independent and possible ER-dependent manner. The anti-proliferative effects of the studied AIs were due to a mechanism of cell death by apoptosis and a disruption in cell cycle progression, with a cell cycle arrest in G0/G1 for AIs **9** and **10** and an arrest in G2/M phase for AI **12**. In addition, using LTEDaro cells, it was observed that this cell line can present different behaviors depending on the steroidal AI. These cells were sensitive to compound **10**. Moreover, the addition of the autophagic inhibitor 3-MA, in both MCF-7aro and LTEDaro cells, indicates that autophagy may play divergent roles depending on the cell line, AI used and time of exposure. Therefore, as AI **10** was the most promising compound, further studies should be undertaken to clarify the mechanisms implicated in the reduction of viability of both cell types.

These results are important not only for the clarification of the cellular effects of steroidal AIs on breast cancer cells, but also to determine which chemical structural features in the molecule of androstenedione are important for inhibiting aromatase and cause the reduction of cell viability, preventing, in this way, tumor growth. This study will contribute to the future design of more potent AIs that may overcome endocrine resistance.

Chapter V

References

Amaral, C., Borges, M., Melo, S., da Silva, E.T., Correia-da-Silva, G. and Teixeira, N., 2012. Apoptosis and autophagy in breast cancer cells following exemestane treatment. *PLoS ONE*, 7(8), p.e42398.

Amaral, C., Varela, C., Azevedo, M., da Silva, E.T., Roleira, F.M., Chen, S., Correia-da-Silva, G. and Teixeira, N., 2013. Effects of steroidal aromatase inhibitors on sensitive and resistant breast cancer cells: aromatase inhibition and autophagy. *J Steroid Biochem Mol Biol*, 135, pp.51–59.

Arpino, G., Wiechmann, L., Osborne, C.K. and Schiff, R., 2008. Crosstalk between the estrogen receptor and the HER tyrosine kinase receptor family: molecular mechanism and clinical implications for endocrine therapy resistance. *Endocrine reviews*, 29(2), pp.217–33.

Berthois, Y., Katzenellenbogen, J. a and Katzenellenbogen, B.S., 1986. Phenol red in tissue culture media is a weak estrogen: implications concerning the study of estrogen-responsive cells in culture. *Proceedings of the National Academy of Sciences of the United States of America*, 83(8), pp.2496–500.

Bhatnagar, A.S., 2007. The discovery and mechanism of action of letrozole. *Breast cancer research and treatment*, 105 Suppl, pp.7–17.

Bliss, J.M., Kilburn, L.S., Coleman, R.E., Forbes, J.F., Coates, A.S., Jones, S.E., Jassem, J., Delozier, T., Andersen, J., Paridaens, R., van de Velde, C.J.H., Lønning, P.E., Morden, J., Reise, J., Cisar, L., Menschik, T. and Coombes, R.C., 2012. Disease-related outcomes with long-term follow-up: an updated analysis of the intergroup exemestane study. *Journal of clinical oncology : official journal of the American Society of Clinical Oncology*, 30(7), pp.709–17.

Brodie, A., Macedo, L. and Sabnis, G., 2010. Aromatase resistance mechanisms in model systems in vivo. *J Steroid Biochem Mol Biol*, 118(4-5), pp.283–287.

Brodie, A. and Sabnis, G., 2011. Adaptive changes result in activation of alternate signaling pathways and acquisition of resistance to aromatase inhibitors. *Clin Cancer Res*, 17(13), pp.4208–4213.

Bulun, S.E., Lin, Z., Zhao, H., Lu, M., Amin, S., Reierstad, S. and Chen, D., 2009. Regulation of aromatase expression in breast cancer tissue. *Annals of the New York Academy of Sciences*, 1155, pp.121–31.

Burris 3rd, H.A., 2013. Overcoming acquired resistance to anticancer therapy: focus on the PI3K/AKT/mTOR pathway. *Cancer Chemother Pharmacol*, 71(4), pp.829–842.

Cannings, E., Kirkegaard, T., Tovey, S.M., Dunne, B., Cooke, T.G. and Bartlett, J.M.S., 2007. Bad expression predicts outcome in patients treated with tamoxifen. *Breast cancer research and treatment*, 102(2), pp.173–9.

Castoria, G., Migliaccio, A., Giovannelli, P. and Auricchio, F., 2010. Cell proliferation regulated by estradiol receptor: Therapeutic implications. *Steroids*, 75(8-9), pp.524–527.

Choueiri, T.K., Alemany, C.A., Abou-Jawde, R.M. and Budd, G.T., 2004. Role of aromatase inhibitors in the treatment of breast cancer. *Clin Ther*, 26(8), pp.1199–1214.

Chumsri, S., Howes, T., Bao, T., Sabnis, G. and Brodie, A., 2011. Aromatase, aromatase inhibitors, and breast cancer. *J Steroid Biochem Mol Biol*, 125(1-2), pp.13–22.

Ciruelos, E., Pascual, T., Arroyo Vozmediano, M.L., Blanco, M., Manso, L., Parrilla, L., Munoz, C., Vega, E., Calderon, M.J., Sancho, B. and Cortes-Funes, H., 2014. The therapeutic role of fulvestrant in the management of patients with hormone receptor-positive breast cancer. *Breast*, 23(3), pp.201–208.

Demura, M. and Bulun, S.E., 2008. CpG dinucleotide methylation of the CYP19 I.3/II promoter modulates cAMP-stimulated aromatase activity. *Molecular and cellular endocrinology*, 283(1-2), pp.127–32.

Dowsett, M., Cuzick, J., Wale, C., Forbes, J., Mallon, E. a, Salter, J., Quinn, E., Dunbier, A., Baum, M., Buzdar, A., Howell, A., Bugarini, R., Baehner, F.L. and Shak, S., 2010. Prediction of risk of distant recurrence using the 21-gene recurrence score in node-negative and node-positive postmenopausal patients with breast cancer treated with anastrozole or tamoxifen: a TransATAC study. *Journal of clinical oncology : official journal of the American Society of Clinical Oncology*, 28(11), pp.1829–34.

Dowsett, M., Nicholson, R.I. and Pietras, R.J., 2005. Biological characteristics of the pure antiestrogen fulvestrant: overcoming endocrine resistance. *Breast Cancer Res Treat*, 93 Suppl 1, pp.S11–8.

Eroles, P., Bosch, A., Perez-Fidalgo, J.A. and Lluch, A., 2012. Molecular biology in breast cancer: intrinsic subtypes and signaling pathways. *Cancer Treat Rev*, 38(6), pp.698–707.

Ferlay J, Soerjomataram I, Ervik M, Dikshit R, Eser S, Mathers C, Rebelo M, Parkin DM, Forman D, Bray, F., 2013. GLOBOCAN 2012 v1.0, Cancer Incidence and Mortality Worldwide: IARC CancerBase No. 11 [Internet]. *Lyon, France: International Agency for Research on Cancer*.

Ford, C.H.J., Al-Bader, M., Al-Ayadhi, B. and Francis, I., 2011. Reassessment of estrogen receptor expression in human breast cancer cell lines. *Anticancer research*, 31(2), pp.521–7.

Garcia-Becerra, R., Santos, N., Diaz, L. and Camacho, J., 2012. Mechanisms of Resistance to Endocrine Therapy in Breast Cancer: Focus on Signaling Pathways, miRNAs and Genetically Based Resistance. *Int J Mol Sci*, 14(1), pp.108–145.

Geisler, J., 2011. Differences between the non-steroidal aromatase inhibitors anastrozole and letrozole--of clinical importance? *British journal of cancer*, 104(7), pp.1059–66.

Ghayee, H.K. and Auchus, R.J., 2007. Basic concepts and recent developments in human steroid hormone biosynthesis. *Reviews in endocrine & metabolic disorders*, 8(4), pp.289–300.

Ghosh, D., Griswold, J., Erman, M. and Pangborn, W., 2009. Structural basis for androgen specificity and oestrogen synthesis in human aromatase. *Nature*, 457(7226), pp.219–223.

Goldhirsch, a, Winer, E.P., Coates, a S., Gelber, R.D., Piccart-Gebhart, M., Thürlimann, B. and Senn, H.-J., 2013. Personalizing the treatment of women with early breast cancer: highlights of the St Gallen International Expert Consensus on the Primary Therapy of

Early Breast Cancer 2013. *Annals of oncology : official journal of the European Society for Medical Oncology / ESMO*, 24(9), pp.2206–23.

Goldhirsch, a, Wood, W.C., Coates, a S., Gelber, R.D., Thürlimann, B. and Senn, H.-J., 2011. Strategies for subtypes--dealing with the diversity of breast cancer: highlights of the St. Gallen International Expert Consensus on the Primary Therapy of Early Breast Cancer 2011. *Annals of oncology : official journal of the European Society for Medical Oncology / ESMO*, 22(8), pp.1736–47.

Gomes, A., Fernandes, E. and Lima, J.L.F.C., 2005. Fluorescence probes used for detection of reactive oxygen species. *Journal of biochemical and biophysical methods*, 65(2-3), pp.45–80.

Goss, P.E., Ingle, J.N., Pritchard, K.I., Ellis, M.J., Sledge, G.W., Budd, G.T., Rabaglio, M., Ansari, R.H., Johnson, D.B., Tozer, R., D'Souza, D.P., Chalchal, H., Spadafora, S., Stearns, V., Perez, E. a, Liedke, P.E.R., Lang, I., Elliott, C., Gelmon, K. a, et al., 2013. Exemestane versus anastrozole in postmenopausal women with early breast cancer: NCIC CTG MA.27--a randomized controlled phase III trial. *Journal of clinical oncology : official journal of the American Society of Clinical Oncology*, 31(11), pp.1398–404.

Gross, A., McDonnell, J.M. and Korsmeyer, S.J., 1999. BCL-2 family members and the mitochondria in apoptosis. *Genes Dev*, 13(15), pp.1899–1911.

Guarneri, V. and Conte, P., 2009. Metastatic breast cancer: therapeutic options according to molecular subtypes and prior adjuvant therapy. *Oncologist*, 14(7), pp.645–656.

Habel, L. a, Shak, S., Jacobs, M.K., Capra, A., Alexander, C., Pho, M., Baker, J., Walker, M., Watson, D., Hackett, J., Blick, N.T., Greenberg, D., Fehrenbacher, L., Langholz, B. and Quesenberry, C.P., 2006. A population-based study of tumor gene expression and risk of breast cancer death among lymph node-negative patients. *Breast cancer research : BCR*, 8(3), p.R25.

Harigopal, M., Heymann, J., Ghosh, S., Anagnostou, V., Camp, R.L. and Rimm, D.L., 2009. Estrogen receptor co-activator (AIB1) protein expression by automated quantitative analysis (AQUA) in a breast cancer tissue microarray and association with patient outcome. *Breast cancer research and treatment*, 115(1), pp.77–85.

Herschkowitz, J.I., Simin, K., Weigman, V.J., Mikaelian, I., Usary, J., Hu, Z., Rasmussen, K.E., Jones, L.P., Assefnia, S., Chandrasekharan, S., Backlund, M.G., Yin, Y., Khramtsov, A.I., Bastein, R., Quackenbush, J., Glazer, R.I., Brown, P.H., Green, J.E., Kopelovich, L., et al., 2007. Identification of conserved gene expression features between murine mammary carcinoma models and human breast tumors. *Genome Biol*, 8(5), p.R76.

Hong, Y. and Chen, S., 2006. Aromatase inhibitors: structural features and biochemical characterization. *Ann N Y Acad Sci*, 1089, pp.237–251.

Hong, Y., Li, H., Yuan, Y.C. and Chen, S., 2009. Molecular characterization of aromatase. *Ann N Y Acad Sci*, 1155, pp.112–120.

Hurtado, A., Holmes, K. a, Geistlinger, T.R., Hutcheson, I.R., Nicholson, R.I., Brown, M., Jiang, J., Howat, W.J., Ali, S. and Carroll, J.S., 2008. Regulation of ERBB2 by oestrogen receptor-PAX2 determines response to tamoxifen. *Nature*, 456(7222), pp.663–6.

Ignatiadis, M. and Sotiriou, C., 2013. Luminal breast cancer: from biology to treatment. *Nature reviews. Clinical oncology*, 10(9), pp.494–506.

Jin, Y., Desta, Z., Stearns, V., Ward, B., Ho, H., Lee, K.-H., Skaar, T., Storniolo, A.M., Li, L., Araba, A., Blanchard, R., Nguyen, A., Ullmer, L., Hayden, J., Lemler, S., Weinshilboum, R.M., Rae, J.M., Hayes, D.F. and Flockhart, D. a, 2005. CYP2D6 genotype, antidepressant use, and tamoxifen metabolism during adjuvant breast cancer treatment. *Journal of the National Cancer Institute*, 97(1), pp.30–9.

Jordan, V.C., 2004. Selective estrogen receptor modulation: concept and consequences in cancer. *Cancer cell*, 5(3), pp.207–13.

Knower, K.C., To, S.Q. and Clyne, C.D., 2013. Intracrine oestrogen production and action in breast cancer: an epigenetic focus. *J Steroid Biochem Mol Biol*, 137, pp.157–164.

Krell, J., Januszewski, A., Yan, K. and Palmieri, C., 2011. Role of fulvestrant in the management of postmenopausal breast cancer. *Expert Rev Anticancer Ther*, 11(11), pp.1641–1652.

Kurokawa, H., Nishio, K., Fukumoto, H., Tomonari, A., Suzuki, T. and Saijo, N., 1999. Alteration of caspase-3 (CPP32/Yama/apopain) in wild-type MCF-7, breast cancer cells. *Oncology Reports*, 6(1), pp.33–37.

Labrie, F., 2014. All sex steroids are made intracellularly in peripheral tissues by the mechanisms of intracrinology after menopause. *The Journal of steroid biochemistry and molecular biology*, pp.1–6.

Lønning, P.E., Bajetta, E., Murray, R., Tubiana-Hulin, M., Eisenberg, P.D., Mickiewicz, E., Celio, L., Pitt, P., Mita, M., Aaronson, N.K., Fowst, C., Arkhipov, A., di Salle, E., Polli, A. and Massimini, G., 2000. Activity of exemestane in metastatic breast cancer after failure of nonsteroidal aromatase inhibitors: a phase II trial. *Journal of clinical oncology : official journal of the American Society of Clinical Oncology*, 18(11), pp.2234–44.

Masri, S., Lui, K., Phung, S., Ye, J., Zhou, D., Wang, X. and Chen, S., 2009. Characterization of the weak estrogen receptor alpha agonistic activity of exemestane. *Breast Cancer Res Treat*, 116(3), pp.461–470.

Masri, S., Phung, S., Wang, X., Wu, X., Yuan, Y.C., Wagman, L. and Chen, S., 2008. Genome-wide analysis of aromatase inhibitor-resistant, tamoxifen-resistant, and long-term estrogen-deprived cells reveals a role for estrogen receptor. *Cancer Res*, 68(12), pp.4910–4918.

McNamara, K.M. and Sasano, H., 2014. The intracrinology of breast cancer. *J Steroid Biochem Mol Biol*.

Miller, W.R., Bartlett, J., Brodie, A.M.H., Brueggemeier, R.W., di Salle, E., Lønning, P.E., Llombart, A., Maass, N., Maudelonde, T., Sasano, H. and Goss, P.E., 2008. Aromatase inhibitors: are there differences between steroidal and nonsteroidal aromatase inhibitors and do they matter? *The oncologist*, 13(8), pp.829–37.

Morishima, N., Nakanishi, K., Takenouchi, H., Shibata, T. and Yasuhiko, Y., 2002. An endoplasmic reticulum stress-specific caspase cascade in apoptosis. Cytochrome c-

independent activation of caspase-9 by caspase-12. *The Journal of biological chemistry*, 277(37), pp.34287–94.

Musgrove, E.A. and Sutherland, R.L., 2009. Biological determinants of endocrine resistance in breast cancer. *Nat Rev Cancer*, 9(9), pp.631–643.

Nelson, L.R. and Bulun, S.E., 2001. Estrogen production and action. *Journal of the American Academy of Dermatology*, 45(3), pp.S116–S124.

O'Hara, J., Vareslija, D., McBryan, J., Bane, F., Tibbitts, P., Byrne, C., Conroy, R.M., Hao, Y., Gaora, P.O., Hill, A.D., McIlroy, M. and Young, L.S., 2012. AIB1:ERalpha transcriptional activity is selectively enhanced in aromatase inhibitor-resistant breast cancer cells. *Clin Cancer Res*, 18(12), pp.3305–3315.

Osborne, C.K., Bardou, V., Hopp, T. a, Chamness, G.C., Hilsenbeck, S.G., Fuqua, S. a W., Wong, J., Allred, D.C., Clark, G.M. and Schiff, R., 2003. Role of the estrogen receptor coactivator AIB1 (SRC-3) and HER-2/neu in tamoxifen resistance in breast cancer. *Journal of the National Cancer Institute*, 95(5), pp.353–61.

Osborne, C.K. and Schiff, R., 2005. Estrogen-receptor biology: continuing progress and therapeutic implications. *J Clin Oncol*, 23(8), pp.1616–1622.

Osborne, C.K., Zhao, H. and Fuqua, S. a, 2000. Selective estrogen receptor modulators: structure, function, and clinical use. *Journal of clinical oncology : official journal of the American Society of Clinical Oncology*, 18(17), pp.3172–86.

Palmieri, C., Patten, D.K., Januszewski, A., Zucchini, G. and Howell, S.J., 2014. Breast cancer: current and future endocrine therapies. *Mol Cell Endocrinol*, 382(1), pp.695–723.

Paridaens, R.J., Dirix, L.Y., Beex, L. V, Nooij, M., Cameron, D. a, Cufer, T., Piccart, M.J., Bogaerts, J. and Therasse, P., 2008. Phase III study comparing exemestane with tamoxifen as first-line hormonal treatment of metastatic breast cancer in postmenopausal women: the European Organisation for Research and Treatment of Cancer Breast Cancer Cooperative Group. *Journal of clinical oncology : official journal of the American Society of Clinical Oncology*, 26(30), pp.4883–90.

Parker, J.S., Mullins, M., Cheang, M.C.U., Leung, S., Voduc, D., Vickery, T., Davies, S., Fauron, C., He, X., Hu, Z., Quackenbush, J.F., Stijleman, I.J., Palazzo, J., Marron, J.S., Nobel, A.B., Mardis, E., Nielsen, T.O., Ellis, M.J., Perou, C.M., et al., 2009. Supervised risk predictor of breast cancer based on intrinsic subtypes. *Journal of clinical oncology : official journal of the American Society of Clinical Oncology*, 27(8), pp.1160–7.

Parrish, A.B., Freel, C.D. and Kornbluth, S., 2013. Cellular mechanisms controlling caspase activation and function. *Cold Spring Harb Perspect Biol*, 5(6).

Perou, C.M., Sørlie, T., Eisen, M.B., van de Rijn, M., Jeffrey, S.S., Rees, C.A., Pollack, J.R., Ross, D.T., Johnsen, H., Akslen, L.A., Fluge, O., Pergamenschikov, A., Williams, C., Zhu, S.X., Lønning, P.E., Børresen-Dale, A.L., Brown, P.O. and Botstein, D., 2000. Molecular portraits of human breast tumours. *Nature*, 406(6797), pp.747–752.

Prat, A. and Perou, C.M., 2011. Deconstructing the molecular portraits of breast cancer. *Mol Oncol*, 5(1), pp.5–23.

Rakha, E.A. and Ellis, I.O., 2011. Modern classification of breast cancer: should we stick with morphology or convert to molecular profile characteristics. *Adv Anat Pathol*, 18(4), pp.255–267.

Richards, J. a and Brueggemeier, R.W., 2003. Prostaglandin E2 regulates aromatase activity and expression in human adipose stromal cells via two distinct receptor subtypes. *The Journal of clinical endocrinology and metabolism*, 88(6), pp.2810–6.

Riggs, B.L. and Hartmann, L.C., 2003. Selective estrogen-receptor modulators -- mechanisms of action and application to clinical practice. *The New England journal of medicine*, 348(7), pp.618–629.

Rouzier, R., Perou, C.M., Symmans, W.F., Ibrahim, N., Cristofanilli, M., Anderson, K., Hess, K.R., Stec, J., Ayers, M., Wagner, P., Morandi, P., Fan, C., Rabiul, I., Ross, J.S., Hortobagyi, G.N. and Pusztai, L., 2005. Breast cancer molecular subtypes respond differently to preoperative chemotherapy. *Clinical cancer research : an official journal of the American Association for Cancer Research*, 11(16), pp.5678–85.

Sainsbury, R., 2013. The development of endocrine therapy for women with breast cancer. *Cancer Treat Rev*, 39(5), pp.507–517.

Salvador, J.A., Carvalho, J.F., Neves, M.A., Silvestre, S.M., Leitao, A.J., Silva, M.M. and Sa e Melo, M.L., 2013. Anticancer steroids: linking natural and semi-synthetic compounds. *Nat Prod Rep*, 30(2), pp.324–374.

Sanderson, J.T., 2006. The steroid hormone biosynthesis pathway as a target for endocrine-disrupting chemicals. *Toxicological sciences : an official journal of the Society of Toxicology*, 94(1), pp.3–21.

Sasano, H., Miki, Y., Nagasaki, S. and Suzuki, T., 2009. In situ estrogen production and its regulation in human breast carcinoma: from endocrinology to intracrinology. *Pathology international*, 59(11), pp.777–89.

Schiavon, G. and Smith, I.E., 2013. Endocrine therapy for advanced/metastatic breast cancer. *Hematol Oncol Clin North Am*, 27(4), pp.715–36, viii.

Simpson, E.R., 2002. Aromatization of androgens in women: current concepts and findings. *Fertility and sterility*, 77 Suppl 4(4), pp.S6–10.

Small, G.W., Shi, Y.Y., Higgins, L.S. and Orlowski, R.Z., 2007. Mitogen-activated protein kinase phosphatase-1 is a mediator of breast cancer chemoresistance. *Cancer research*, 67(9), pp.4459–66.

Thiantanawat, A., Long, B.J. and Brodie, A.M., 2003. Signaling pathways of apoptosis activated by aromatase inhibitors and antiestrogens. *Cancer research*, 63(22), pp.8037–8050.

Thompson, E.A. and Siiteri, P.K., 1974. Utilization of oxygen and reduced nicotinamide adenine dinucleotide phosphate by human placental microsomes during aromatization of androstenedione. *Journal of Biological Chemistry*, 249(17), pp.5364–5372.

To, S.Q., Knower, K.C., Cheung, V., Simpson, E.R. and Clyne, C.D., 2014. Transcriptional control of local estrogen formation by aromatase in the breast. *J Steroid Biochem Mol Biol*.

Turkistani, A. and Marsh, S., 2012. Pharmacogenomics of third-generation aromatase inhibitors. *Expert Opin Pharmacother*, 13(9), pp.1299–1307.

Tyagi, A.K., Singh, R.P., Agarwal, C., Chan, D.C.F. and Agarwal, R., 2002. Silibinin strongly synergizes human prostate carcinoma DU145 cells to doxorubicin-induced growth inhibition, G2-M arrest, and apoptosis. *Clinical Cancer Research*, 8(11), pp.3512–3519.

Varela, C., Tavares da Silva, E.J., Amaral, C., Correia da Silva, G., Baptista, T., Alcaro, S., Costa, G., Carvalho, R.A., Teixeira, N.A. and Roleira, F.M., 2012. New structure-activity relationships of A- and D-ring modified steroidal aromatase inhibitors: design, synthesis, and biochemical evaluation. *J Med Chem*, 55(8), pp.3992–4002.

Varela, C.L., Amaral, C., Correia-da-Silva, G., Carvalho, R.A., Teixeira, N.A., Costa, S.C., Roleira, F.M. and Tavares-da-Silva, E.J., 2013. Design, synthesis and biochemical studies of new 7alpha-allylandrostanes as aromatase inhibitors. *Steroids*, 78(7), pp.662–669.

Veer, L. van't, Dai, H. and Vijver, M. Van De, 2002. Gene expression profiling predicts clinical outcome of breast cancer. *nature*, 415(345).

Yang, Z.J., Chee, C.E., Huang, S. and Sinicrope, F.A., 2011. The role of autophagy in cancer: therapeutic implications. *Mol Cancer Ther*, 10(9), pp.1533–1541.

Zhou, D.J., Pompon, D. and Chen, S.A., 1990. Stable expression of human aromatase complementary DNA in mammalian cells: a useful system for aromatase inhibitor screening. *Cancer research*, 50(21), pp.6949–6954.